

Aus dem Max-Planck-Institut für Neurobiologie

Abteilung Neuroimmunologie

Direktor: Professor Dr. med. Hartmut Wekerle

**Habilitationsschrift zur Erlangung der *venia legendi*  
für das Fach Neuroimmunologie  
an der Fakultät für Medizin  
der Ludwig-Maximilians-Universität München**

**Modeling central nervous system autoimmunity:  
Triggers and pathogenic processes**

Vorgelegt von  
Dr. rer. nat. Gurumoorthy Krishnamoorthy  
München

# Table of Contents

<b>1. INTRODUCTION .....</b>	<b>1</b>
1.1. EXPERIMENTAL AUTOIMMUNE ENCEPHALOMYELITIS: AN ANIMAL MODEL OF MULTIPLE SCLEROSIS .....	2
1.1.1. <i>Spontaneous EAE models</i> .....	2
1.2. TRIGGERS AND PATHOGENIC EVENTS IN CNS AUTOIMMUNITY .....	3
<b>2. QUESTIONS .....</b>	<b>5</b>
<b>3. RESULTS AND DISCUSSION .....</b>	<b>6</b>
3.1. SPONTANEOUS EAE MODELS OF MS .....	6
3.2. B CELLS IN SPONTANEOUS EAE MODELS .....	8
3.3. CUMULATIVE AUTOIMMUNITY .....	11
3.4. GUT MICROBIOTA AS A TRIGGER OF SPONTANEOUS CNS AUTOIMMUNITY .....	13
<b>4. SUMMARY .....</b>	<b>15</b>
<b>5. REFERENCES .....</b>	<b>16</b>
<b>6. PUBLICATIONS .....</b>	<b>21</b>
<b>7. CURRICULUM VITAE .....</b>	<b>60</b>
<b>8. ACKNOWLEDGMENT .....</b>	<b>61</b>

## 1. Introduction

Multiple Sclerosis (MS), an autoimmune demyelinating disease affecting the central nervous system (CNS), causes tremendous disability in young adults and inflicts a huge economic burden on the society. Currently, more than 2.5 million people are affected by MS worldwide and the incidence is steadily increasing in most countries (Pugliatti et al., 2002). The disease progression in individual patients often takes different courses eventually leading to severe functional deficits which include inability to walk without support, cognitive decline etc. Functional deficits in MS are caused by focal lesions in the CNS white matter predominantly composed of immune cell infiltrates (Hauser and Oksenberg, 2006; Sospedra and Martin, 2005). These infiltrating immune cells recruit additional immune cells and also activate local resident cells to orchestrate a pathogenic cascade inflicting demyelination and axonal damage.

Genetic factors clearly predispose a particular individual to the development of MS. In support of this, genome wide association studies identified many genes, in particular immunologically relevant genes, as risk factors for MS susceptibility (Sawcer et al., 2011). However, the low concordance rate of approximately 30% between monozygotic twins to develop MS indicates an important and significant role of environmental factors in disease initiation. Moreover, the striking increase in the incidence of MS within the last few decades cannot be entirely attributed to genetic changes. Although clear causative environmental factors are not known, analysis of epidemiological data suggests vitamin D, smoking and Epstein-Barr-Virus (EBV) infection as potential risk factors for triggering MS (Ascherio and Munger, 2008). The high prevalence of MS also coincides with the improved lifestyle and high standards of hygiene which reduce the burden of infections but can also limit exposure to microbes that are potentially beneficial for healthy activation of the immune system (Bach, 2002; Okada et al., 2010). While the importance of the immune mediated pathology in MS has been firmly established, how the CNS-specific autoimmune responses are initiated is poorly understood. Moreover, it is not clear what triggers relapses of clinical episodes in relapsing-remitting MS patients. While the currently available animal models greatly allow us to understand the effector phase of the autoimmune disease, they were not useful to study the triggering phase of the disease.

## 1.1. Experimental autoimmune encephalomyelitis: an animal model of multiple sclerosis

Experimental autoimmune encephalomyelitis (EAE) induced in rodents is the common model of choice to study CNS autoimmune responses. Typically, two types of models have been used: actively induced EAE or passive transfer EAE. The active EAE induction protocols require complete Freund's adjuvant (CFA) as an adjuvant which facilitates the gradual release of antigen into the draining lymph nodes and at the same time amplifies the immune response by activating innate immune system. Pertussis toxin is also combined with EAE induction in mice (Linthicum et al., 1982). Passive EAE induction relies on the transfer of encephalitogenic T cells clones or lines obtained from immunized animals and stimulated *in vitro* by the autoantigen (Wekerle et al., 1994). However, these induced models have several drawbacks. These artificial models poorly reflect the true pathogenic mechanisms of MS and are often too simplistic, focusing mainly on T cell responses. Later, many transgenic models have been developed to interrogate the pathogenic mechanisms of CNS autoimmunity. These include transgenic mice expressing the susceptible human leucocyte antigen (HLA) genes from patients, targeted expression of the cytokines and chemokines in the CNS and T cell receptor and B cell receptor transgenic mice (Krishnamoorthy et al., 2007).

### 1.1.1. Spontaneous EAE models

The development of alternative class of models which overexpress myelin-specific T- or B-cell receptors resulted in spontaneous neurological symptoms with varied incidence and clinical patterns (Krishnamoorthy et al., 2007). These models are entirely murine or "humanized" for the T cell receptor (TCR) and associated antigen presenting molecules. The first TCR transgenic mouse model was generated by Goverman and colleagues which recognized the I-A<sup>u</sup> restricted myelin basic protein (MBP) Ac1-11 peptide (Goverman et al., 1993; Lafaille et al., 1994). The MBP-specific TCR transgenic mice spontaneously developed neurological symptoms (~14 - 44%) under conventional housing but not in specific pathogen free (SPF) conditions (Goverman et al., 1993). Interestingly, the spontaneous EAE incidence reached 100% in the absence of regulatory T cells (Treg) and B cells in mice lacking functional RAG genes. Later, proteolipid protein (PLP) 139-151 specific TCR transgenic mice were developed which showed severe spontaneous EAE on the susceptible SJL/J background and remained healthy in resistant B10.S background (Waldner et al., 2000). Following this, a myelin oligodendrocyte glycoprotein (MOG) 35-55 specific TCR transgenic mouse in C57BL/6 background was generated which showed signs of isolated optic neuritis (>30%) and low grade EAE (4%) (Bettelli et al., 2003). While these spontaneous EAE models stressed the

important role of T cells in CNS autoimmunity, the role of other immune cells in particular B cells were not addressed in these models.

## 1.2. Triggers and pathogenic events in CNS autoimmunity

Many cellular players contribute to CNS autoimmunity. The ease with which myelin-specific CD4<sup>+</sup> T lymphocytes are isolated from rodents and humans as well as their ability to transfer EAE to naïve recipients suggests that CD4<sup>+</sup> T lymphocytes are the main culprits inducing CNS damage (Wekerle, 1993). Animal models that were used to mimic MS are predominately based on CD4<sup>+</sup> T cells. Numerous efforts were undertaken to define the effector phenotype of CD4<sup>+</sup> T cells, which alone can induce inflammation in the CNS. However, it became clear that all CD4<sup>+</sup> T cell-subsets, be it IFN- $\gamma$ -producing T<sub>H</sub>1 cells or IL-17-producing T<sub>H</sub>17 cells, are capable of mediating EAE in different settings (Domingues et al., 2010; Jäger et al., 2009). Nevertheless, MS lesions contain higher frequencies of CD8<sup>+</sup> than CD4<sup>+</sup> T lymphocytes (Babbe et al., 2000). Reports showed that myelin-specific CD8<sup>+</sup> T cells can also induce EAE (Ford and Evavold, 2005; Sun et al., 2001) and cytotoxic T cells are able to contribute to CNS pathology (Na et al., 2008; Saxena et al., 2008). The type II histological patterns of MS lesions as well as the presence of oligoclonal bands in the cerebrospinal fluid (CSF) of MS patients suggests, in addition to T cells, a contribution of B lymphocytes to the pathogenesis of the disease (Lucchinetti et al., 2000; Owens et al., 2006). Moreover, rituximab, a B cell-depleting monoclonal antibody, was effective in a subset of MS patients (Owens et al., 2006).

The central question, which remains still unanswered, is how the CNS autoimmune responses are initiated. For long time, pathogenic infections were suspected to be the triggers of MS. Among viral infections, human herpes virus 6 (HHV-6) and Epstein-Barr virus (EBV) were widely studied as initiators of the disease (Ascherio and Munch, 2000; Challoner et al., 1995). Similarly, bacterial pathogens such as *Chlamydia pneumoniae*, a Gram-negative intracellular bacterium, have been associated with MS, although the data is controversial (Sriram et al., 1999). However, none of the proposed infectious trigger has been definitively proven.

The overall rise in incidence of many autoimmune diseases including MS suggests a common causative environmental factor. The hygiene hypothesis states that the lack of childhood exposure to infections increases the susceptibility to autoimmune and allergic disorders (Bach, 2002; Okada et al., 2010). Emerging evidence from various autoimmune disease models suggests a role for resident gut microbiota in the pathogenesis of autoimmune diseases (Chervonsky, 2010). So far, there is no direct evidence implicating gut microbiota in triggering MS. The indirect evidence for a

role of gut microbiota stems from the fact that dietary factors (potent modulators of gut microbiota composition and function (David et al., 2014; Maslowski and Mackay, 2011)) like milk, animal fat and meat are positive influencers of MS incidence (Lauer, 1994, 1997). Interestingly, recent studies have linked MS incidence to lifestyle factors that have been shown to interfere with the establishment of healthy bacterial populations in the gastrointestinal tract, such as early-life antibiotics (Norgaard et al., 2011), formula feeding (Conradi et al., 2013), and caesarian sections (Maghzi et al., 2012). Although the role of gut microbiota was not directly investigated in these studies, these lifestyle factors may hurt the transmission of microbiota, likely leading to aberrations of the gut microbiota. Another interesting data showed that the MS disease course was milder in inflammatory bowel disease (IBD) patients, who are known to have an altered gut microbial profile (Zépher et al., 2013).

The potential involvement of gut microbiota in CNS autoimmunity came from work in the animal models of MS. Early studies using MBP-specific TCR transgenic mice showed that SPF mice (with a normal gut microbiota) were less prone to develop EAE than mice housed in a conventional, “dirty” facility (Goverman et al., 1993). However, a specific trigger has not been identified to date. Later studies using antibiotic treatments to reduce the gut bacterial load also showed that EAE severity is reduced in mice and rats (Ochoa-Repáraz et al., 2009; Wekerle et al., 2013; Yokote et al., 2008). Two recent studies suggested that the hallmark of westernized life style, “high salt” diet consumption led to severe EAE in mice (Kleinewietfeld et al., 2013; Wu et al., 2013), indirectly supporting a role for gut microbiota. Attempts to relate the influence of gut microbiota to the susceptibility of EAE by active immunization have yielded contradictory results. One group noted no difference between germ free (GF) and SPF mice (Lampropoulou et al., 2008) while a very recent report (Lee et al., 2011) found reduced EAE susceptibility in GF C57BL/6 mice. Obviously the use of CFA immunization will supersede a potential role of commensal microbiota. Spontaneous models sparing any artificial immunization will be superior in addressing these important questions in natural settings.

## 2. Questions

Although we have learned a lot about the immunopathogenesis of MS using induced EAE models, there remains a knowledge gap regarding the disease triggering mechanisms.

The central question of my work is:

### **What are the triggers of CNS autoimmunity?**

To answer this question, the following developments were made

- Generation of spontaneous EAE models (described in publications 1 & 2)
- Contribution of B cells to spontaneous EAE pathogenesis (described in publications 1 & 2)
- Cumulative autoimmunity (described in publication 3)
- Gut microbiota as a trigger of CNS autoimmunity (described in publication 4)

### 3. Results and discussion

#### 3.1. Spontaneous EAE models of MS

To investigate the triggering mechanisms of CNS autoimmunity, it is essential to use the animal model which develops spontaneous neuroinflammation at high frequency. We developed two new mouse models based on the transgenic expression of myelin antigen-specific T and B cell receptors. The first mouse model utilizes the TCR transgenic mice (2D2; TCR<sup>MOG</sup>) whose T cells recognize the MOG 35-55 peptide in the context of I-A<sup>b</sup> and express the rearranged TCR $\alpha$  and  $\beta$  chain from the pathogenic T cell clone obtained from immunized animals (Bettelli et al., 2003). A significant proportion (>30%) of these mice develop spontaneous optic neuritis without evidence of clinical or histological signs of EAE and around 4% of the mice developed spontaneous EAE at older age. B cell receptor (BCR) knock-in mice (IgH<sup>MOG</sup>) were produced by gene targeting of the rearranged heavy chain VDJ sequence from the MOG specific hybridoma 8.18-C5 to its natural locus (Litzenburger et al., 1998). This heavy chain recognizes the conformational epitope present in the extracellular portion of MOG. B cells in IgH<sup>MOG</sup> mice develop normally and secrete high titers of pathogenic antibodies. However, these mice never show autoimmunity, but enhanced kinetics of EAE after immunization was observed.

In an attempt to shed light on the involvement of myelin autoantigen specific T and B cells and their products in CNS autoimmunity, we crossed 2D2 mice with IgH<sup>MOG</sup> mice (Figure 1). Unexpectedly, we observed that a high proportion of these double-transgenic mice spontaneously developed severe EAE at young age. CNS inflammation in the double-transgenic mice was focused to spinal cord and optic nerve, leaving unaffected the brain and cerebellum, leading us to dub these animals as Opticospinal Encephalomyelitis (OSE) mice. The lesions presented severe demyelination and infiltration by inflammatory cells, predominantly macrophages and CD4<sup>+</sup> T cells, but also eosinophilic leukocytes (Krishnamoorthy et al., 2006) (**Publication 1**).

Spontaneous EAE in OSE mice takes a chronic-progressive course. This is not surprising, since it is known that C57BL/6 mice respond to active induction of EAE with chronic, not relapsing-remitting disease. In an attempt to develop an experimental model which would present spontaneous relapsing remitting disease, we used the SJL/J mouse strain, which is known to develop relapsing-remitting EAE following active immunization or passive transfer. We raised a highly encephalitogenic and MOG-specific SJL/J T cell clone which uses a TCR composed of V $\alpha$ 8.3/V $\beta$ 4 chains. We generated a transgenic SJL/J mouse expressing this MOG-specific TCR by



pronuclear injection. These animals developed spontaneous relapsing-remitting EAE, hence dubbed as RR mice (Figure 1).

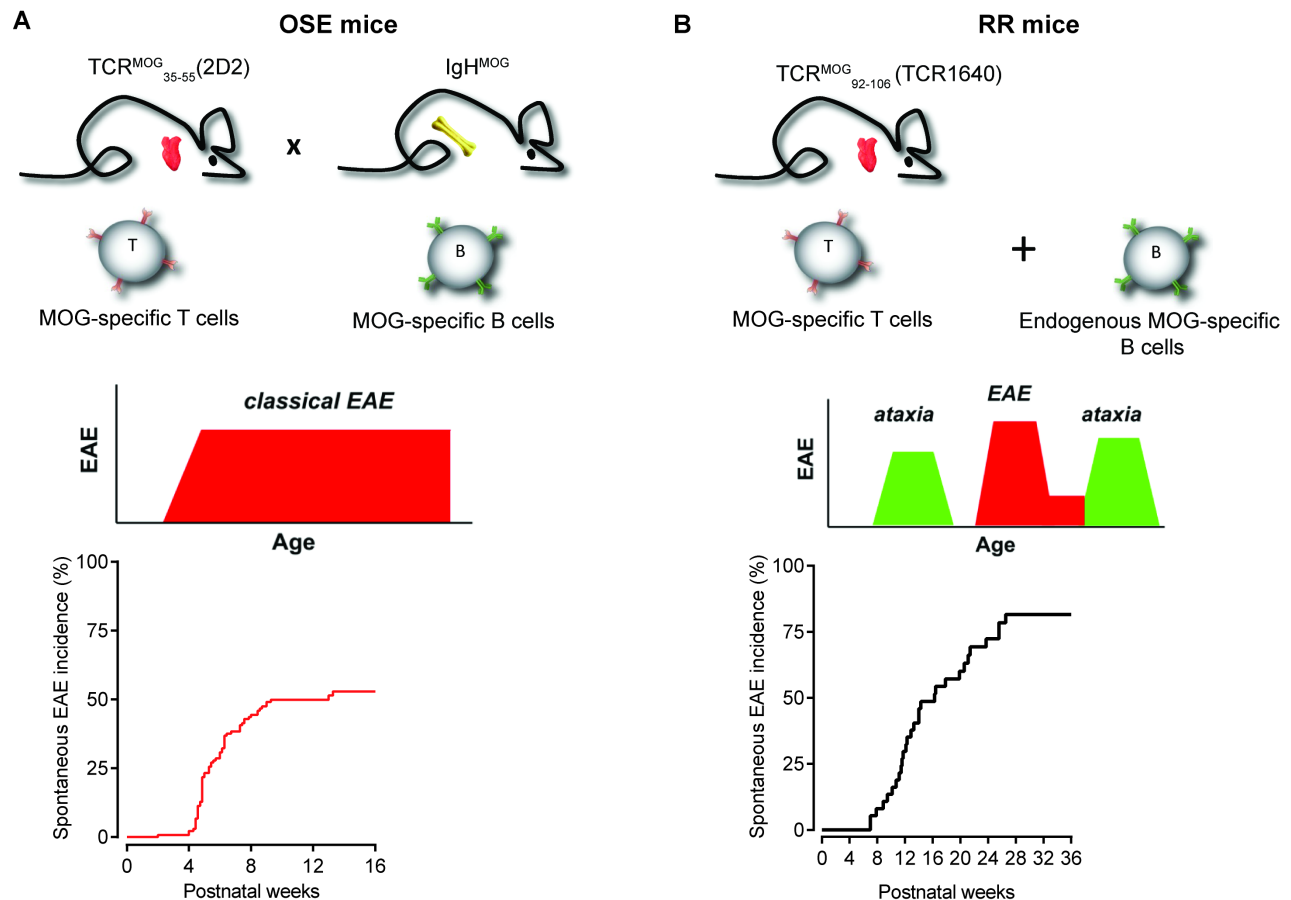


**Figure 1. Spontaneous EAE mouse models representing two distinct forms of human MS.**

A) OSE mice are double transgenic mice expressing MOG<sub>35-55</sub>-specific TCR and MOG-specific immunoglobulin heavy chain. The middle panel depicts that OSE mice develop classical EAE. The bottom panel shows the incidence of spontaneous EAE in OSE mice. B) Relapsing-remitting (RR) mice are TCR transgenic mice specific for MOG<sub>92-106</sub> peptide. MOG-specific T cells in these mice recruit endogenous MOG-specific B cells that produce demyelinating autoantibodies. The middle panel depicts that RR mice develop relapsing-remitting EAE with clinical episodes of ataxia and paralytic symptoms. The bottom panel shows the incidence of spontaneous EAE in RR mice. (Adapted from Krishnamoorthy, G et al J Clin Invest 2006 & Pöllinger, B et al J Exp Med 2009).

The large confluent demyelinating plaque-like lesions were located in the cerebellum and the spinal cord. Importantly, RR mouse lesions feature local immunoglobulin deposits along with activated complement complexes. This is remarkable, considering that the only change of these mice is the expression of transgenic TCR genes, resulting in an overrepresentation of MOG-specific T cells in their CD4<sup>+</sup> T cell repertoire. Consequently, the autoantibody-producing B cells must be recruited from the natural B cell repertoire. Evidence indicates that the selection, activation and differentiation of autoantibody-producing B cells takes place in germinal centers of the cervical lymph nodes, which are directly connected to the CNS via lymphatic vessels. The process of B cell recruitment is critically dependent on the presence of CNS-derived MOG autoantigen since the

MOG-specific antibodies were not present in the MOG-deficient RR mice (Pöllinger et al., 2009) **(Publication 2)**.

### 3.2. B cells in spontaneous EAE models

While the role of T cells has been extensively explored in EAE models, the role of B cells in the immunopathogenesis of EAE was not clear. B cells can serve as APCs, produce cytokines/chemokines or secrete antibodies. Especially our two spontaneous EAE mouse models, OSE mouse (Bettelli et al., 2006; Krishnamoorthy et al., 2006) and RR mouse (Pöllinger et al., 2009), highlight the importance of B cell functions in disease pathogenesis.

To explore the role of B cells in our mouse models, we cultured spleen cells from OSE mice with serially diluted concentrations of recombinant MOG protein. We found that MOG-specific B cells in OSE mice enhanced the activation of MOG-reactive T cells even at very low concentrations of MOG. This was due to their specific membrane receptors through which they can specifically capture and concentrate MOG and hence present it more efficiently to T cells. In this co-culture, we observed that both T and B cells proliferated vigorously and expressed activation markers such as CD25 and CD86, respectively. In sharp contrast, single transgenic T cells required more than 100 fold higher MOG protein amounts to exhibit a similar proliferation while B cells responded only weakly. The efficient presentation of MOG required conformational MOG since MOG-specific B cells were not as efficient to present the MOG 35-55 compared to MOG protein (Figure 2).

Since B cells can also produce autoantibodies, we measured MOG-specific antibodies in the serum of OSE mice. We found high titers of isotype switched MOG-specific IgG1 or IgG2a antibodies in the serum of both healthy and EAE affected OSE mice (Bettelli et al., 2006; Krishnamoorthy et al., 2006). In contrast, isotype switched antibodies were present in much lower concentrations in single transgenic IgH<sup>MOG</sup> mice, suggesting a T cell driven activation and subsequent isotype switching of MOG-specific B cells. However, we did not find a deposition of antibodies in the CNS lesions of EAE-affected OSE mice. Moreover, the onset of clinical symptoms did not affect the level or nature of MOG-specific antibodies. Finally, MOG-deficient OSE mice also harbored higher amounts of MOG-specific antibodies suggesting their generation occurred independently of MOG antigen (Figure 2). Collectively, the OSE mouse model supports the concept that B cells could act as efficient antigen presenting cells to initiate autoimmunity.

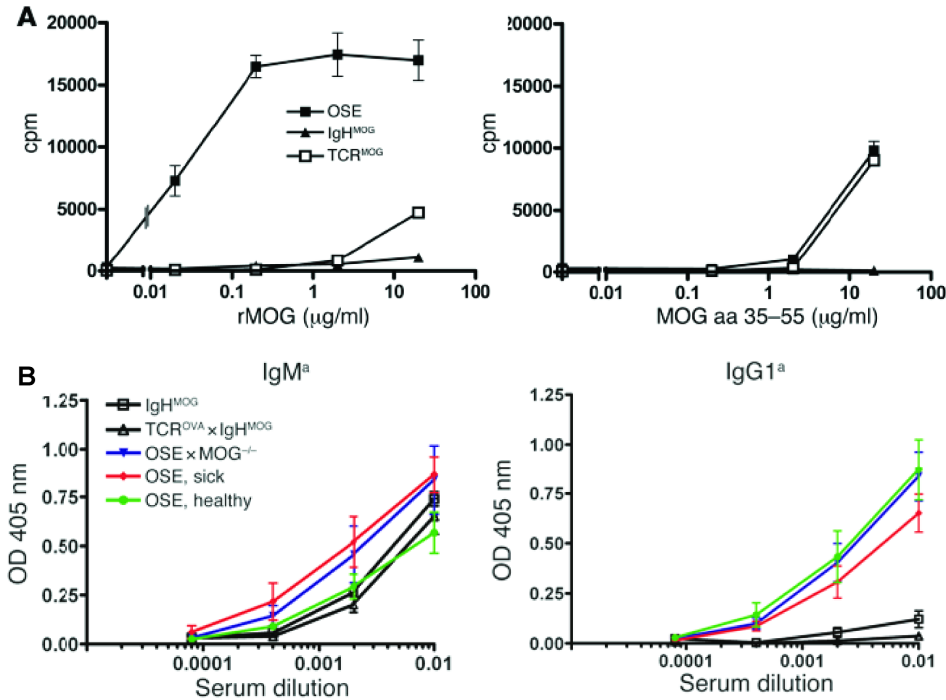


**Figure 2: Enhanced antigen presentation and autoantibody production in OSE mice.** A) Enhanced autoreactivity of lymphocytes from OSE mice to rMOG. Proliferation of splenocytes from OSE, TCR<sup>MOG</sup> single-transgenic and IgH<sup>MOG</sup> single-transgenic mice in response to increasing concentrations of rMOG and MOG<sub>35-55</sub> peptide. B) Relative concentrations of MOG-specific serum Ig antibodies. MOG-binding IgM<sup>a</sup> and IgG1<sup>a</sup> antibodies were detected by ELISA in serially diluted sera obtained from healthy and sick OSE, healthy IgH<sup>MOG</sup>, healthy TCR<sup>OVA</sup>xIgH<sup>MOG</sup> and healthy OSE x MOG<sup>-/-</sup> mice. Mean absorbance at OD405 nm is shown; error bars indicate SEM. (Adapted from Krishnamoorthy, G et al JCI 2006).

We performed similar antigen presentation assays in RR mice but failed to find appreciably higher antigen presentation capacity of B cells from RR mice compared to controls. Surprisingly, however, we found that RR mice spontaneously produced MOG-specific autoantibodies presumably due to the recruitment of MOG-reactive B cells from the endogenous B cell repertoire by activated T cells (Pöllinger et al., 2009). We also found extensive deposits of MOG-binding antibodies in the CNS lesions of RR mice, suggesting the importance of MOG-specific antibodies in the pathogenesis. The B cell response in RR mice was a specific response to MOG rather than a broad autoreactivity since we did not find antibodies against other autoantigens. The autoantibodies appeared in serum from 5 weeks of age, and persisted up to 6 months of age and started declining thereafter (Pöllinger et al., 2009). There is evidence that conformational epitope but not linear epitope binding autoantibodies are involved in EAE pathogenesis (von Büdingen et al., 2002). We tested the serum of RR mice on cell bound MOG and found that majority of these antibodies were indeed recognizing conformationally intact MOG expressed on the cell surface. We next performed experiments to test the pathogenic potential of these antibodies by injecting them along with low

dose PLP peptide immunization. We noted a significant aggravation of EAE in mice that received RR mouse serum compared to non-transgenic littermate serum recipients. To examine the importance of B cells, we performed B cell depletion experiments using anti-CD20 antibodies. B cell depletion had contrasting impact on spontaneous EAE depending upon the time point of depletion. While neonatal B cell depletion suppressed spontaneous EAE (Figure 3), adult B cell depletion increased EAE incidence. It can be concluded that while B cells are necessary for the efficient priming of T cells in early life, in adulthood B cells are important for its regulatory functions.

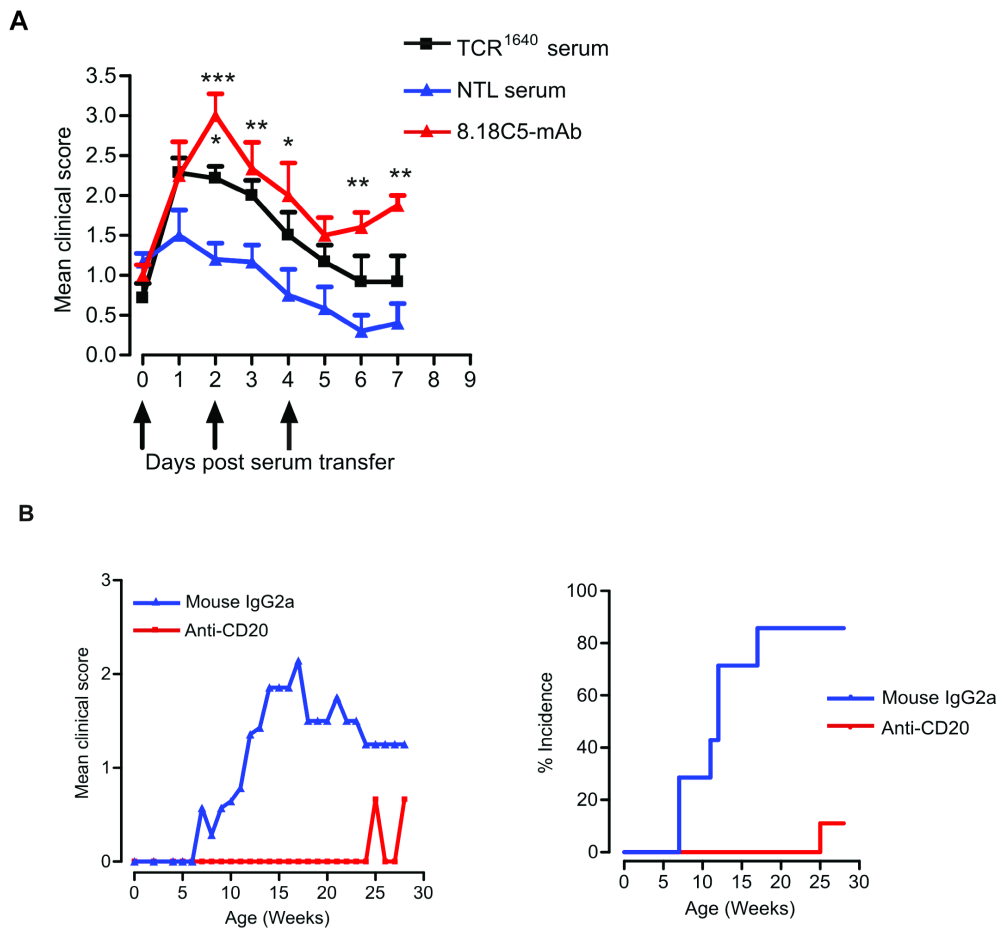


**Figure 3. B cells and anti-MOG antibodies are essential for spontaneous EAE in RR mice.**

A) Pathogenic potential of spontaneously developed MOG-specific autoantibodies were tested by transferring serum to WT SJL/J mice immunized with low-dose PLP<sub>139-151</sub>. Serum from TCR<sup>1640</sup> (RR) mice, NTL mice or control monoclonal 8.18c5 mAb were transferred after mice showed first clinical symptoms. Error bars indicate SEM. \*, P < 0.05; \*\*, P < 0.01; \*\*\*, P < 0.001. B) B cells were depleted from RR mice by twice weekly injections of anti-CD20 antibodies from day 3 after birth and control mice received mouse IgG2a antibodies. Although 85% of isotype control antibody-treated mice developed spontaneous EAE, treatment with CD20 antibodies protected RR mice from disease development. (Adapted from Pöllinger, B et al J Exp Med 2009).

Overall, our and other studies indicate a diverse role for B cells in MS. Unraveling the pathophysiological effects mediated by B cells and/or antibodies in patients is essential if we are to exploit these observations to develop new therapeutic strategies for MS, particularly in view of the clinical and mechanistic heterogeneity of the disease.

### 3.3. Cumulative autoimmunity

Molecular mimicry, a cross-reaction of autoaggressive T cells to pathogen-derived molecules, has been suggested as a mechanism by which tolerance against autoantigens can be broken (Fujinami et al., 1983; Oldstone, 1987). While studying the role of the autoantigen in spontaneous MOG-directed EAE, we bred the MOG-specific TCR transgenic 2D2 mice on a MOG-deficient background. Unexpectedly, we noted spontaneous EAE in MOG-deficient 2D2 mice with incidence and kinetics indistinguishable from their wild type counterparts (Krishnamoorthy et al., 2009). EAE in MOG-deficient 2D2 mice could have been due to several possibilities: aberrant expression of truncated protein, recruitment of endogenous TCR specific for other myelin antigen or 2D2 TCR cross reacting with another myelin autoantigen. Our western blot analysis ruled out any residual MOG protein in MOG knock out mice. The flow cytometry analysis also did not find endogenous TCR expression that is reactive to other myelin antigens.

After excluding incomplete ablation of MOG or an autoimmune attack by T cells from the residual endogenous repertoire as possible explanations, we probed the possibility that other CNS protein(s) could serve as an alternative autoantigen in the paradoxical EAE response. Using a purification strategy to separate the CNS proteins from MOG-deficient mice and subsequent in vitro recall assay with 2D2 T cells, we identified several fractions that efficiently activated 2D2 T cells. We performed mass spectrometry analysis of the 2D2 T cell activating fractions and identified the medium sized neurofilament (NF-M) as an alternative target for 2D2 T cells. An in silico search identified a seven amino acid peptide of NF-M that is nearly identical to the core region of the antigenic peptide MOG<sub>38-50</sub>. The dominant epitopes of MOG and NF-M shared several important TCR contact positions that contain the amino acids Arg41, Phe44, Arg46 and Val47, which are known to be the crucial contact amino acids for the 2D2 TCR and other MOG-specific T cell lines (Ben-Nun et al., 2006; Petersen et al., 2004). We confirmed the reactivity of 2D2 T cells to NF-M by using synthetic peptide and the recombinant NF-M protein (Figure 4). Interestingly, the cross-reactivity between NF-M and MOG-specific T cells is not a phenomenon unique to the transgenic TCR 2D2; we found this response pattern in a significant proportion of CD4<sup>+</sup> T cells selected for MOG-reactivity.

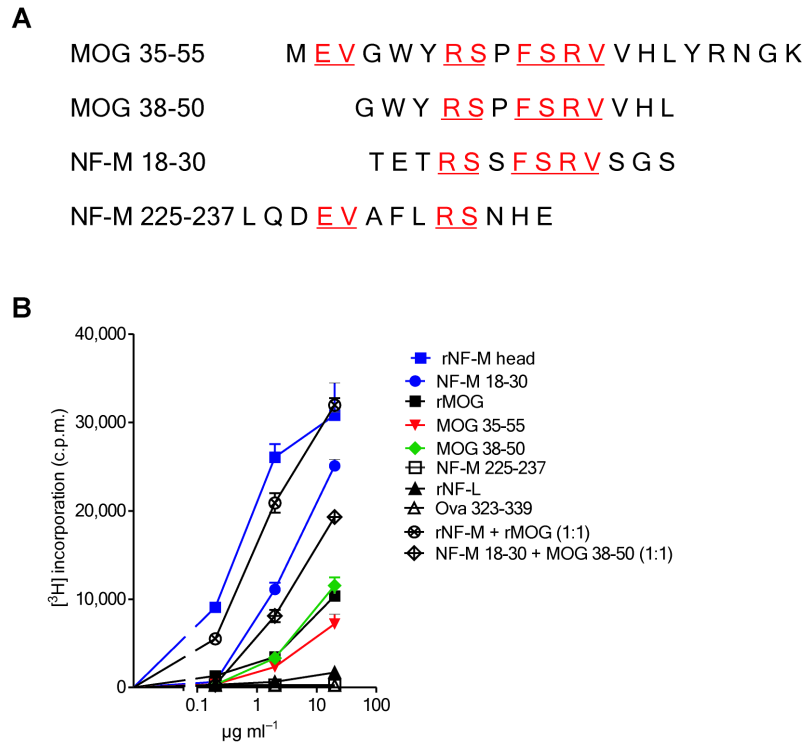


**Figure 4. Identification of a neuronal protein that cross-reacts with MOG-specific 2D2 T cells.**

A) Amino acid alignment of the immunodominant epitopes of MOG and NF-M. MOG<sub>35-55</sub> and the minimal epitope MOG<sub>38-50</sub> were aligned with NF-M. Shown in red and underlined is the amino acid identity of MOG and NF-M peptides. B) 2D2 splenocytes were cultured with increasing concentrations of the indicated proteins, peptides or mixtures and proliferation was measured by <sup>3</sup>H-thymidine incorporation assay. (Adapted from Krishnamoorthy, G et al Nat Med 2009)

To determine the *in vivo* recognition of NF-M by 2D2 T cells, we transferred activated 2D2 T cells into RAG<sup>-/-</sup> and RAG<sup>-/-</sup> x MOG<sup>-/-</sup> mice. Whereas both recipient groups developed EAE, in MOG-deficient Rag2<sup>-/-</sup> mice the disease was delayed. Similarly, NF-M-activated 2D2-expressing T cells also triggered EAE in WT hosts with the same incidence and kinetics as that of MOG-activated 2D2 T cells. Thus, we found the first example of immunological self-mimicry, i.e., the response of one T cell population against two target autoantigens in the same tissue, MOG and NF-M (Krishnamoorthy et al., 2009). We postulate that the combined response of a T cell clone against two independent autoantigens presented within the same target tissue initiates a particularly vigorous autoimmune attack. Such a cumulative autoimmune response may explain why the MOG epitope 35-55 elicits EAE in C57BL/6 mice, which otherwise are resistant against most other CNS autoantigens.

### 3.4. Gut Microbiota as a trigger of spontaneous CNS autoimmunity

While the triggering mechanisms of autoimmune diseases still remain an unanswered question, the overall rise in the incidence of many autoimmune diseases suggests a common causative environmental factor. The hygiene hypothesis states that the lack of childhood exposure to infections increases the susceptibility to autoimmune and allergic disorders (Bach, 2002; Okada et al., 2010). Emerging evidence from various autoimmune disease models suggests a role for the resident gut microbiota in the pathogenesis of autoimmune diseases (Chervonsky, 2010). So far, there is no direct evidence implicating gut microbiota in triggering MS. The indirect evidence for the role of gut microbiota stems from the fact that dietary factors (potent modulators of gut microbiota composition and function (David et al., 2014; Maslowski and Mackay, 2011)) like milk, animal fat and meat are positive influencers of MS incidence (Lauer, 1994, 1997).

Having distributed our RR mice to different pathogen-free facilities, we noted incidences of spontaneous EAE ranging between 35–90%, a variation, which could simply not be explained by varying “hygienic conditions”. To test the possible contribution of non-pathogenic commensal microbiota to EAE triggering, we re-derived RR mice into GF, devoid of commensal flora, conditions. Strikingly, we noted a complete protection from spontaneous RR EAE in GF mice compared to our normal SPF housed mice (Berer et al., 2011). Re-colonization of GF RR mice with regular flora from SPF mice promptly restored spontaneous EAE suggesting a vital role for commensal flora in disease induction (Figure 5).

Protection from EAE went along with a drastic reduction in the frequency of T<sub>H</sub>17 cells in the lamina propria and Peyer’s patches of GF mice suggesting a possible activation of MOG-specific T cells in the gut associated lymphoid tissue (GALT) (Berer et al., 2011). Indeed, CFSE labeled T cells transferred into SPF mice proliferated predominantly in the GALT, a response abolished after short-term antibiotic treatment. There is increasing evidence that the gut microbiota not only activates the pro-inflammatory effector T cells but also induces autoimmune disease suppressing regulatory T cells depending upon the presence of particular species. For example, segmented filamentous bacteria (SFB) predominantly induce pro-inflammatory T<sub>H</sub>1 and T<sub>H</sub>17 cells (Gaboriau-Routhiau et al., 2009; Ivanov et al., 2009) whereas clostridium species from both humans and mice induce regulatory T cells (Atarashi, 2011; Atarashi et al., 2013). However, mono-association of GF RR mice with SFB did not restore spontaneous EAE (Berer et al., 2011).

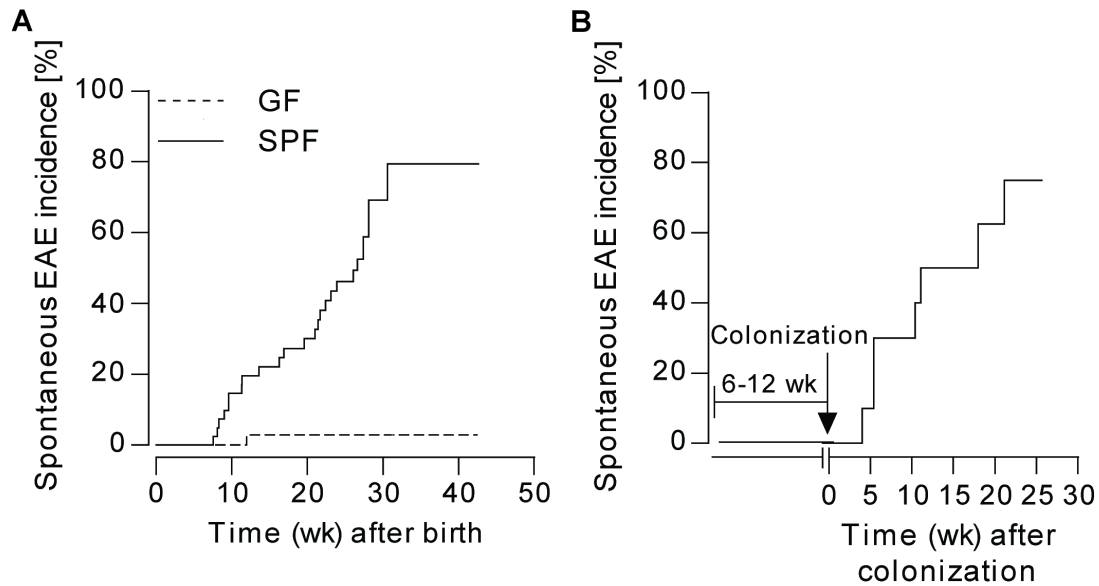


**Figure 5. Gut microbiota is required for spontaneous EAE development.**

A) Incidence of spontaneous EAE in a cohort of RR mice housed in germ-free (GF) or specific pathogen free (SPF) conditions. B) Incidence of spontaneous EAE in germ-free RR mice re-colonized with conventional flora from SPF mice. (Adapted from Berer, K et al Nature 2011))

Activation of MOG-specific T cells is necessary but not sufficient for full clinical EAE. MOG-specific B cells recruited from the native immune repertoire by T cells play an additional crucial role in the EAE development by producing demyelinating antibodies. In GF mice, in the absence of T cell activation, B cell recruitment was impaired, as reflected by reduced production of MOG-binding serum antibodies. Spontaneous production of anti-MOG antibodies also required the expression of MOG antigen in the CNS. RR mice deficient in MOG (RR x MOG<sup>-/-</sup>) failed to develop anti-MOG autoantibody titers despite their normal microbial status. We localized the recruitment of MOG-specific B cells to CNS draining lymph nodes by transferring GFP-labeled transgenic MOG-specific B cells. We found that MOG-specific B cells specifically accumulated in the germinal centers of cervical lymph nodes of SPF mice but not in any other peripheral lymph nodes. This migration was not seen in RR x MOG<sup>-/-</sup> recipients (Berer et al., 2011). Together, our work identifies a sequence of events triggering a spontaneous autoimmune demyelinating disease.



## 4. Summary

It is widely believed that autoimmune diseases arise due to the combination of several factors such as genetic susceptibility and environmental triggers. Epidemiological studies strongly suggest that allergic and autoimmune diseases are clearly on the rise in developed countries. But infectious agents show a complex relationship with autoimmunity. While lack of infection favours autoimmunity, infection can also precipitate autoimmunity (Bach, 2002);(Christensen, 2005). In the case of MS, there were numerous studies that show that immune cells, in particular T cells, play a major role in disease pathogenesis. However, there is a huge gap in understanding the triggers of autoimmune reactivity.

To understand **“What are the triggers of CNS autoimmunity?”** new spontaneous EAE mouse models were developed. These models differed in their clinical characteristics, pathology and pathogenesis. While in OSE mice B cells primarily served as antigen presenting cells, autoantibodies played a crucial role in the demyelination in RR mice. Also, these models led us to identify a novel phenomenon of autoimmune cross reactivity, i.e., self-molecular mimicry which we termed as “Cumulative autoimmunity”.

One of the most important uses of these models was to investigate the actual triggering mechanism of the CNS autoimmunity. Our studies identified that the commensal gut microbiota through modulating the immune functions triggered CNS autoimmune reactivity. Mechanistically, how the gut microbiota modulates autoimmune responses against the remote CNS is yet to be understood. The gut microbiota effects can be transmitted to remote organs through a) trafficking of adaptive and innate immune cells stimulated in the intestine b) transport of bacterial metabolites c) translocation of live bacteria due to impaired epithelial integrity. These are the potential lines of investigations in our future experiments.

## 5. References

- Ascherio, A., and Munch, M. (2000). Epstein-Barr virus and multiple sclerosis. *Epidemiology* *11*, 220-224.
- Ascherio, A., and Munger, K. (2008). Epidemiology of multiple sclerosis: from risk factors to prevention. *Semin Neurol* *28*, 17-28.
- Atarashi, K. (2011). Induction of colonic regulatory T cells by indigenous *Clostridium* species. *Science* *331*, 337-341.
- Atarashi, K., Tanoue, T., Oshima, K., Suda, W., Nagano, Y., Nishikawa, H., Fukuda, S., Saito, T., Narushima, S., Hase, K., *et al.* (2013). Treg induction by a rationally selected mixture of *Clostridia* strains from the human microbiota. *Nature* *500*, 232-236.
- Babbe, H., Roers, A., Waisman, A., Lassmann, H., Goebels, N., Hohlfeld, R., Friese, M., Schröder, R., Deckert, M., Schmidt, S., *et al.* (2000). Clonal expansion of CD8<sup>+</sup> T cells dominate the T cell infiltrate in active multiple sclerosis lesions shown by micromanipulation and single cell polymerase chain reaction. *J Exp Med* *192*, 393-404.
- Bach, J.F. (2002). The effect of infections on susceptibility to autoimmune and allergic diseases. *N Engl J Med* *347*, 911-920.
- Ben-Nun, A., Kerlero de Rosbo, N., Kaushansky, N., Eisenstein, M., Cohen, L., Kaye, J.F., and Mendel, I. (2006). Anatomy of T cell autoimmunity to myelin oligodendrocyte glycoprotein (MOG): Prime role of MOG44F in selection and control of MOG-reactive T cells in H-2<sup>b</sup> mice *Eur J Immunol* *36* 478-493.
- Berer, K., Mues, M., Koutroulos, M., Al Rasbi, Z., Boziki, M., Johner, C., Wekerle, H., and Krishnamoorthy, G. (2011). Commensal microbiota and myelin autoantigen cooperate to trigger autoimmune demyelination. *Nature* *479*, 538-541.
- Bettelli, E., Baeten, D., Jäger, A., Sobel, R.A., and Kuchroo, V.K. (2006). Myelin oligodendrocyte glycoprotein-specific T and B cells cooperate to induce a Devic-like disease in mice. *J Clin Invest* *116*, 2393-2402.
- Bettelli, E., Pagany, M., Weiner, H.L., Linington, C., Sobel, R.A., and Kuchroo, V.K. (2003). Myelin oligodendrocyte glycoprotein-specific T cell receptor transgenic mice develop spontaneous autoimmune optic neuritis. *J Exp Med* *197*, 1073-1081.
- Challoner, P.B., Smith, K.T., Parker, J.D., and *et al.* (1995). Plaque associated expression of human herpesvirus 6 in multiple sclerosis. *Proc Natl Acad Sci U S A* *92*, 7440-7444.
- Chervonsky, A.V. (2010). Influence of microbial environment on autoimmunity. *Nat Immunol* *11*, 28-35.
- Christensen, T. (2005). Association of human endogenous retroviruses with multiple sclerosis and possible interactions with herpes viruses. *RevMedVirol* *15*, 179-211.

Conradi, S., Malzahn, U., Paul, F., Quill, S., Harms, L., Then Bergh, F., Ditzenbach, A., Georgi, T., Heuschmann, P., and Rosche, B. (2013). Breastfeeding is associated with lower risk for multiple sclerosis. *Mult Scler* 19, 553-558.

David, L.A., Maurice, C.F., Carmody, R.N., Gootenberg, D.B., Button, J.E., Wolfe, B.E., Ling, A.V., Devlin, A.S., Varma, Y., Fischbach, M.A., *et al.* (2014). Diet rapidly and reproducibly alters the human gut microbiome. *Nature* 505, 559-563.

Domingues, H.S., Mues, M., Lassmann, H., Wekerle, H., and Krishnamoorthy, G. (2010). Functional and pathogenic differences of Th1 and Th17 cells in experimental autoimmune encephalomyelitis. *PLoS ONE* 5, e15531.

Ford, M.L., and Evavold, B.D. (2005). Specificity, magnitude, and kinetics of MOG-specific CD8<sup>+</sup> T cell responses during experimental autoimmune encephalomyelitis. *Eur J Immunol* 35 76-85.

Fujinami, R.S., Oldstone, M.B.A., Wroblewska, Z., Frankel, M.E., and Koprowski, H. (1983). Molecular mimicry in virus infection: Cross-reaction of measles virus phosphoprotein or of herpes simplex virus protein with human intermediate filaments. *Proc Natl Acad Sci U S A* 80, 2346-2350.

Gaboriau-Routhiau, V., Rakotobe, S., Lévuyet, E., Mulder, I., Lan, A., Bridonneau, C., Rochet, V., Pisi, A., De Paepe, M., Brandi, G., *et al.* (2009). The key role of segmented filamentous bacteria in the coordinated maturation of gut helper T cell responses. *Immunity* 31, 677-689.

Goverman, J., Woods, A., Larson, L., Weiner, L.P., Hood, L., and Zaller, D.M. (1993). Transgenic mice that express a myelin basic protein-specific T cell receptor develop spontaneous autoimmunity. *Cell* 72, 551-560.

Hauser, S.L., and Oksenberg, J.R. (2006). The neurobiology of multiple sclerosis: genes, inflammation, and neurodegeneration. *Neuron* 52, 61-76.

Ivanov, I.I., Atarashi, K., Manel, N., Brodie, F.L., Shima, T., Karaoz, U., Wei, D.G., Goldfarb, K.C., Santee, C.A., Lynch, S.V., *et al.* (2009). Induction of intestinal Th17 cells by segmented filamentous bacteria. *Cell* 139, 485-498.

Jäger, A., Dardalhon, V., Sobel, R.A., Bettelli, E., and Kuchroo, V.K. (2009). Th1, Th17, and Th9 effector cells induce experimental autoimmune encephalomyelitis with different pathological phenotypes. *J Immunol* 183, 7169-7177.

Kleinewietfeld, M., Manzel, A., Titze, J., Kvakana, H., Yosef, N., Linker, R.A., Muller, D.N., and Hafler, D.A. (2013). Sodium chloride drives autoimmune disease by the induction of pathogenic TH17 cells. *Nature* 496, 518-522.

Krishnamoorthy, G., Holz, A., and Wekerle, H. (2007). Experimental models of spontaneous autoimmune disease in the central nervous system. *J Mol Med* 85, 1161-1173.

Krishnamoorthy, G., Lassmann, H., Wekerle, H., and Holz, A. (2006). Spontaneous opticospinal encephalomyelitis in a double-transgenic mouse model of autoimmune T cell/B cell cooperation. *J Clin Invest* 116, 2385-2392.

Krishnamoorthy, G., Saxena, A., Mars, L.T., Domingues, H.S., Mentele, R., Ben-Nun, A., Lassmann, H., Dornmair, K., Kurschus, F.C., Liblau, R., *et al.* (2009). Myelin specific T cells also

recognize neuronal autoantigen in a transgenic mouse model of multiple sclerosis. *Nat Med* *15*, 626-632.

Lafaille, J.J., Nagashima, K., Katsuki, M., and Tonegawa, S. (1994). High incidence of spontaneous autoimmune encephalomyelitis in immunodeficient anti-myelin basic protein T cell receptor transgenic mice. *Cell* *78*, 399-408.

Lampropoulou, V., Hoehlig, K., Roch, T., Neves, P., Gómez, E.C., Sweenie, C.H., Hao, Y., Freitas, A.A., Steinhoff, U., Anderton, S.M., *et al.* (2008). TLR-activated B cells suppress T cell-mediated autoimmunity. *J Immunol* *180* 4763-4773.

Lauer, K. (1994). The risk of multiple sclerosis in the U.S.A. in relation to sociogeographic features: a factor-analytic study. *J Clin Epidemiol* *47*, 43-48.

Lauer, K. (1997). Diet and multiple sclerosis. *Neurology* *49*, S55-S61.

Lee, Y.K., Menezes, J.S., Umesaki, Y., and Mazmanian, S.K. (2011). Proinflammatory T-cell responses to gut microbiota promote experimental autoimmune encephalomyelitis. *Proc Natl Acad Sci U S A* *108*, 4615-4622.

Linthicum, D.S., Munoz, J.J., and Blaskett, A. (1982). Acute experimental autoimmune encephalomyelitis in mice. I. Adjuvant action of Bordetella pertussis is due to vasoactive amine sensitization and increased vascular permeability of the central nervous system. *Cell Immunol* *73*, 299-310.

Litzenburger, T., Fässler, R., Bauer, J., Lassmann, H., Linington, C., Wekerle, H., and Iglesias, A. (1998). B lymphocytes producing demyelinating autoantibodies: Development and function in gene-targeted transgenic mice. *J Exp Med* *188*, 169-180.

Lucchinetti, C.F., Brück, W., Parisi, J., Scheithauer, B., Rodriguez, M., and Lassmann, H. (2000). Heterogeneity of multiple sclerosis lesions: Implications for the pathogenesis of multiple sclerosis. *Ann Neurol* *47*, 707-717.

Maghzi, A.H., Etemadifar, M., Heshmat-Gahdarijani, K., Nonahal, S., Minagar, A., and Moradi, V. (2012). Cesarean delivery may increase the risk of multiple sclerosis. *Mult Scler* *18*, 468-471.

Maslowski, K.M., and Mackay, C.R. (2011). Diet, gut microbiota and immune responses. *Nat Immunol* *12*, 5-9.

Na, S.Y., Cao, Y., Toben, T., Nitschke, L., Stadelmann, C., Gold, R., Schimpl, A., and Hünig, T. (2008). Naïve CD8 T-cells initiate spontaneous autoimmunity to a sequestered model antigen of the central nervous system. *Brain* *131*, 2353-2365.

Norgaard, M., Nielsen, R.B., Jacobsen, J.B., Gradus, J.L., Stenager, E., Koch-Henriksen, N., Lash, T.L., and Sorensen, H.T. (2011). Use of penicillin and other antibiotics and risk of multiple sclerosis: A population-based case-control study. *Am J Epidemiol* *174*, 945-948.

Ochoa-Repáraz, J., Mielcarz, D.W., Ditrio, L.E., Burroughs, A.R., Foureau, D.M., Haque-Begum, S., and Kasper, L.H. (2009). Role of gut commensal microflora in the development of experimental autoimmune encephalomyelitis. *J Immunol* *183*, 6041-6050.

Okada, H., Kuhn, C., Feillet, H., and Bach, J.F. (2010). The 'hygiene hypothesis' for autoimmune and allergic diseases: an update. *Clin Exp Immunol* *160*, 1-9.

Oldstone, M.B.A. (1987). Molecular mimicry and autoimmune disease. *Cell* *50*, 819-820.

Owens, G.P., Bennett, J.L., Gilden, D.H., and Burgoon, M.P. (2006). The B cell response in multiple sclerosis. *Neurol Res* *28*, 236-244.

Petersen, T.R., Bettelli, E., Sidney, J., Sette, A., Kuchroo, V., and Bäckström, B.T. (2004). Characterization of MHC- and TCR-binding residues of the myelin oligodendrocyte glycoprotein 38-51 peptide. *Eur J Immunol* *34*, 165-173.

Pöllinger, B., Krishnamoorthy, G., Berer, K., Lassmann, H., Bösl, M., Dunn, R., Domingues, H.S., Holz, A., Kurschus, F.C., and Wekerle, H. (2009). Spontaneous relapsing-remitting EAE in the SJL/J mouse: MOG-reactive transgenic T cells recruit endogenous MOG-specific B cells. *J Exp Med* *206*, 1303-1316.

Pugliatti, M., Sotgiu, S., and Rosati, G. (2002). The worldwide prevalence of multiple sclerosis. *Clin Neurol Neurosurg* *104*, 182-191.

Sawcer, S., Hellenthal, G., Pirinen, M., Spencer, C.C.A., Patsopoulos, N.A., Moutsianas, L., Dilthey, A., Su, Z., Freeman, C., Hunt, S.E., *et al.* (2011). Genetic risk and a primary role for cell-mediated immune mechanisms in multiple sclerosis. *Nature* *476*, 214-219.

Saxena, A., Bauer, J., Scheikl, T., Zappulla, J., Audebert, M., Desbois, S., Waisman, A., Lassmann, H., Liblau, R.S., and Mars, L.T. (2008). Multiple sclerosis-like lesions induced by effector CD8 T cells recognizing a sequestered antigen on oligodendrocytes. *J Immunol* *181* 1617-1621

Sospedra, M., and Martin, R. (2005). Immunology of multiple sclerosis. *Annu Rev Immunol* *23*, 683-747.

Sriram, S., Stratton, C.W., Yao, S., Tharp, A., Ding, L., Bannan, J.D., and Mitchell, W.M. (1999). Chlamydia pneumoniae infection of the central nervous system in multiple sclerosis. *Ann Neurol* *46*, 6-14.

Sun, D., Whitaker, J.N., Huang, Z., Liu, D., Coleclough, C., Wekerle, H., and Raine, C.S. (2001). Myelin antigen-specific CD8+ T cells are encephalitogenic and produce severe disease in C57BL/6 mice. *J Immunol* *166*, 7579-7587.

von Büdingen, H.C., Hauser, S.L., Fuhrmann, A., Nabavi, C.B., Lee, J.I., and Genain, C.P. (2002). Molecular characterization of antibody specificities against myelin/oligodendrocyte glycoprotein in autoimmune demyelination. *Proc Natl Acad Sci U S A* *99*, 8207-8212.

Waldner, H., Whitters, M.J., Sobel, R.A., Collins, M., and Kuchroo, V.K. (2000). Fulminant spontaneous autoimmunity of the central nervous system in mice transgenic for the myelin proteolipid protein-specific T cell receptor. *Proc Natl Acad Sci U S A* *97* 3412-3417.

Wekerle, H. (1993). T-cell autoimmunity in the central nervous system. *Intervirol* *35*, 95-100.

Wekerle, H., Berer, K., and Krishnamoorthy, G. (2013). Remote control—triggering of brain autoimmune disease in the gut. *Curr Opin Immunol* *25*, 683-689.

Wekerle, H., Kojima, K., Lannes-Vieira, J., Lassmann, H., and Linington, C. (1994). Animal models. *Ann Neurol* 36 *Suppl*, S47-S53.

Wu, C., Yosef, N., Thalhamer, T., Zhu, C., Xiao, S., Kishi, Y., Regev, A., and Kuchroo, V.K. (2013). Induction of pathogenic TH17 cells by inducible salt-sensing kinase SGK1. *Nature* 496, 513-517.

Yokote, H., Miyake, S., Croxford, J.L., Oki, S., Mizusawa, H., and Yamamura, T. (2008). NKT cell-dependent amelioration of a mouse model of multiple sclerosis by altering gut flora. *Am J Pathol* 173, 1714-1723.

Zéphir, H., Gower-Rousseau, C., Salleron, J., Simon, A., Debouverie, M., Le Page, E., Bouhnik, Y., Lebrun-Frenay, C., Papeix, C., Vigneron, B., *et al.* (2013). Milder multiple sclerosis course in patients with concomitant inflammatory bowel disease. *Mult Scler* 20, 1135-1139.

## 6. Publications

# Publication 1



# Spontaneous opticospinal encephalomyelitis in a double-transgenic mouse model of autoimmune T cell/B cell cooperation

Gurumoorthy Krishnamoorthy,<sup>1</sup> Hans Lassmann,<sup>2</sup> Hartmut Wekerle,<sup>1</sup> and Andreas Holz<sup>1</sup>

<sup>1</sup>Department of Neuroimmunology, Max Planck Institute for Neurobiology, Martinsried, Germany. <sup>2</sup>Division of Neuroimmunology, Center for Brain Research, Medical University of Vienna, Vienna, Austria.

We describe a double-transgenic mouse strain (opticospinal EAE [OSE] mouse) that spontaneously develops an EAE-like neurological syndrome closely resembling a human variant of multiple sclerosis, Devic disease (also called neuromyelitis optica). Like in Devic disease, the inflammatory, demyelinating lesions were located in the optic nerve and spinal cord, sparing brain and cerebellum, and the murine lesions showed histological similarity with their human correlates. OSE mice have recombination-competent immune cells expressing a TCR- $\alpha\beta$  specific for myelin oligodendrocyte glycoprotein (MOG) aa 35–55 peptide in the context of I-A<sup>b</sup> along with an IgJ region replaced by the recombined heavy chain of a monoclonal antibody binding to a conformational epitope on MOG. OSE mouse B cells bound even high dilutions of recombinant MOG, but not MOG peptide, and processed and presented it to autologous T cells. In addition, in OSE mice, but not in single-transgenic parental mice, anti-MOG antibodies were switched from IgM to IgG1.

## Introduction

MS is the most important demyelinating disease in the northern hemisphere. It arises without known trigger and either progresses in isolated bouts or worsens steadily from the very beginning. In the classical form of MS the demyelinating plaques are spread throughout the CNS. Usually the plaques appear in certain preferred locations, such as around the periventricular areas, but there are also variants in which the disease is limited to individual regions of the CNS. In Devic disease, for example, the lesions are restricted to the optic nerve and the spinal cord, sparing the cerebrum and the cerebellum (1). MS and its subgroups also have distinct histological patterns of pathological changes (2).

The factors determining onset, course, distribution, and cellular composition of autoimmune lesions in MS are largely unknown. In particular, it is unclear which processes are involved in triggering the onset of the disease and which drive inflammation during the further course of the disorder. While some investigators link the trigger(s) of MS to microbial infection (3), the opposite has been proposed as well, namely that the propensity to autoimmune disorders is related to the decreasing prevalence of infections (4). Our ignorance of these vital issues is largely due to the lack of suitable experimental models that would develop human CNS disease spontaneously and reproduce its essential clinical and structural aspects.

Here we describe a double-transgenic mouse strain that may fill this gap. These animals spontaneously developed a neurological condition that strikingly resembled the Devic variant of human MS. The majority of these opticospinal EAE (OSE) mice had a paralytic disease caused by inflammatory demyelinating

lesions in the spinal cord and the optic nerve. The causative CNS lesions, again much like human Devic lesions, sometimes contained a high proportion of eosinophilic leukocytes besides T cells and macrophages.

## Results

*Spontaneous EAE-like disease in OSE double-transgenic mice.* Myelin oligodendrocyte glycoprotein-specific (MOG-specific) TCR transgenic mice on a C57BL/6 background (TCR<sup>MOG</sup> mice; also referred to as 2D2 mice; ref. 5) express a transgenic TCR recognizing MOG aa 35–55 peptide in the context of I-A<sup>b</sup> on most CD4<sup>+</sup> T cells. TCR<sup>MOG</sup> transgenic animals rarely have classic EAE, although a major proportion of the older ones develop optic neuritis. MOG-specific Ig heavy-chain knock-in mice on a C57BL/6 background (IgH<sup>MOG</sup> mice; also referred to as Th mice) contain B lymphocytes that produce antibodies with the heavy chain of a demyelinating MOG-specific antibody (8.18C5) (6, 7). Despite high titers of pathogenic serum antibodies, the spontaneous development of autoimmunity has not previously been observed (8).

TCR<sup>MOG</sup> and IgH<sup>MOG</sup> single-transgenic animals were crossed, both on a C57BL/6 background. EAE-like signs (a disease score of at least 3; see Methods) were observed in 51% of the mice kept under specific pathogen-free (SPF) conditions (Figure 1) and in 46% of mice housed under conventional conditions (Supplemental Figure 1; supplemental material available online with this article; doi:10.1172/JCI28330DS1). All single-transgenic littermates remained healthy throughout the 12-week observation period (Figure 1). The mean maximum disease score among TCR<sup>MOG</sup> × IgH<sup>MOG</sup> double-transgenic animals, termed OSE (opticospinal EAE) mice, was 3.4 ± 1.2 with a mean onset at 6.1 ± 2.0 postnatal weeks. Female and male OSE mice developed EAE-like disease at similar rates (Figure 1). Neurological disease followed a chronic course with no marked remissions, and disease onset in the mice coincided with substantial weight loss (see Supplemental Figure 2).

There was no spontaneous EAE in F1 crosses of IgH<sup>MOG</sup> mice with OVA-specific TCR transgenic mice on a C57BL/6 background

**Nonstandard abbreviations used:** FACS, fluorescence-activated cell sorting; IgH<sup>MOG</sup> mice, MOG-specific Ig heavy-chain knock-in mice on a C57BL/6 background; MBP, myelin basic protein; MOG, myelin oligodendrocyte glycoprotein; OSE, opticospinal EAE; rMOG, recombinant MOG aa 1–125; SPF, specific pathogen-free; TCR<sup>MOG</sup> mice, MOG-specific TCR transgenic mice on a C57BL/6 background; TCR<sup>OVA</sup> mice, OVA-specific TCR transgenic mice on a C57BL/6 background.

**Conflict of interest:** The authors have declared that no conflict of interest exists.

**Citation for this article:** *J. Clin. Invest.* 116:2385–2392 (2006). doi:10.1172/JCI28330.



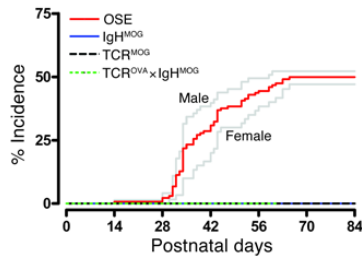


**Figure 1**

Spontaneous EAE-like disease in  $\text{TCR}^{\text{MOG}} \times \text{IgH}^{\text{MOG}}$  double-transgenic (OSE) mice. Spontaneous incidence after birth of severe EAE-like disease (clinical score  $\geq 3$ ) was observed in double-transgenic mice housed under SPF conditions (red line;  $n = 133$ , 60 females and 73 males). Single-transgenic littermates ( $\text{IgH}^{\text{MOG}}$ ,  $n = 69$ ;  $\text{TCR}^{\text{MOG}}$ ,  $n = 34$ ) and  $\text{TCR}^{\text{OVA}} \times \text{IgH}^{\text{MOG}}$  double-transgenic mice ( $n = 11$ ) remained free of clinical signs during the observation period. Gray lines show disease incidence for male and female OSE mice. The difference in the disease kinetics between sexes was not statistically significant ( $P = 0.2263$ ).

( $\text{TCR}^{\text{OVA}}$  mice, also referred to as OT-II mice) specific for OVA aa 323–339 (9) (Figure 1) nor in OSE mice lacking MOG antigen ( $\text{MOG}^{-/-}$  mice; ref. 10; data not shown).

**The pathological CNS lesion.** In OSE mice with spontaneous EAE kept under conventional conditions, CNS lesions were located almost exclusively in the optic nerve and in the spinal cord (Figure 2). The lesions were circumscribed rather than diffuse and were characterized by massive infiltration of inflammatory cells along with profound demyelination and moderate axonal loss. In sharp contrast, inflammation in the spinal cords and optic nerves in  $\text{TCR}^{\text{MOG}}$  and  $\text{IgH}^{\text{MOG}}$  single-transgenic littermates of

the same age was sparse or absent. Only in exceptional animals was it associated with some perivascular tissue damage. Healthy OSE mice showed only sparse inflammatory infiltrates in the CNS (Supplemental Figure 3).

The inflammatory infiltrates were dominated by mononuclear cells (Figure 2). Immunocytochemistry identified macrophages and  $\text{CD4}^+$  T cells, but only very few  $\text{B220}^+$  B cells or  $\text{CD8}^+$  T cells (Figure 2, L–O), in the optic nerve and the spinal cord. It is noteworthy that using the same antibody staining of the brain did not reveal immunoreactivity. In addition, some actively demyelinating lesions contained abundant eosinophilic granulocytes.

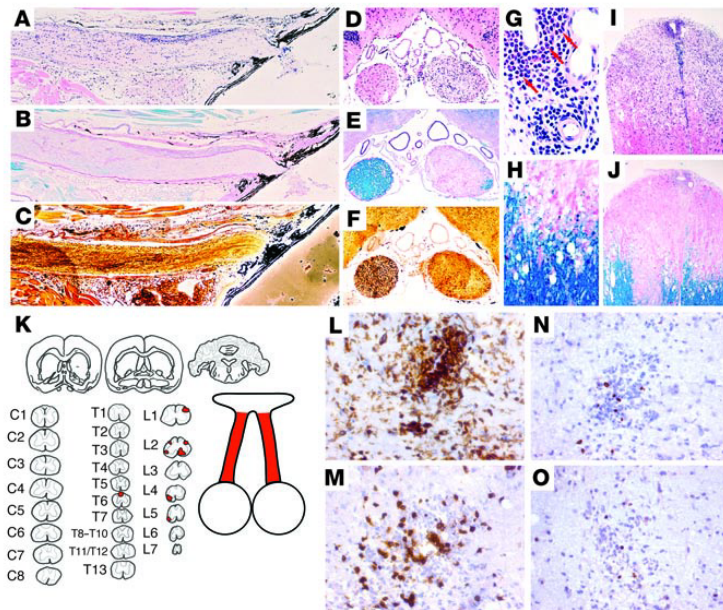
Double-transgenic mice that were kept under SPF conditions also showed profound inflammatory demyelination in their optic nerves and spinal cords. In addition, SPF-bred animals exhibited extensive inflammation that formed thick mononuclear infiltrates in the meninges and perivascular spaces. Demyelination was associated with mononuclear cell infiltration of the tissue, but eosinophilic granulocytes were generally absent (Supplemental Figure 4).

**Activation of CNS-infiltrating  $\text{CD4}^+$  T cells.** In contrast to healthy  $\text{TCR}^{\text{MOG}}$  and  $\text{IgH}^{\text{MOG}}$  single-transgenic animals, which yielded only very few inflammatory cells, large numbers of inflammatory cells were recovered from the spinal cords of sick OSE mice. Percoll gradient-separated infiltrate cells were predominantly  $\text{CD4}^+\text{CD3}^+$  T lymphocytes, along with a  $\text{CD11b}^+$  macrophage/monocyte component (Figure 3). The  $\text{CD4}^+$  T cells were stained by antibodies directed against  $\text{V}\alpha 3.2$  and  $\text{V}\beta 11$  (Figure 3F), the V region specificities of the transgenic  $\text{TCR}^{\text{MOG}}$  mouse.

Of note,  $\text{CD4}^+\text{CD3}^+$  T lymphocytes from the CNS of sick OSE mice showed a highly activated phenotype indicated by the markers  $\text{CD69}$  and  $\text{CD25}$  (Figure 3D) as well as  $\text{CD44}$  (data not shown). In contrast,  $\text{CD3}$  and  $\text{CD62L}$  (data not shown) were partly down-regulated. Splenic T cells from the same sick OSE animals were not activated (Figure 3B).

**Figure 2**

Histological analysis of the CNS from sick OSE mice. (A–J and L–O) The optic nerves (A–F) and spinal cords (G–J and L–O) from OSE mice that developed neurological disease in a non-SPF environment showed severe infiltration, demyelination, and axonal damage as visualized by H&E (A, D, G, and I), luxol fast blue (B, E, H, and J), and Bielschowsky silver impregnation (C and F). Arrows in G indicate eosinophilic granulocytes. (K) Demyelinating lesions (red shading) were specifically localized in the optic nerves and spinal cords of OSE mice, thus resembling the lesion distribution observed in human Devic disease. Cervical sections are labeled C1–C8; thoracic sections are labeled T1–T13; lumbar sections of the spinal cord are labeled L1–L7. (L–O) Cellular infiltrates were predominantly composed of  $\text{CD11b}^+$  macrophages/microglia (L) and  $\text{CD4}^+$  T cells (M), while only few  $\text{CD8}^+$  T (N) and B cells (O) were found exclusively in the optic nerves and spinal cords of sick mice. Note that healthy OSE littermates remained free of demyelinating CNS lesions (see Supplemental Figure 3). Furthermore, OSE mice housed under SPF conditions showed slightly stronger infiltration/demyelination (see Supplemental Figure 4).



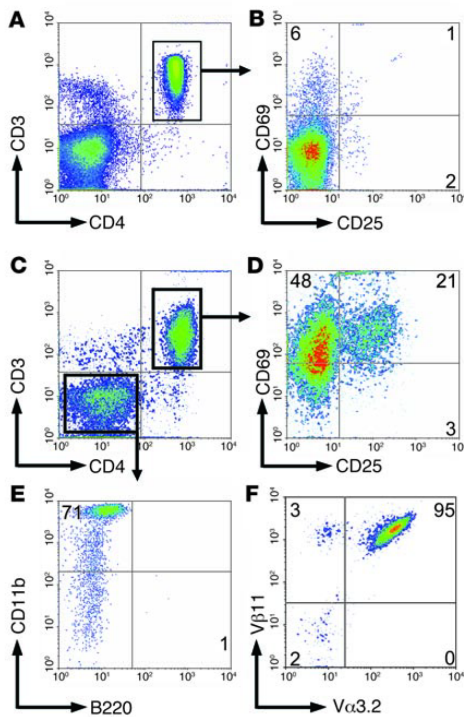


**Figure 3**

Activated pathogenic CD4<sup>+</sup> T cells infiltrate the spinal cord of OSE mice. (A–D) Living splenocytes (A and B) and CNS mononuclear cells (C and D) isolated by Percoll gradient centrifugation from a sick OSE mouse were stained with CD4 and CD3 (A and C), and CD25 and CD69 expression was analyzed among gated CD4<sup>+</sup>CD3<sup>+</sup> double-positive T cells (B and D). (E) Gated CD4<sup>−</sup>CD3<sup>−</sup> CNS cells were stained with anti-CD11b and anti-B220 in a separate reaction. (F) CD4<sup>+</sup>CD3<sup>+</sup> T cells infiltrating the CNS of sick OSE mice predominantly expressed the pathogenic TCR composed of V $\alpha$ 3.2 and V $\beta$ 11 chains. Numbers indicate the percentage of stained cells in the respective quadrant. Flow cytometric data are representative of 7 sick OSE animals analyzed in 4 independent experiments.

of 0.02  $\mu$ g/ml caused massive proliferation of double-transgenic splenocytes, while TCR<sup>MOG</sup> single-transgenic cells required more than 100-fold protein concentrations. IgH<sup>MOG</sup> single-transgenic splenocytes scarcely or only weakly responded to rMOG, even at high concentrations (Figure 5A).

In sharp contrast, the immunodominant peptide MOG aa 35–55 was recognized equally by OSE and single-transgenic TCR<sup>MOG</sup> mice (Figure 5B). Both required relatively high peptide concentrations for measurable activation, whereas spleen cells from single-transgenic IgH<sup>MOG</sup> mice completely failed to respond to MOG aa 35–55.

In an initial attempt to elucidate the relative contribution of MOG-reactive T and B cells to the enhanced reactivity of OSE spleen cells, single-transgenic IgH<sup>MOG</sup> splenocytes were mixed with cells from single-transgenic TCR<sup>MOG</sup> spleens. The combination of both single-transgenic populations potentiated rMOG reactivity (see Supplemental Figure 5A). A similar supra-additive effect was produced by combining B and T cells purified (>90% by fluorescence-activated cell sorting [FACS] analysis) from single-transgenic TCR<sup>MOG</sup> and IgH<sup>MOG</sup> spleens. Figure 5C shows that the combination of MOG-reactive T and B cells from single-transgenic TCR<sup>MOG</sup> and IgH<sup>MOG</sup> mice fully reproduced the high reactivity of unseparated double-transgenic OSE mouse splenocytes. In contrast, transgenic T cells from TCR<sup>MOG</sup> mice combined with nontransgenic B cells and transgenic B cells from IgH<sup>MOG</sup> mice together with nontransgenic T cells showed comparable proliferative responses (Figure 5C). Finally, the mixing of highly purified transgenic T and B cells from OSE mice restored the enhanced proliferative kinetics of unseparated OSE splenocytes (Supplemental Figure 5B).

The contribution of transgenic T or B lymphocytes to the proliferative response of rMOG was determined by labeling OSE splenocytes with CFSE and exposing them to optimal antigen doses in vitro. Both T and B cells were driven to proliferate (Figure 5D). In

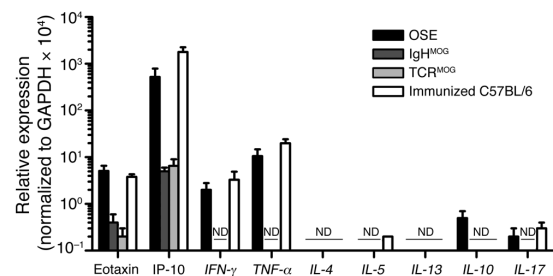
**Cytokine and chemokine expression in CNS lesions.** Quantitative real-time PCR was used to compare the transcription of cytokines and chemokines in the spinal cords of OSE animals with spontaneous EAE and WT C57BL/6 mice with actively induced EAE. Both profiles were almost identical. The cytokine genes *IFN- $\gamma$*  and *TNF- $\alpha$*  were substantially enhanced, while *IL-4*, *IL-5*, *IL-10*, *IL-13*, and *IL-17* transcripts remained practically undetectable (Figure 4). In healthy single-transgenic TCR<sup>MOG</sup> and IgH<sup>MOG</sup> littermates, none of these transcripts were found.

The chemokines IP-10 and eotaxin were transcribed at similar high levels in sick OSE animals and C57BL/6 mice with MOG aa 35–55-induced EAE (Figure 4).

**Enhanced anti-MOG response and cytokine production by lymphocytes from OSE mice.** Spleen cells from OSE mice responded to recombinant MOG aa 1–125 (rMOG) much more efficiently than did TCR<sup>MOG</sup> single-transgenic control cells (Figure 5A). Antigen doses

**Figure 4**

Cytokine milieu in the spinal cords of sick OSE mice. Relative expression level of various cytokine and chemokine genes was assessed by quantitative PCR in the spinal cords of sick OSE mice ( $n = 5$ ; clinical score  $\geq 3$ ), healthy IgH<sup>MOG</sup> mice ( $n = 3$ ), healthy TCR<sup>MOG</sup> mice ( $n = 3$ ), and C57BL/6 mice immunized with MOG aa 35–55 ( $n = 3$ ; clinical score  $\geq 3$ ). Error bars represent SEM from the measurement of individual animals within each experimental group. ND, no gene expression was detectable.



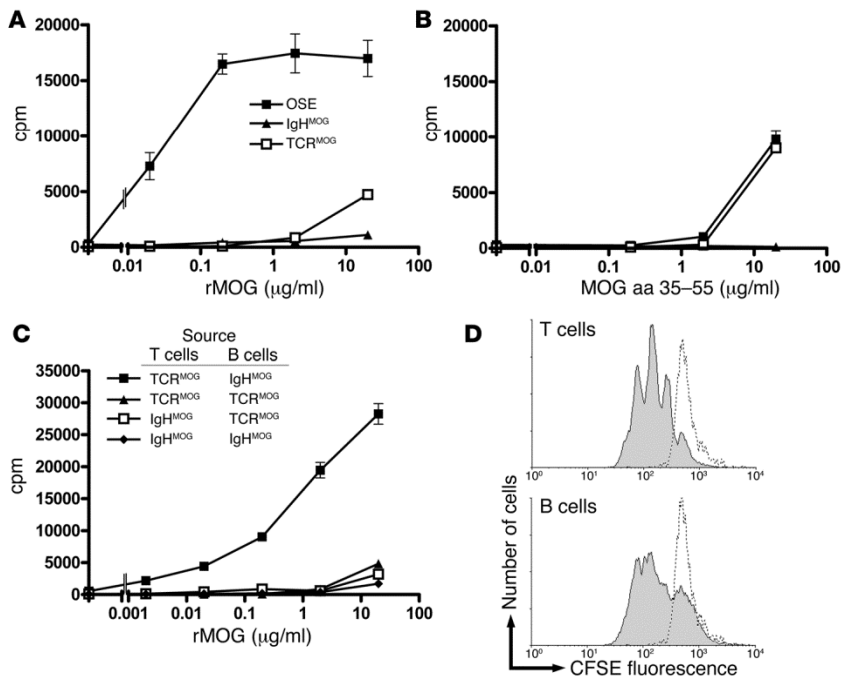


**Figure 5** Enhanced autoreactivity of lymphocytes from OSE mice to rMOG. (A and B) Proliferation of splenocytes from OSE, TCR<sup>MOG</sup> single-transgenic, and IgH<sup>MOG</sup> single-transgenic mice in response to increasing concentrations of (A) rMOG and (B) MOG aa 35–55 peptide. (C) Proliferation of CD4<sup>+</sup> T cells and B cells isolated from IgH<sup>MOG</sup> and TCR<sup>MOG</sup> single-transgenic mice that were combined as indicated after their purification (>90% purity) and stimulated with increasing amounts of rMOG. Note that the combination of MOG-reactive T and B cells caused a substantial increase in proliferation in response to rMOG, comparable to that of OSE splenocytes. (D) Splenocytes from an OSE mouse were labeled with CFSE and stimulated with optimal concentrations of rMOG in vitro. The dilution of cellular CFSE due to proliferation of live-gated CD4<sup>+</sup>CD3<sup>+</sup> T lymphocytes (top) and live-gated CD19<sup>+</sup> B lymphocytes (bottom) is shown. Splenocytes that remained without stimulus are represented by dotted lines. In A–C, each data point was run in triplicate, and error bars indicate SEM. Experiments in A and B were replicated on multiple occasions (>10), those in C and D were repeated twice.

addition, both responding lymphocyte populations were activated. T cells expressed CD25, and B cells CD86, as activation markers (Supplemental Figure 6).

The cytokines secreted by MOG-stimulated splenocytes from OSE mice in vitro were measured by ELISA. Predominantly, the cytokines IL-2, IFN- $\gamma$ , and IL-17 (albeit to a lesser extent) were released from OSE and TCR<sup>MOG</sup> T cells in the dose-response pattern previously found in proliferation assays. In contrast, IL-4 was only marginally detectable in the supernatants, while low levels of IL-5 were seen in responding OSE but not TCR<sup>MOG</sup> T cell cultures (Figure 6A). While stimulation with high doses of MOG aa 35–55 peptide released IL-2, IFN- $\gamma$ , IL-17, and IL-5 cytokines from OSE splenocytes, low peptide doses did not trigger any detectable cytokine secretion (Figure 6B).

**Production of anti-MOG autoantibodies.** OSE mice, either with or without EAE, did not visibly differ in absolute number and cellular composition of splenocytes (Supplemental Table 1) or in cellular function (data not shown). In particular, the capability of MOG-specific transgenic B cells to bind rMOG was unaltered during disease onset and progression. Finally, the proliferation

kinetics and expression of T and B cell activation markers as well as the quantity and quality of cytokines secreted by transgenic splenocytes in response to rMOG remained unaffected by the clinical status of OSE animals (our unpublished observations).

However, OSE mice differed strikingly from age-matched single-transgenic IgH<sup>MOG</sup> or double-transgenic TCR<sup>OVA</sup> $\times$ IgH<sup>MOG</sup> mice by their high titers of the IgG1 isotype of anti-MOG autoantibody (Figure 7). While TCR<sup>MOG</sup> single-transgenic mice did not spontaneously develop any anti-MOG antibodies (Supplemental Figure 7), most of the anti-MOG autoantibodies in single-transgenic IgH<sup>MOG</sup> and in TCR<sup>OVA</sup> $\times$ IgH<sup>MOG</sup> mice were IgM.

The onset of clinical EAE did not affect the level or nature of anti-MOG IgG1 antibodies (Figure 7). Furthermore, longitudinal studies of individual OSE mice showed constant amounts of MOG-specific IgM, IgG1, and IgG2 antibodies (see Supplemental Figure 7). Finally, OSE mice that lacked MOG antigen (i.e., triple-transgenic TCR<sup>MOG</sup> $\times$ IgH<sup>MOG</sup> $\times$ MOG<sup>-/-</sup> animals) exhibited increased amounts of anti-MOG IgG1 serum antibodies, indicating that their generation occurred independently of MOG antigen (Figure 7).

## Discussion

The OSE double-transgenic mouse EAE model described here stands out in several respects. The inflammatory demyelinating disease developed spontaneously, it resulted from pathogenic interaction between myelin autoimmune T and B cells, and the distribution and cellular composition of its lesions resembled that of Devic disease, a variant of human MS.

Spontaneously developing organ-specific autoimmune disease models in rodents are rare. Most notably, the NOD mouse develops type 1 diabetes mellitus at variable frequency within 40 weeks (4). Spontaneous autoimmune disease was also reported in the CNS. Spontaneous EAE was seen in transgenic mice with a TCR specific for myelin basic protein (MBP) in the context of I-A<sup>b</sup> (11, 12) at low frequency: <15% under conventional and 0% under SPF conditions (11). Higher frequencies were observed in the absence of regulatory lymphocytes in double-transgenic MBP-specific TCR transgenic mice on a B10.PL background (TCR<sup>MBP</sup>) crossed with recombinase activating gene-deficient mice (TCR<sup>MBP</sup> $\times$ RAG<sup>-/-</sup> mice; ref. 12). Of interest, these transgenic mice, very similar to our double-transgenic model, showed activated antigen-specific T cells only in the CNS that remained undetectable in peripheral organs (12).

OSE mice developed the disease at rates of about 50% within the first 10 weeks of age, although neither of the 2 parental T and B

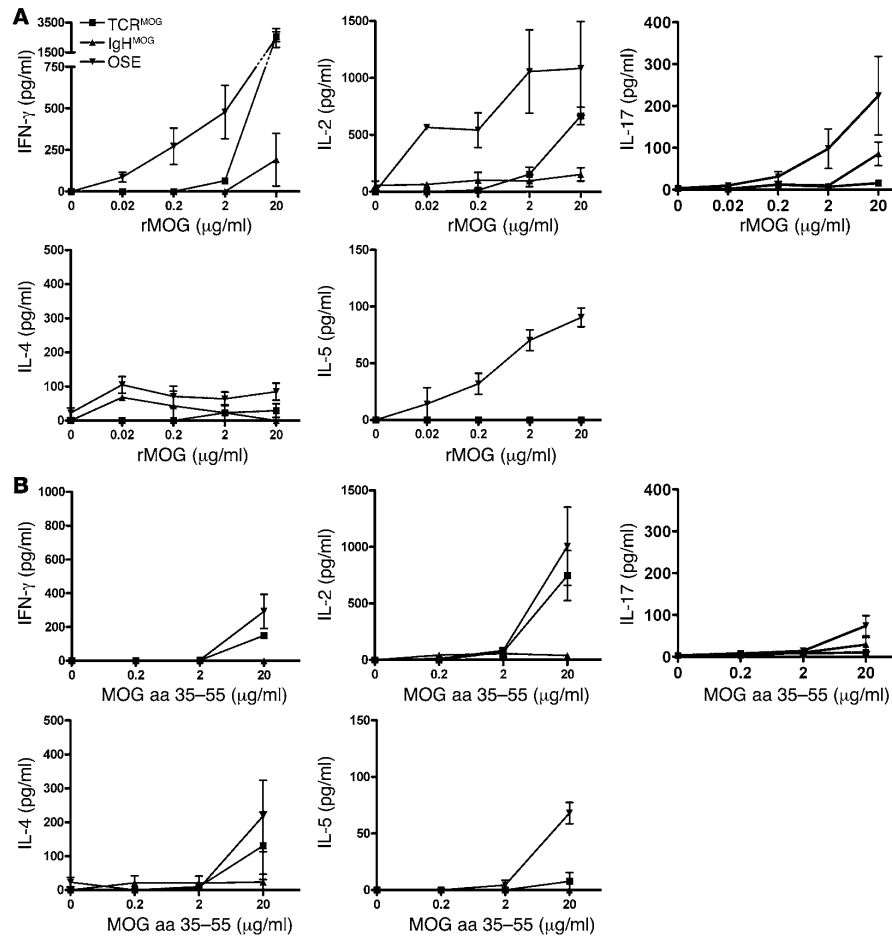


**Figure 6**

Cytokine production by transgenic splenocytes in vitro. (A and B) Splenocytes from OSE, TCR<sup>MOG</sup>, and IgH<sup>MOG</sup> mice were stimulated with increasing amounts of (A) rMOG or (B) MOG aa 35–55 peptide, and secreted IFN- $\gamma$ , IL-2, IL-4, IL-5, and IL-17 cytokines were detected by ELISA. Representative results of a total of 7 OSE, 3 TCR<sup>MOG</sup>, and 3 IgH<sup>MOG</sup> animals analyzed during 3 independent experiments are shown. Error bars indicate SEM.

cell transgenic strains did. The question arises as to which events trigger EAE in OSE mice. In principle, both positive and negative triggers could be envisaged that weaken downregulatory control mechanisms. In human autoimmune disease the triggering events are commonly related to the inflammatory responses surrounding infection. The signals may include molecular mimicry among microbial and autoimmune determinants (13), microbial superantigens (14), and inflammatory milieus created by innate immune responses (15). The data from experimental models of spontaneous autoimmunity are, however, contradictory. Thus in transgenic mice with T cell receptors for MBP, spontaneous EAE was frequently noted in colonies with low hygienic standards, while mice of the same strain remained healthy when kept clean (11). In striking contrast, spontaneous type 1 diabetes mellitus in NOD mice arose more frequently in “clean” than in “dirty” colonies (4, 16). OSE mice from our colony, raised under either SPF or conventional conditions, developed spontaneous EAE at very similar rates.

EAE bouts have been elicited by signals of innate immune responses that mostly act on local APCs. For example, treatment of proteolipid protein-reactive, TCR transgenic mice with bacterial CpG or *Bordetella pertussis* toxin strikingly enhanced the incidence of spontaneous EAE (17). These stimuli did not affect EAE development in OSE mice (data not shown).

Alternatively, autoimmune disease has been precipitated in animals after weakening their regulatory T cell populations (18). Depletion of putative regulatory T cells from partly resistant B10.S mice increased the inducibility of EAE (19) or exacerbated established EAE in SJL/J mice (20). Applying current depletion protocols using anti-IL-2R and anti-GITR antibodies, we were unable to influence the occurrence of spontaneous Devic disease in our mouse colony. However, we noted a low frequency (<2%) of CD4<sup>+</sup>CD25<sup>+</sup>CD69<sup>-</sup> T cells in the mice (Supplemental Figure 8). Furthermore, we were unable to detect differences in the frequency of Foxp3 regulatory cell in healthy versus sick OSE mice (see Supplemental Figure 8 for details).

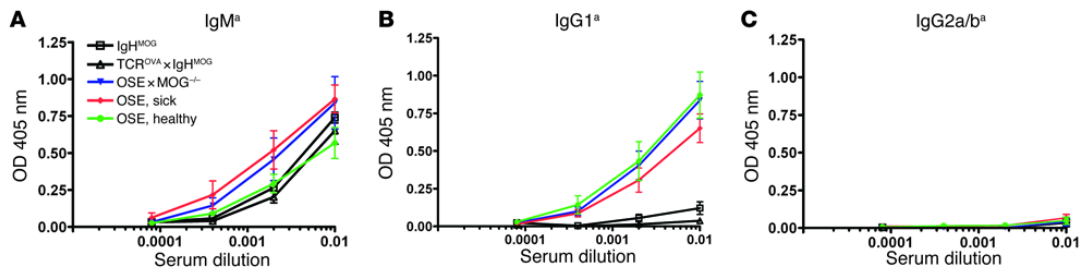


**Figure 7**

Relative concentrations of MOG-specific serum Ig antibodies in transgenic mice. MOG-binding antibodies were detected by ELISA in serially diluted sera obtained from healthy ( $n = 6$ ) and sick ( $n = 7$ ) OSE, healthy IgH<sup>MOG</sup> ( $n = 6$ ), healthy TCR<sup>OVA</sup> × IgH<sup>MOG</sup> ( $n = 6$ ), and healthy OSE × MOG<sup>-/-</sup> ( $n = 3$ ) mice. Sera (diluted at  $10^{-2}$ ,  $5 \times 10^{-2}$ ,  $2.5 \times 10^{-3}$ , and  $1.25 \times 10^{-4}$ ) were incubated with plates precoated with rMOG. Bound anti-MOG Ig was detected by allotype-specific antibodies recognizing IgM<sup>a</sup> (A), IgG1<sup>a</sup> (B), or IgG2a/b<sup>a</sup> (C). Mean absorbance at OD 405 nm is shown; error bars indicate SEM.

Human organ-specific autoimmune diseases like rheumatoid arthritis (21) and myasthenia gravis (22) seem to be the result of pathogenic interactions between autoreactive T and B lymphocytes. There is emerging evidence that, at least in a subset of MS cases, B and T cells cooperate to produce disease (2). Indeed, B cells and plasma cells are quite common components of MS lesions (23, 24). Further, the cerebrospinal fluid characteristically contains B cell products, the oligoclonal Ig bands, which seem to be the results of an antigen-driven immune response (25, 26). Finally, immunotherapies targeted to B cells and their products have been successful in classical MS (27) and Devic disease (28).

While to date EAE models have been used mainly to study the role of T cells in CNS autoimmunity, there are still only a few studies on autoimmune B cells. Several studies explored the contribution of B cells to the pathogenesis of EAE, either by depletion (29, 30) or by using transgenic mice with crippled Ig genes (31–33), but the role of autoantigen-specific B cells has been largely neglected.

The double-transgenic mouse strain described here, which we believe to be novel, fills this gap. OSE mice are double-transgenic for T and B cell receptors specific for the same myelin autoantigen, MOG. Autoimmune T and B cells thus may interact on several levels to create disease. First, antigen-specific B cells are known to efficiently capture even highly diluted protein antigen via their surface Ig receptors, to process the antigen, and then to present it to specific T cells in the context of appropriate MHC determinants (34). This is definitely the case in OSE mice. The transgenic B cells have receptors that bind only conformational epitopes formed by rMOG protein (8) and fail to bind MOG aa 35–55 peptide. Consequently, in these mice, the MOG-specific B cells were able to pick up and concentrate rMOG present at enormous dilutions and present it efficiently to specific T cells. However, the same B cells failed to concentrate MOG peptide.

The role of MOG-specific B cells is, however, not restricted to antigen presentation. We have shown that in double-transgenic spleen cultures, both T and B cells responded to MOG by activation and proliferation. Furthermore, MOG-specific T cells, activated by MOG, can drive their B cell partners into differentiation pathways, toward either Ig-producing plasma cells or long-lived memory B cells. Further, these T cell/B cell interactions control Ig affinity maturation and isotype switching, as indicated by our finding that anti-MOG Igs underwent a class switch from IgM to IgG1 — a switch pattern commonly related to Th2 responses

— in OSE mice. This did not occur in IgH<sup>MOG</sup> mice or in double-transgenic TCR<sup>OVA</sup> × IgH<sup>MOG</sup> mice. Remarkably, however, OSE mice showed a cytokine pattern (high levels of IFN- $\gamma$  and IL-2, low levels of IL-5 and IL-17, and no detectable IL-4) that dominated the transgenic T cells both in vitro and in the CNS milieu. Factors other than the known switch cytokines must have contributed to the IgG1 isotype switch of anti-MOG autoantibodies.

Following conventional concepts, the Ig switch to IgG1 should be the consequence of presentation and recognition of the nominal autoantigen, MOG, between both partner cells. It is thus another major surprise that the IgG1 switch of anti-MOG autoantibodies was seen in OSE mice not only on a MOG<sup>+/+</sup> background but also on a MOG<sup>-/-</sup> background. This raises the question of the (auto)antigen linking T and B cells in vivo. In a previous study of double-transgenic mice expressing the IgH<sup>MOG</sup> gene replacement plus the light chain from the donor hybridoma, Litzberger et al. observed B cell receptor editing (35), a phenomenon involving B cell contact with self antigen (36). MOG-reactive B cells showed evidence of receptor editing in both MOG<sup>+/+</sup> and MOG<sup>-/-</sup> mice, a finding that suggests a non-MOG self protein mimicking MOG epitopes (35).

In OSE mice, the particular localization of lesions in the optic nerve and in the spinal cord differs from most actively induced or passively transferred EAE variants. Presumably, lesion distribution depends both on the nature of the target autoantigen and on genetic factors. While classic EAE induced in Lewis rats by MBP-specific T cells affects the spinal cord in a caudocranial gradient of intensity, other CNS autoantigens produce very different patterns in the same strain (37). Conversely, immunization of BN rats with rMOG produces EAE with distribution like that in OSE mice, while sensitization of DA rats results in inflammation throughout the CNS (38). Furthermore, single-transgenic TCR<sup>MOG</sup> mice frequently show isolated optic neuritis, but rarely spinal cord lesions (5).

The distribution of the demyelinating lesions within the optic nerve and the spinal cord along with their particular cellular composition in our transgenic mice are similar to that in Devic disease. However, TCR<sup>MOG</sup> × IgH<sup>MOG</sup> double-transgenic OSE mice were not able to replicate all aspects of the complex clinical and pathological patterns observed in human Devic disease. Most importantly, in Devic disease long monofocal lesions are observed that are predominantly located in the cervical spinal cord segments. Highly destructive and necrotic lesions are symmetrical and mainly affect the central portions of the spinal cord over several segments. Despite



impressive and severe pathology in OSE mice, we were unable to see such devastating pathology (Figure 2), probably due in part to the fact that affected animals rapidly developed severe clinical symptoms after onset of disease, often requiring the early scarification of such animals (see Supplemental Figure 2). Furthermore, human Devic disease seems to be associated with massive perivascular IgM, IgG, and complement deposition, which are not specifically located on myelin sheaths. We, however, were unable to detect comparable complement deposition within the CNS of sick OSE mice (data not shown). Antibodies binding to aquaporin-4, which have been recently described in the sera of Devic disease patients (39), seemed to be absent in OSE mice (data not shown). This discrepancy may, however, be of limited importance, as anti-aquaporin antibodies were missing in about 30% of Devic patient sera. Moreover, the distribution of aquaporin within the human CNS does not coincide with the distribution of demyelinating lesions in Devic disease (39, 40).

OSE mice offer important new features, which will make them of use for a number of purposes. Most interestingly, they may lend themselves to the study of mechanisms that precipitate spontaneous autoimmune disease. OSE mice may also be useful for exploring factors that determine the localization of lesions and their cellular composition. Finally, as a model of spontaneous, non-adjuvant-induced autoimmunity, OSE mice may be helpful in the preclinical validation of novel therapies of autoimmune CNS disease.

## Methods

**Animals and disease scoring.** The transgenic IgH<sup>MOG</sup> (also referred to as Th; ref. 8), TCR<sup>MOG</sup> (also referred to as 2D2; ref. 5), and MOG<sup>-/-</sup> mice (10) along with C57BL/6 mice were bred in the animal facilities of the Max Planck Institute of Biochemistry. TCR<sup>MOG</sup> mice were generated directly on the C57BL/6 genetic background (5). IgH<sup>MOG</sup> and MOG<sup>-/-</sup> mice were originally made using 129-derived ES cells but were backcrossed against the C57BL/6 strain for more than 12 and 8 generations, respectively. Homozygous TCR<sup>OVA</sup> mice ( $n = 6$ ) were purchased from Jackson Laboratory.

F1 animals resulting from the intercross of IgH<sup>MOG</sup> with TCR<sup>MOG</sup> or TCR<sup>OVA</sup> mice were weighed and examined every 2–3 days for clinical signs of disease. Clinical scoring of animals was according to the classic EAE disease determination: 0, healthy animal; 1, animal with a flaccid tail; 2, animal with impaired righting reflex and/or gait; 3, animal with 1 paralyzed hind leg; 4, animal with both hind legs paralyzed; 5, moribund animal or death of the animal after preceding clinical disease.

All animal procedures used in this report were in accordance with guidelines of the committee on animals of the Max Planck Institute for Neurobiology and with the license of the Regierung von Oberbayern (Munich, Germany).

**Antigens.** rMOG was purified from bacterial inclusion bodies (41). MOG aa 35–55 peptide was synthesized at BioTrend, Germany.

**Immunization of animals.** Mice were injected s.c. at the tail base with an emulsion of equal amounts of CFA and 200  $\mu$ g MOG aa 35–55 in PBS. CFA was supplemented with 5 mg/ml *Mycobacterium tuberculosis* (strain H37Ra). Pertussis toxin (400 ng) was injected i.p. on days 0 and 2 relative to immunization.

**Histological analysis.** Animals were perfused with 4% paraformaldehyde in PBS, stored in the same fixative for 24 hours, and then washed twice with PBS. Brain and spinal cord tissue was dissected and in part embedded in paraffin or snap frozen for immunocytochemistry. Adjacent serial sections were stained with H&E, luxol fast blue, or Bielschowsky silver impregnation.

**Immunohistochemistry.** Immunohistochemical stainings were performed as described previously (42). Tissue sections (8–12  $\mu$ m) were incubated with primary rat antibodies recognizing mouse CD4, CD11b, CD8a, IgM, CD19, or B220 (all obtained from BD Biosciences Pharmingen). A secondary biotinylated anti-rat antibody, a streptavidin-HRP complex (both

from Vector Laboratories), and diaminobenzidine (Zymed) allowed the cell type specific detection of mononuclear cells. Slides were counterstained with Meyer's hematoxylin and embedded in AquaMount (Fisher Scientific) prior to microscopic analysis.

**Flow cytometric analysis.** Mononuclear cells were isolated from the CNS by Percoll gradient centrifugation. For the detection of cell surface markers by FACS analysis, cells were stained with fluorochrome-labeled antibodies (BD Biosciences Pharmingen; see Supplemental Methods for details). MOG-binding cells were detected with biotinylated rMOG protein (41) and a streptavidin-allophycocyanin complex (BD Biosciences Pharmingen). Intracellular Foxp3 staining was performed according to the manufacturer's instructions (eBioscience). Data acquisition was done with a FACSCalibur system and CellQuest software (BD). For data analysis CellQuest software and WinMDI software (version 2.8; <http://facs.scripps.edu/software.html>) were used.

**In vitro proliferation assay.** Single-cell suspensions from spleens were prepared, and  $2 \times 10^5$  cells/well were seeded in 96-well, round-bottomed plates in a total volume of 200  $\mu$ l complete RPMI medium containing 10% FCS (Invitrogen). After a culture period of 48 hours, 1  $\mu$ Ci <sup>3</sup>H-labeled thymidine was added per well. Samples were harvested 16 hours later, and tritium incorporation was measured. Each sample was run in triplicate.

**Cell purification.** Lymphocyte subpopulations were purified from the spleens of transgenic mice using B cell or T cell Negative Selection kits (Dyna). Their viability and purity were evaluated by FACS analysis. The cell purification procedure generally resulted in cell populations that were more than 90% pure.

**CFSE labeling of lymphocytes.** Cells ( $2 \times 10^7$ ) were incubated at 37°C for 10 minutes with 1% FCS/PBS containing 5  $\mu$ M CFSE (Invitrogen) and were subsequently washed extensively with cold PBS.

**ELISA.** Cells were plated and stimulated as described for proliferation assays. After 72 hours cell supernatants were collected. Cytokine concentrations were determined using matching antibody pairs for mouse IL-2, IFN- $\gamma$ , IL-4, IL-5 (BD Biosciences Pharmingen), and IL-17 (R&D Systems). For colorimetric cytokine determination, 2',2'-azino-bis (3-ethylbenzthiazoline-6-sulphonic acid (ABTS; Sigma-Aldrich) was used as a substrate, and plates were read at 405 nm.

**Determination of serum titers of MOG-specific antibodies.** Serially diluted serum collected from transgenic mice were transferred to 96-well ELISA plates (Nunc) precoated with rMOG. After extensive washes, bound Ig was detected by a sandwich consisting of a biotinylated allotype- and isotype-specific anti-mouse Ig (all BD Biosciences Pharmingen; see Supplemental Methods for details) and a streptavidin-HRP complex (BD Biosciences Pharmingen). ABTS was used as a color substrate that was measured at 405 nm.

**Quantitative real-time TaqMan PCR analysis.** Total RNA was isolated from the spinal cord and optic nerves by TRI Reagent extraction (Sigma-Aldrich) and, following DNase I treatment, was converted into cDNA using either hexanucleotide or oligo-dT primers and SuperScript II Reverse Transcriptase (Invitrogen). Sense and antisense primers in combination with FAM/TAMRA TaqMan probes and gene-specific primers (synthesized at Metabion) were used for PCR analysis. A list of used primer sequences for the IFN- $\gamma$ , TNF- $\alpha$ , IL-4, IL-5, IL-10, IL-13, IP-10, eoraxin, Foxp3, and GAPDH genes is provided in Supplemental Methods. Where possible the primer/probe sequence combinations spanned contact sequences of subsequent exons. For amplification the Absolute QPCR mix was used (ABgene). Each reaction was run in triplicate on an ABI 5700 machine (Applied Biosystems) and was normalized to house-keeping gene GAPDH transcripts. Primary data was analyzed with GeneAmp SDS 5700 software (Applied Biosystems).

**Statistics.** Descriptive statistical analysis was performed using Excel 2003 (Microsoft) and Prism version 4 (GraphPad) software. Differential



## research article

EAE incidence was analyzed by log-rank test (by an in-built survival curve analysis from Prism version 4). *P* values less than 0.05 were considered to be significant.

### Acknowledgments

We thank Irene Arnold-Ammer for exceptional technical assistance; Edgar Meinel, Florian Kurschus, and Klaus Dornmair for critical review of the manuscript; Estelle Bettelli and Vijay Kuchroo for providing 2D2 transgenic mice; Danielle Pham-Dinh for MOG<sup>-/-</sup> animals; and Shimon Sakaguchi for the DTA-1 and PC61 hybridoma. This work was supported in part by the Max Planck society, the Deutsche Forschungsgemeinschaft (SFB 571), and the National Multiple Sclerosis Society (grant RG3335A1/T).

Received for publication February 23, 2006, and accepted in revised form June 13, 2006.

Address correspondence to: Andreas Holz or Hartmut Wekerle, Department of Neuroimmunology, Max Planck Institute for Neurobiology, Am Klopferspitz 18, D-82152 Martinsried, Germany. Phone: 48-89-8578-3561; Fax: 49-89-8995-0170; E-mail: holz@neuro.mpg.de (A. Holz). Phone: 49-89-8578-3551; Fax: 49-89-8578-3790; E-mail: hwekerle@neuro.mpg.de (H. Wekerle).

Andreas Holz's present address is: Technical University of Braunschweig – Biocenter, Department of Cell and Molecular Biology, Braunschweig, Germany.

- O'Riordan, J.L., et al. 1996. Clinical, CSF and MRI findings in Devic's neuromyelitis optica. *J. Neurol. Neurosurg. Psychiatry*. **60**:382–387.
- Lassmann, H., Brück, W., and Lucchinetti, C. 2001. Heterogeneity of multiple sclerosis pathogenesis: implications for diagnosis and therapy. *Trends Mol. Med.* **7**:115–121.
- Kurtzke, J.F. 1993. Epidemiologic evidence for multiple sclerosis as an infection. *Clin. Microbiol. Rev.* **6**:382–427.
- Bach, J.-F. 2002. The effect of infections on susceptibility to autoimmune and allergic diseases. *N. Engl. J. Med.* **347**:911–920.
- Bettelli, E., et al. 2003. Myelin oligodendrocyte glycoprotein-specific T cell receptor transgenic mice develop spontaneous autoimmune optic neuritis. *J. Exp. Med.* **197**:1073–1081.
- Linington, C., Webb, M., and Woodhams, P.L. 1984. A novel myelin-associated glycoprotein defined by a mouse monoclonal antibody. *J. Neuroimmunol.* **6**:387–396.
- Linington, C., Bradl, M., Lassmann, H., Brunner, C., and Vass, K. 1988. Augmentation of demyelination in rat acute allergic encephalomyelitis by circulating mouse monoclonal antibodies directed against a myelin/oligodendrocyte glycoprotein. *Am. J. Pathol.* **130**:443–454.
- Litzenburger, T., et al. 1998. B lymphocytes producing demyelinating autoantibodies: development and function in gene-targeted transgenic mice. *J. Exp. Med.* **188**:169–180.
- Barnden, M.J., Allison, J., Heath, W.R., and Carbone, F.R. 1998. Defective TCR expression in transgenic mice constructed using cDNA-based  $\alpha$ - and  $\beta$ -chain genes under the control of heterologous regulatory elements. *Immunol. Cell Biol.* **76**:34–40.
- Delarasse, C., et al. 2003. Myelin/oligodendrocyte glycoprotein-deficient (MOG-deficient) mice reveal lack of immune tolerance to MOG in wild-type mice. *J. Clin. Invest.* **112**:544–553. doi:10.1172/JCI200315861.
- Goverman, J., et al. 1993. Transgenic mice that express a myelin basic protein-specific T cell receptor develop spontaneous autoimmunity. *Cell*. **72**:551–560.
- Lafaille, J., Nagashima, K., Katsuki, M., and Tonegawa, S. 1994. High incidence of spontaneous autoimmune encephalomyelitis in immunodeficient anti-myelin basic protein T cell receptor mice. *Cell*. **78**:399–408.
- Oldstone, M.B.A. 1987. Molecular mimicry and autoimmune disease. *Cell*. **50**:819–820.
- Schiffenbauer, J., Soos, J.M., and Johnson, H. 1998. The possible role of bacterial superantigen in the pathogenesis of autoimmune disorders. *Immunol. Today*. **19**:117–120.
- Bachmann, M.F., and Kopf, M. 2001. On the role of the innate immunity in autoimmune disease. *J. Exp. Med.* **193**:F47–F50.
- Pozzilli, P., Signore, A., Williams, A.J.K., and Beales, P.E. 1993. NOD mouse colonies around the world - recent facts and figures. *Immunol. Today*. **14**:193–196.
- Waldner, H., Collins, M., and Kuchroo, V.K. 2004. Activation of antigen-presenting cells by microbial products breaks self tolerance and induces autoimmune disease. *J. Clin. Invest.* **113**:990–997. doi:10.1172/JCI200419388.
- Bach, J.-F. 2003. Regulatory T cells under scrutiny. *Nat. Rev. Immunol.* **3**:189–198.
- Reddy, J., et al. 2004. Myelin proteolipid protein-specific CD4<sup>+</sup>CD25<sup>+</sup> regulatory cells mediate genetic resistance to experimental autoimmune encephalomyelitis. *Proc. Natl. Acad. Sci. U. S. A.* **101**:15434–15439.
- Kohm, A.P., Williams, J.S., and Miller, S.D. 2004. Ligation of the glucocorticoid-induced TNF receptor enhances autoreactive CD4<sup>+</sup> T cell activation and experimental autoimmune encephalomyelitis. *J. Immunol.* **172**:4684–4690.
- Dörner, T., and Burmester, G.R. 2003. The role of B cells in rheumatoid arthritis: mechanisms and therapeutic targets. *Curr. Opin. Rheumatol.* **15**:246–252.
- Hohlfeld, R., and Wekerle, H. 1999. The immunopathogenesis of myasthenia gravis. In *Myasthenia gravis and myasthenic syndromes*. A.G. Engel, editor. Oxford University Press. Oxford, United Kingdom. 87–110.
- Esiri, M.M. 1980. Multiple sclerosis: a quantitative and qualitative study of immunoglobulin-containing cells in the central nervous system. *Neuropathol. Appl. Neurobiol.* **6**:9–21.
- Baranzini, S.E., et al. 1999. B cell repertoire diversity and clonal expansion in multiple sclerosis brain lesions. *J. Immunol.* **163**:5133–5144.
- Qin, Y.F., et al. 2003. Intrathecal B-cell clonal expansion, an early sign of humoral immunity, in the cerebrospinal fluid of patients with clinically isolated syndrome suggestive of multiple sclerosis. *Lab. Invest.* **83**:1081–1088.
- Owens, G.C., et al. 2003. Single-cell repertoire analysis demonstrates that clonal expansion is a prominent feature of the B cell response in multiple sclerosis cerebrospinal fluid. *J. Immunol.* **171**:2725–2733.
- Keegan, M., et al. 2005. Relation between humoral pathological changes in multiple sclerosis and response to therapeutic plasma exchange. *Lancet*. **366**:579–582.
- Cree, B.A.C., et al. 2005. An open label study of the effects of rituximab in neuromyelitis optica. *Neurology*. **64**:1270–1272.
- Gausas, J., Paterson, P.Y., Day, B.D., and Dal Canto, M.C. 1982. Intact B-cell activity is essential for complete expression of experimental allergic encephalomyelitis in Lewis rats. *Cell. Immunol.* **72**:360–366.
- Myers, K.J., Sprent, J., Dougherty, J.P., and Ron, Y. 1992. Synergy between encephalitogenic T cells and myelin basic protein-specific antibodies in the induction of experimental autoimmune encephalomyelitis. *J. Neuroimmunol.* **41**:1–8.
- Wolf, S.D., Dittel, B.N., Hardardottir, F., and Jane-way, C.A. 1996. Experimental autoimmune encephalomyelitis induction in genetically B cell-deficient mice. *J. Exp. Med.* **184**:2271–2278.
- Hjelmström, P., Juedes, A.E., Fjell, J., and Ruddle, N.H. 1998. B cell deficient mice develop experimental allergic encephalomyelitis with demyelination after myelin oligodendrocyte glycoprotein immunization. *J. Immunol.* **161**:4480–4483.
- Lyons, J.-A., San, M., Happ, M.P., and Cross, A.H. 1999. B cells are critical to induction of experimental allergic encephalomyelitis by protein but not by a short encephalitogenic peptide. *Eur. J. Immunol.* **29**:3432–3439.
- Lanzavecchia, A. 1990. Receptor-mediated antigen uptake and its effects on antigen presentation to class II-restricted T lymphocytes. *Annu. Rev. Immunol.* **8**:773–794.
- Litzenburger, T., et al. 2000. Development of MOG autoreactive transgenic B lymphocytes: receptor editing in vivo following encounter of a self-antigen distinct from MOG. *J. Immunol.* **165**:5360–5366.
- Verkoczy, L.K., Mårtensson, A.S., and Nemezei, D. 2004. The scope of receptor editing and its association with autoimmunity. *Curr. Opin. Immunol.* **16**:808–816.
- Berger, T., et al. 1997. Experimental autoimmune encephalomyelitis: the antigen specificity of T-lymphocytes determines the topography of lesions in the central and peripheral nervous system. *Lab. Invest.* **76**:355–364.
- Storch, M.E., et al. 1998. Autoimmunity to myelin oligodendrocyte glycoprotein in rats mimics the spectrum of multiple sclerosis pathology. *Brain Pathol.* **8**:681–694.
- Lennon, V.A., Kryzer, T.J., Pittock, S.J., Verkman, A.S., and Hinson, S.R. 2005. IgG marker of optic-spinal multiple sclerosis binds to the aquaporin-4 water channel. *J. Exp. Med.* **202**:473–477.
- Lennon, V.A., et al. 2004. A serum autoantibody marker of neuromyelitis optica: distinction from multiple sclerosis. *Lancet*. **364**:2106–2112.
- Adelmann, M., et al. 1995. The N-terminal domain of the myelin oligodendrocyte glycoprotein (MOG) induces acute demyelinating experimental autoimmune encephalomyelitis in the Lewis rat. *J. Neuroimmunol.* **63**:17–27.
- Holz, A., Brett, K., and Oldstone, M.B.A. 2001. Constitutive  $\beta$ -cell expression of IL-12 does not perturb self-tolerance but intensifies established autoimmune diabetes. *J. Clin. Invest.* **108**:1749–1758. doi:10.1172/JCI200113915.

## **Publication 2**



## Spontaneous relapsing-remitting EAE in the SJL/J mouse: MOG-reactive transgenic T cells recruit endogenous MOG-specific B cells

Bernadette Pöllinger,<sup>1</sup> Gurumoorthy Krishnamoorthy,<sup>1</sup> Kerstin Berer,<sup>1</sup> Hans Lassmann,<sup>3</sup> Michael R. Bösl,<sup>2</sup> Robert Dunn,<sup>4</sup> Helena S. Domingues,<sup>1</sup> Andreas Holz,<sup>1</sup> Florian C. Kurschus,<sup>1</sup> and Hartmut Wekerle<sup>1</sup>

<sup>1</sup>Department of Neuroimmunology and <sup>2</sup>Transgenic Service, Max Planck Institute of Neurobiology, D-82152 Martinsried, Germany

<sup>3</sup>Center for Brain Research, Medical University of Vienna, A-1090 Vienna, Austria

<sup>4</sup>Department of Immunology, Biogen Idec, San Diego, CA 92122

We describe new T cell receptor (TCR) transgenic mice (relapsing-remitting [RR] mice) carrying a TCR specific for myelin oligodendrocyte glycoprotein (MOG) peptide 92–106 in the context of I-A<sup>b</sup>. Backcrossed to the SJL/J background, most RR mice spontaneously develop RR experimental autoimmune encephalomyelitis (EAE) with episodes often altering between different central nervous system tissues like the cerebellum, optic nerve, and spinal cord. Development of spontaneous EAE depends on the presence of an intact B cell compartment and on the expression of MOG autoantigen. There is no spontaneous EAE development in B cell-depleted mice or in transgenic mice lacking MOG. Transgenic T cells seem to expand MOG autoreactive B cells from the endogenous repertoire. The expanded autoreactive B cells produce autoantibodies binding to a conformational epitope on the native MOG protein while ignoring the T cell target peptide. The secreted autoantibodies are pathogenic, enhancing demyelinating EAE episodes. RR mice constitute the first spontaneous animal model for the most common form of multiple sclerosis (MS), RR MS.

### CORRESPONDENCE

Hartmut Wekerle:  
hwekerle@neuro.mpg.de  
OR  
Florian C. Kurschus:  
kurschus@neuro.mpg.de

Abbreviations used: cDNA, complementary DNA; CNS, central nervous system; EAE, experimental autoimmune encephalomyelitis; MOG, myelin oligodendrocyte glycoprotein; MS, multiple sclerosis; NTL, nontransgenic littermate; OSE, opticospinal EAE; OSMS, opticospinal MS; PI, propidium iodide; rMOG, recombinant rat MOG; R.R., relapsing-remitting.

Autoimmune diseases can affect most organs of the body including liver, heart, the endocrine system, the musculoskeletal apparatus, and the central nervous system (CNS). They commonly start off at a young age and then last throughout life, often resulting in severe disability. The factors that trigger the onset, modulate the course, and determine the clinical character of autoimmune diseases have remained obscure, a deficit of knowledge which sets limits to the design of specific and efficient therapies.

Yet there is increasing evidence that organ-specific autoimmune diseases, such as rheumatoid arthritis, type 1 diabetes mellitus, and multiple

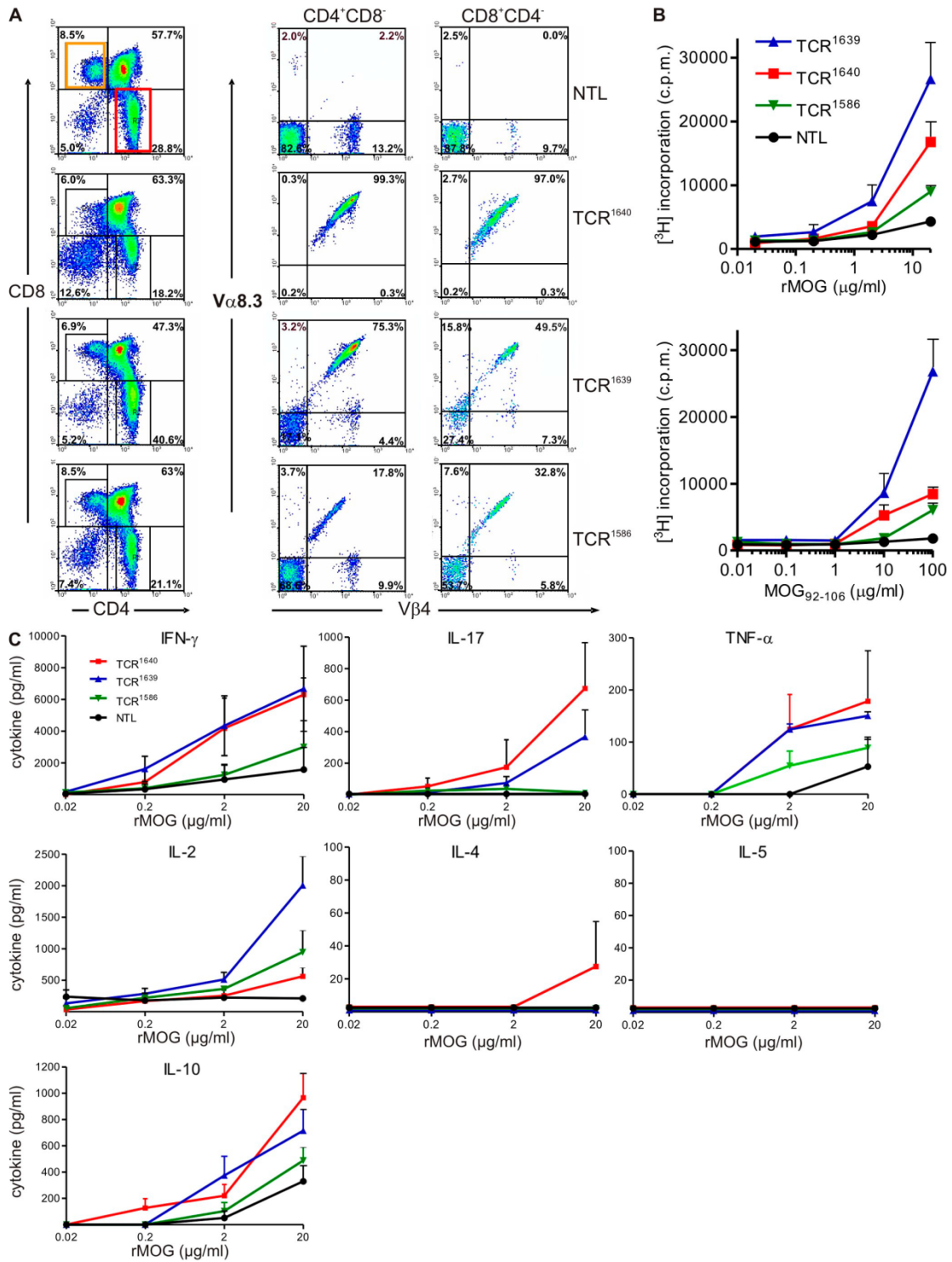
sclerosis (MS), are the result of a pathogenic interaction of autoimmune T and B cells. There is substantial information on the role of T cells in organ-specific autoimmunity. Some act as effector cells attacking self-tissues, either directly or via recruiting accessory cells like macrophages. Other T cells regulate the time course of the response and still others provide help to autoantibody-producing B cells. The contribution of autoimmune B cells to the inflammatory pathogenesis seems to be complex as well. Beyond producing humoral autoantibodies, B cells serve as APCs activating pathogenic T cells, and, through their capacity of releasing cytokines, B cells are involved in shaping local microenvironments favorable to evolving cellular autoimmune responses.

A. Holz's present address is Department of Cellular and Molecular Biology, Technical University of Braunschweig, D-38106 Braunschweig, Germany.

B. Pöllinger's present address is Novartis Pharma AG, CH-4056 Basel, Switzerland.

F.C. Kurschus's present address is I. Medizinische Klinik und Poliklinik, Johannes Gutenberg Universität, D-55131 Mainz, Germany.

© 2009 Pöllinger et al. This article is distributed under the terms of an Attribution-Noncommercial-Share Alike-No Mirror Sites license for the first six months after the publication date (see <http://www.jem.org/misc/terms.shtml>). After six months it is available under a Creative Commons License (Attribution-Noncommercial-Share Alike 3.0 Unported license, as described at <http://creativecommons.org/licenses/by-nc-sa/3.0/>).



Deciphering the interactions between T and B cells in the spontaneous development of organ-specific autoimmune responses requires suitable animal models. Naturally occurring models are available for type 1 diabetes mellitus and systemic lupus erythematosus but not for autoimmunity in the CNS (1). Recently, we and others described a double-transgenic mouse model, which simulates opticospinal MS (OSMS) remarkably well, a variant of which is also known as Devic's disease (2, 3). These mice, termed opticospinal experimental autoimmune encephalomyelitis (EAE [OSE]) mice, express myelin oligodendrocyte glycoprotein (MOG)-specific receptors on T and B cells and spontaneously develop demyelinating inflammatory disease at frequencies >50%. Like in human OSMS (4), the lesions in affected mice are restricted to optic nerve and spinal cord, and, in most cases, the disease takes a chronic progressive course without remissions and marked relapses. It should, however, be noted that the type of MS that most prevalently affects Caucasian populations differs fundamentally from OSMS (5). Typically, MS starts out with a relapsing-remitting (RR) course, where disease episodes may completely resolve only to be followed by a subsequent relapse. In this disease variant, the pathogenic lesions, demyelinating plaques, may be located throughout the CNS, thus causing the notoriously varied neurological defect patterns.

In this paper, we describe a new transgenic mouse model that spontaneously develops RR-EAE and, thus, recapitulates the "Western" variant of MS. Furthermore, and most importantly, we found that in these mice transgenic autoimmune T cells expand autoimmune B cells from the endogenous immune repertoire and guide them to produce antibodies against conformational epitopes of the MOG protein, which, together with complement, may initiate the destruction of MOG-expressing target cells.

## RESULTS

### New MOG-specific TCR transgenic SJL/J mice

We generated transgenic mice expressing a TCR specific for the rat/mouse MOG peptide 92–106 in the context of I-A<sup>b</sup>. This TCR, which uses V $\alpha$ 8.3 and V $\beta$ 4 genes, was derived from a MOG-specific encephalitogenic Th1-CD4<sup>+</sup> T cell clone isolated from a WT SJL/J mouse immunized against recombinant rat MOG (rMOG; Fig. S1). We selected three founder lines differing in markedly distinct proportions of transgenic V $\alpha$ 8.3<sup>+</sup>/V $\beta$ 4<sup>+</sup> CD4<sup>+</sup> T cells in central and peripheral immune repertoires (Fig. 1 A and Fig. S2). In low frequency TCR<sup>1586</sup> mice, 18% of single-positive CD4<sup>+</sup>CD8<sup>-</sup> thymocytes expressed the transgenic TCR. The proportion was 75% in

medium frequency TCR<sup>1639</sup> mice and 99% in high frequency TCR<sup>1640</sup> mice (Fig. 1 A). In all three transgenic mouse lines, transgene expression levels in the peripheral immune system were proportional to the ones in the central thymic repertoires (Fig. S2).

The density of the transgenic TCR on the surface of mature CD4<sup>+</sup> T cells in the spleen varied markedly (Fig. S2). Especially in high frequency TCR<sup>1640</sup> spleens, T cells could be distinguished based on the low and high densities of surface TCR (dim and bright TCR). The dim TCR population expressed higher levels of CD25 and CD69 and lower levels of CD62L (unpublished data).

Stimulation of nonimmunized transgenic spleen cells with rMOG or MOG<sub>92-106</sub> peptide *in vitro* led to dose-dependent proliferative responses (Fig. 1 B). Concomitant cytokine responses largely followed the proliferation pattern. Although the secretion of proinflammatory IFN- $\gamma$ , IL-17, and antiinflammatory IL-10 was similar in TCR<sup>1640</sup> and TCR<sup>1639</sup> lines, IL-2 secretion was higher in TCR<sup>1639</sup> T cells. The Th2-related cytokines IL-4 and IL-5 were absent in nearly all samples tested (Fig. 1 C).

### Spontaneous EAE in single- and double-transgenic SJL/J anti-MOG mice: RR course with varied clinical syndromes

While continuously backcrossing the line TCR<sup>1640</sup> into the SJL/J background, we noted spontaneous EAE-like disease developing at a high frequency (Fig. 2 A and Table S1). In the eighth backcross generation, >80% of all females developed EAE within 160 d. During the same period, the EAE rate in males was >60%. EAE was rare in transgenic SJL/J mice with low frequency TCR<sup>1586</sup> and surprisingly absent in medium frequency TCR<sup>1639</sup> mice and in *Mog*-deficient TCR<sup>1640</sup> (TCR<sup>1640</sup>  $\times$  *Mog*<sup>-/-</sup>) mice (Table S1).

We and others previously described a double-transgenic mouse strain, OSE mice (2, 3), which expressed a MOG-specific TCR transgene, 2D2 (specific for MOG peptide 35–55 in context of I-A<sup>b</sup>), along with the gene coding for the rearranged IgH variable chain of the classical anti-MOG monoclonal antibody, 8.18-C5 (IgH<sup>MOG</sup> mice) (6). We have now created similar double-transgenic mice by mating TCR<sup>1640</sup> SJL/J mice to IgH<sup>MOG</sup> on SJL/J background. Double-transgenic TCR<sup>1640</sup>  $\times$  IgH<sup>MOG</sup> mice developed spontaneous EAE very similar to TCR<sup>1640</sup> single transgenics, with some apparently minor differences. Almost all double-transgenic females came down with disease by 120 d of age, whereas males of the same age showed an EAE rate of <40%. This gender gap was highly significant but narrowed during the subsequent weeks (Fig. 2 A).

**Figure 1. Characterization of a new MOG-specific TCR transgenic SJL/J mouse.** (A) Thymocytes from 8–10-wk-old TCR transgenic mice or NTLs were stained with antibodies to CD4, CD8, TCR-V $\beta$ 4, and TCR-V $\alpha$ 8.3 and cells were analyzed by flow cytometry. Representative figures of three to seven analyzed mice are shown. Transgenic V $\alpha$ 8.3 and V $\beta$ 4 are shown on cells gated as indicated, either CD4<sup>+</sup>/CD8<sup>-</sup> or CD4<sup>-</sup>/CD8<sup>+</sup>. (B) Proliferative response to recombinant MOG protein (rMOG) or MOG peptide 92–106 measured as <sup>3</sup>H-thymidine incorporation. Splenocytes from TCR transgenic mice (8–10-wk-old healthy) were cultured with indicated concentrations of rMOG (top) and MOG<sub>92-106</sub> (bottom). (C) Cytokine responses to rMOG. Indicated cytokines were measured in supernatants harvested 48 h after rMOG activation by ELISA. Pooled data from three independent experiments are shown. Error bars indicate SEM. B and C: TCR<sup>1640</sup>, *n* = 3; TCR<sup>1639</sup>, *n* = 3; TCR<sup>1586</sup>, *n* = 3; NTL, *n* = 2.

**Table 1.** Spontaneous EAE in TCR transgenic SJL/J mice: course of disease

Mice (gender)	RR (n)		Progressive (n)
	With full remission	With partial remission	
	%	%	%
TCR <sup>1640</sup> (f)	71.4 (5/7)	14.3 (1/7)	14.3 (1/7)
TCR <sup>1640</sup> (m)	35.3 (6/17)	11.7 (2/17)	53 (9/17)
TCR <sup>1640</sup> × IgH <sup>M0G</sup> (f)	43.7 (7/16)	25.0 (4/16)	31.2 (5/16)
TCR <sup>1640</sup> × IgH <sup>M0G</sup> (m)	6.2 (1/16)	25.0 (4/16)	68.8 (11/16)
rMOG imm. SJL/J (f)	10.0 (1/10)	70.0 (7/10)	20 (2/10)

f, female; m, male; imm., immunized.

We also crossed IgH<sup>M0G</sup> mice to the medium and low frequency lines TCR<sup>1639</sup> and TCR<sup>1586</sup>, respectively. Only 1 out of 17 medium frequency TCR<sup>1639</sup> × IgH<sup>M0G</sup> mice displayed EAE and none of the low frequency TCR<sup>1586</sup> × IgH<sup>M0G</sup> showed any clinical symptoms (Table S1).

The CNS disease spontaneously developing in TCR transgenic SJL/J mice differed dramatically from spontaneous OSE seen in OSE mice (2, 3). In TCR transgenic SJL/J mice, single-transgenic TCR<sup>1640</sup> mice, and double-transgenic TCR<sup>1640</sup> × IgH<sup>M0G</sup> mice, disease was extremely variable both in course and

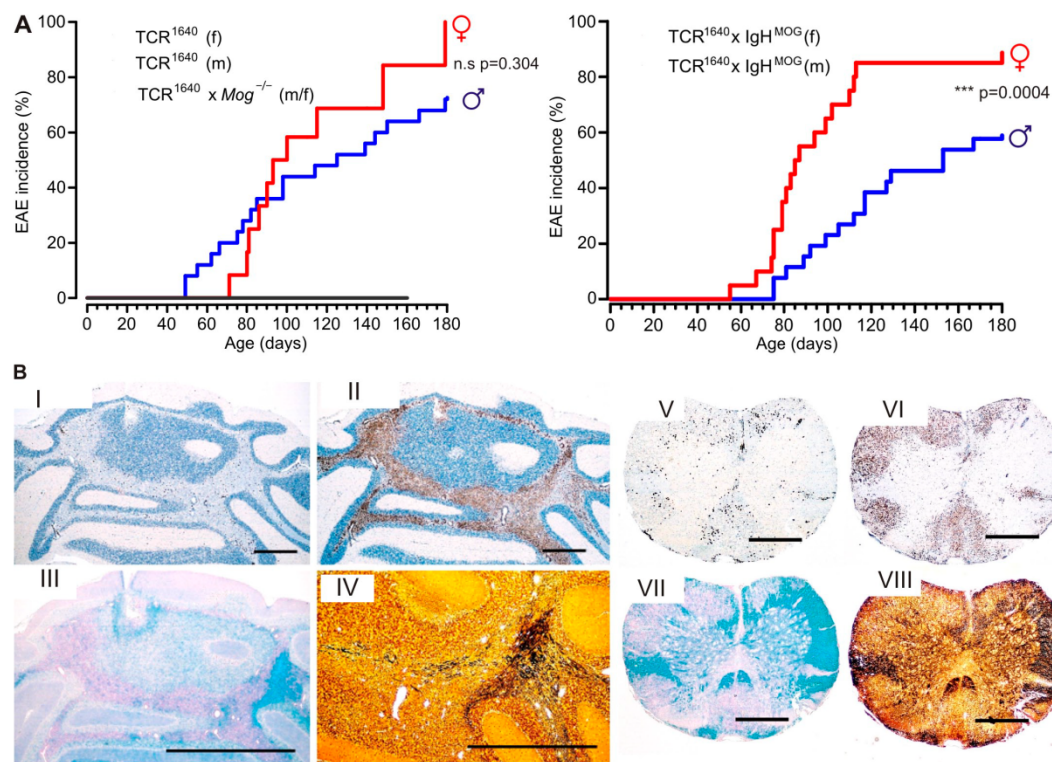


**Figure 2.** Spontaneous RR-EAE in TCR transgenic SJL/J mice. (A) Male and female single-transgenic TCR<sup>1640</sup> compared with double-transgenic TCR<sup>1640</sup> × IgH<sup>M0G</sup> mice. Shown is the spontaneous incidence of first signs of ataxia or classical EAE-like symptoms in TCR<sup>1640</sup> (left) and double-transgenic TCR<sup>1640</sup> × IgH<sup>M0G</sup> (right) mice. TCR<sup>1640</sup> females (f), *n* = 12; males (m), *n* = 27; TCR<sup>1640</sup> × IgH<sup>M0G</sup> females, *n* = 20; males, *n* = 26; TCR<sup>1640</sup> × *Mog*<sup>-/-</sup> mice, *n* = 6. Disease kinetic of genders in TCR<sup>1640</sup> mice was not statistically significant (*P* = 0.304) but differed significantly between sexes of TCR<sup>1640</sup> × IgH<sup>M0G</sup> mice (*P* = 0.0004). (B) Histological analysis of cerebellum and spinal cord from a sick TCR<sup>1640</sup> mouse (RR mouse) with ataxia and classical paralysis. Cerebellum (I–IV) and spinal cord (V–VIII) showed severe infiltration, demyelination, and axonal damage as visualized by immunohistochemistry using anti-CD3 (I and V) and anti-Mac3 antibodies (II and VI), Luxol fast blue staining (III and VII), and Bielschowsky silver impregnation (IV and VIII). I, II, V, and VI were counterstained by hematoxylin and eosin (H&E). Magnification: ×17 (cerebellum) and ×30 (spinal cord). Bars, 1 mm. Data are representative of at least two independent experiments consisting of more than three mice per group.

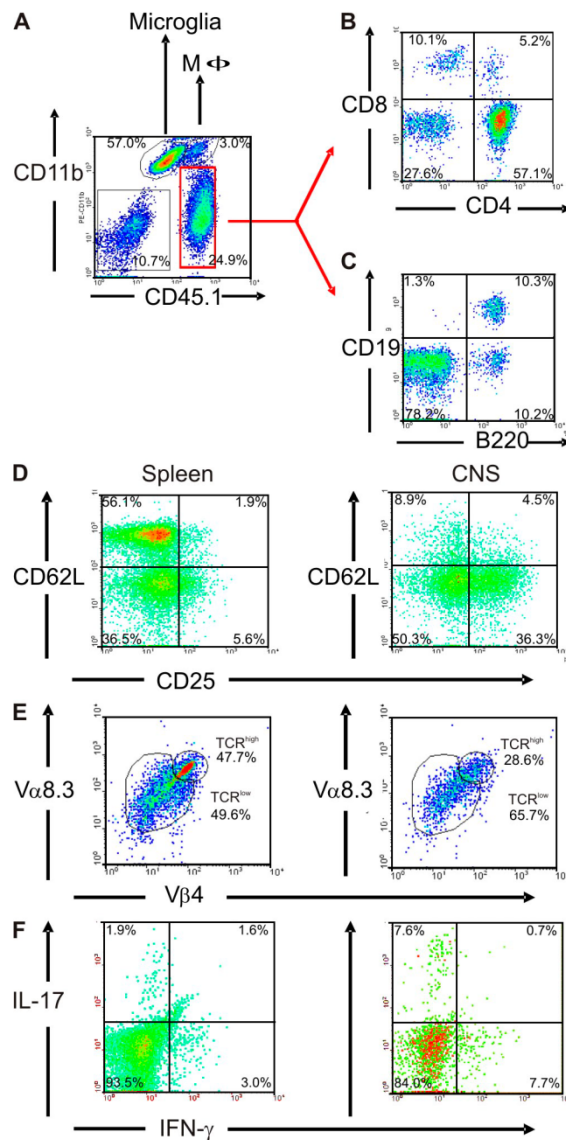


**Figure 3. Inflammatory cell infiltrates in RR-EAE lesions.** (A–C) Cellular infiltrate into the CNS of sick TCR<sup>1640</sup> mice (score 3) is composed of macrophages, T cells, and B cells. CNS mononuclear cells were isolated from a sick TCR<sup>1640</sup> mouse and stained against CD11b and CD45.1 (A), together with CD8 and CD4 (B) or together with CD19 and B220 (C). Cells in B and C were analyzed among gated CD45.1<sup>+</sup>CD11b<sup>+</sup> cells (red region as indicated). (D–F) Activation and Th1/Th17 cytokine expression of infiltrating CD4<sup>+</sup> T cells. (D) CNS infiltrate cells express CD25, but not CD62L, and partially down-modulate their TCR (V $\alpha$ 8.3 and V $\beta$ 4). Activation status and TCR expression was compared between splenocytes (left) and CNS-isolated cells (right). (E) CD4<sup>+</sup>CD3<sup>+</sup> T cells infiltrating the CNS of sick TCR<sup>1640</sup> mice predominantly expressed the pathogenic TCR composed of V $\alpha$ 8.3 and V $\beta$ 4 chains in a low expression level (TCR<sup>low</sup>) compared with the spleen. Numbers indicate the percentage of stained cells in the re-

clinical nature. Typically, in females EAE started with an RR course. Often, the first attacks resolved completely but were followed by further bouts. Intriguingly, individual EAE bouts often differed radically in their neurological defects. In a substantial number of cases, the initial bout was dominated by ataxia rather than by classical EAE defects. Affected mice were unable to walk along a straight line, deviating and falling to the side, but did not show limb weakness or paralysis (Video 1). In many cases, the mice recovered completely until a first relapse, which commonly showed a completely different clinical picture, for example, hind limb paralysis as seen in typical EAE. Again, this second disease episode subsided, giving way to partial remission. Later disease episodes mostly showed classical paralytic EAE (Table I and Fig. S3).

Although there was no clear distinction between single- and double-transgenic SJL/J mice, EAE course differed between females and males. As detailed in Table I, RR disease was more common in females. A minority of female mice developed progressive EAE from the beginning, but more than half of the males developed primary progressive EAE.

#### CNS changes representing different clinical EAE episodes

The clinical deficiencies developing in affected mice were reflected by the location and character of underlying CNS lesions. Ataxic mice displayed large inflammatory and demyelinated lesions in cerebellum and brain stem (Fig. 2 B). In contrast, in mice suffering from conventional EAE, lesions were distributed throughout the spinal cord, brain stem, and optic nerve (Table S2).

Irrespective of their location within the CNS, the inflammatory lesions were characterized by numerous CD3<sup>+</sup> T cells in the middle of a plethora of Mac3-positive activated macrophage-like cells (Fig. 2 B). The inflammatory infiltrates were embedded in large areas of demyelination and axon destruction. In line with their comparable clinical score, the histological patterns were similar between TCR<sup>1640</sup> single-transgenic and TCR<sup>1640</sup>  $\times$  IgH<sup>MOG</sup> double-transgenic mice (Table S2).

Cytofluorimetric analyses confirmed that, within the CNS, the major infiltrating inflammatory lymphocytes were CD4<sup>+</sup> T cells and B cells together with a minor population of macrophages and CD8<sup>+</sup> T cells (Fig. 3, A–C), with only minor contributions from CD8<sup>+</sup> T cells. Notably, most transgenic CD4<sup>+</sup> T cells infiltrating the CNS were activated. Many cells expressed the activation marker CD25 and were CD62L negative (Fig. 3 D). Additionally, infiltrating CD4<sup>+</sup> T cells expressed the activation markers CD44, VLA4, and ICOS (unpublished data). Furthermore, a high proportion (>65%) of CNS-infiltrating transgenic T cells partly down-modulated

spective quadrant or region. (F) Intracellular cytokine staining after stimulation with PMA/ionomycin in brefeldin A. Th1 (IFN- $\gamma$ <sup>+</sup>/IL-17<sup>-</sup>) and Th17 (IFN- $\gamma$ <sup>-</sup>/IL-17<sup>+</sup>) cells are enriched in CNS infiltrates of sick TCR<sup>1640</sup> (score 3.5) mice compared with splenocytes. D–F were analyzed among gated CD45.1<sup>+</sup>CD4<sup>+</sup> cells. Flow cytometry data are representative of three to five sick TCR<sup>1640</sup> mice analyzed in three to five independent experiments.

their transgenic V $\beta$ 4 and V $\alpha$ 8.3 determinants, which is in contrast to peripheral splenic populations, where the modulated subpopulations comprised less than half of the entire transgenic CD4<sup>+</sup> T cell subset (Fig. 3 E).

In agreement with previous EAE studies (7–10), we found CNS-infiltrating Th1 (IFN- $\gamma$ <sup>+</sup>/IL-17<sup>-</sup>) and Th17 (IFN- $\gamma$ <sup>-</sup>/IL-17<sup>+</sup>) cells. Compared with spleen, Th17 cells were enriched in CNS threefold and Th1 cells more than twofold (Fig. 3 F). A substantial part of the activated CD4<sup>+</sup>CD25<sup>+</sup> infiltrate T cells express transcription factor Foxp3, a marker of regulatory T cells (not depicted) (11).

Next, we measured the cytokine milieu in brain and spinal cord of TCR<sup>1640</sup> mice in different disease stages by real-time PCR in comparison to rMOG immunized SJL/J mice (Fig. S4). Most cytokines followed an infiltration pattern proportional to CD4 expression. As expected from our infiltrate analysis (Fig. 3), we found expression of both IFN- $\gamma$  and IL-17 in diseased mice. In accordance with this, TNF- $\alpha$  and IFN- $\gamma$  inducible protein 10 (IP-10/CXCL10) were strongly up-regulated during disease. Of the Th2 cytokines analyzed (IL-4, IL-5, and IL-13), only IL-5 was at measurable levels. This cytokine may support B cell proliferation, differentiation, and antibody secretion (12). The levels of the regulatory cytokine IL-10 and of the T reg cell transcription factor FoxP3 paralleled the observed expression of

CD4 in diseased mice. Interestingly, we found no major differences between immunized WT SJL/J mice and TCR<sup>1640</sup> mice, which suffered from classical paralytic EAE. In line with their clinical picture, ataxic mice showed higher expression levels of the analyzed genes in brain (which also includes cerebellum and brain stem) than did paralytic relapsed mice. Conversely, expression in spinal cord was higher in paralytic relapsed mice than in ataxic mice. Intriguingly, most analyzed factors were elevated even in healthy TCR<sup>1640</sup> mice (score 0) as compared with healthy nontransgenic littermate (N1L) mice, likely indicating subclinical inflammation. Finally, during the remission phase, expression of all analyzed genes dropped down to similar values as in score 0–TCR<sup>1640</sup> mice (Fig. S4).

#### Expansion of MOG-specific B cells in TCR<sup>1640</sup> single-transgenic SJL/J mice

Single-transgenic TCR<sup>1640</sup> mice showed evidence of a strong MOG-specific B cell response. Spontaneous EAE lesions of single-transgenic TCR<sup>1640</sup> animals displayed prominent deposits of Ig and some activated complement (Fig. 4). Furthermore, the inflamed CNS tissue contained, besides CD4<sup>+</sup> and CD8<sup>+</sup> lymphocytes, substantial numbers of B cells (5–40% of infiltrated lymphocytes) expressing CD19 or B220 as revealed by immunocytochemistry and flow cytometry (Fig. 3 and Fig. 4 E).

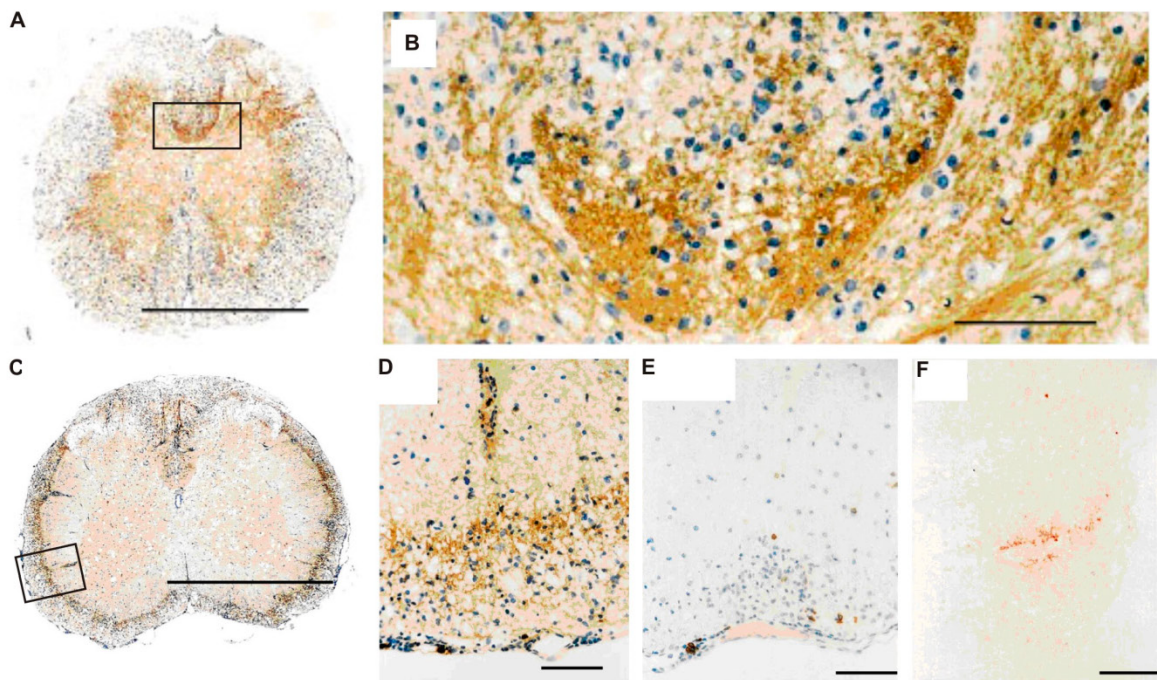


**Figure 4.** Ig deposition and B cell infiltrates in spinal cord of sick TCR<sup>1640</sup> × IgH<sup>MOG</sup> and TCR<sup>1640</sup> mice. (A–D) Histological analysis of spinal cord using anti-Ig antibodies shows deposition of Ig in sick TCR<sup>1640</sup> × IgH<sup>MOG</sup> (A and B) and TCR<sup>1640</sup> (C and D) mice (B and D show magnifications of marked areas in A and C, respectively). (E) Anti-B220 staining revealed some B cells among cellular infiltrates in sick TCR<sup>1640</sup> mice. (F) Deposition of complement C9neo within CNS lesions of TCR<sup>1640</sup> mice. Mononuclear cells were stained with H&E. Magnifications: A and C, ×50; B, ×425; D and E, ×200; F, ×450. Bars: (A and C) 1 mm; (B and D–F) 100  $\mu$ m. Data are representative of at least two independent experiments consisting of more than three mice per group.

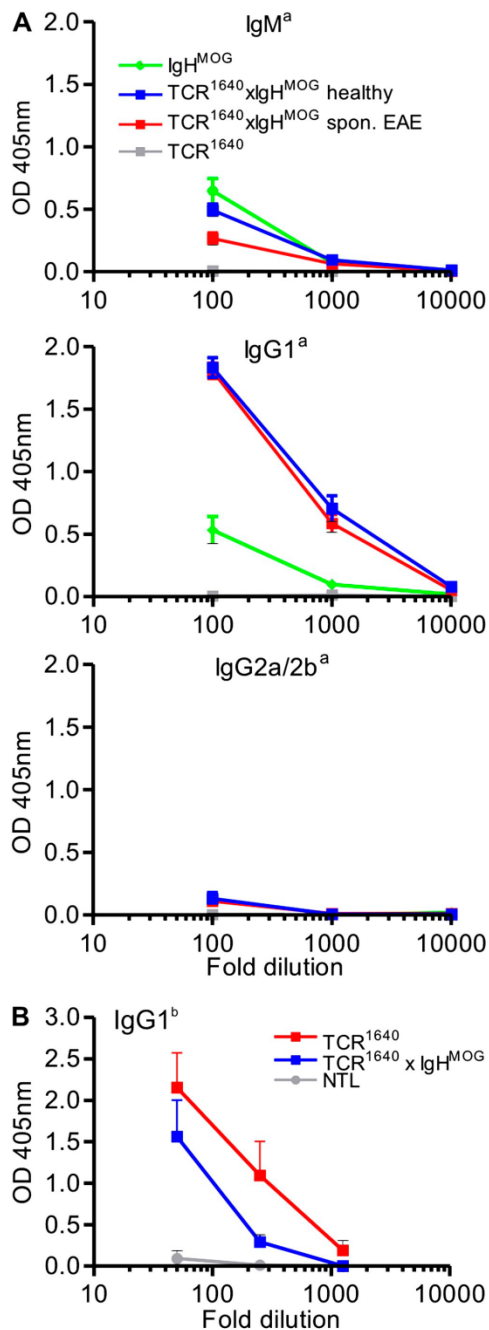


**Figure 5. MOG-specific antibodies in double-transgenic TCR<sup>1640</sup> × IgH<sup>MOG</sup> and single TCR transgenic mice.** (A) MOG binding allotype *a* autoantibodies were detected by ELISA in sera of indicated groups (each five to six mice). (B) Spontaneous anti-MOG IgG1 allotype *b* antibodies in TCR<sup>1640</sup> and TCR<sup>1640</sup> × IgH<sup>MOG</sup> but not in NTL (*n* = 5 for each group). Sera at the indicated dilutions were incubated with plates precoated with rMOG. Bound anti-MOG Ig was detected by allotype-specific antibodies as

Double-transgenic TCR<sup>1640</sup> × IgH<sup>MOG</sup> animals showed an anti-MOG antibody response dominated by the transgene-specific allotype *Igh<sup>a</sup>*. In addition, however, a minor part of the MOG-specific antibodies expressed the endogenous nontransgenic *Igh<sup>b</sup>* allotype (Fig. 5 B). Both antibody species were switched from IgM to IgG1 (Fig. 5, A and B).

Single-transgenic TCR<sup>1640</sup> mice also produced anti-MOG autoantibodies (of endogenous *Igh<sup>b</sup>*-allotype) reaching titers similar to those from WT mice immunized with rMOG (Fig. 6 A). The anti-MOG Igs were mainly of IgG1 and IgG2a/b isotypes, with very little IgM. The spontaneously appearing anti-MOG transgenic high frequency TCR<sup>1640</sup> mice formed autoantibodies irrespective of their EAE status. This contrasted with low frequency single-transgenic TCR<sup>1586</sup>, where anti-MOG autoantibodies were noted solely in the few animals with spontaneous EAE but not in resistant mice (Fig. 6 B). Also, mice of the EAE-resistant medium frequency line TCR<sup>1639</sup> did not produce spontaneous MOG-specific antibodies. Development of spontaneous MOG antibodies was dependent on the presence of the autoantigen. Sera of MOG-deficient TCR<sup>1640</sup> mice (bred on the *Mog*-deficient [*Mog*<sup>-/-</sup>] background [reference 13]) did not contain any MOG-specific antibodies (Fig. 6 B). The B cell response in TCR<sup>1640</sup> mice was specific to MOG and did not extend to other autoantigens (Fig. 6 C). In single-transgenic TCR<sup>1640</sup> mice, autoantibodies became demonstrable from 5 wk of life and, in our series of measurements, persisted up to 9–10 wk, but very young mice, up to 4 wk of age, had no anti-MOG Igs (IgG1 and IgG2a/b isotypes) (Fig. 6 D).

#### Contribution of endogenous B cells and anti-MOG autoantibodies to RR spontaneous EAE

There is evidence that only autoantibodies directed against conformational epitopes, not linear epitopes, are involved in the pathogenesis of EAE (14) and that SJL/J mice, but not C57BL/6 mice, are able to produce such antibodies upon immunization with rMOG in CFA (15). The anti-MOG autoantibodies formed spontaneously in TCR<sup>1640</sup> mice also bound to correctly folded MOG expressed on the surface of transduced EL4 cells and, thus, behaved like the classical anticonformational MOG mAb 8.18-C5 and its H chain transgene in TCR<sup>1640</sup> × IgH<sup>MOG</sup> mice (16) (Fig. 7 A). Binding of autoantibodies from TCR<sup>1640</sup> and sick TCR<sup>1586</sup> mice to EL4-MOG cells (dilutions of 1:20 and 1:200) followed by rabbit complement (Fig. 7 B) resulted in the specific lysis of the target cells. Sera from healthy TCR<sup>1586</sup> and TCR<sup>1639</sup> or *Mog*-deficient TCR<sup>1640</sup> did not support lysis (unpublished data).

We confirmed the pathogenic potential of antibodies, *in vivo*. We immunized WT SJL/J mice with a low dose of PLP 139–151 and with incipient clinical EAE symptoms (between scores 0.5 and 1), we transferred serum either from TCR<sup>1640</sup> mice (high titers of anti-MOG antibodies documented by ELISA) or NTLs, and compared the effects with the standard

indicated. Mean absorbance at OD 405 nm is shown. Error bars indicate SEM. Data are representative of two to three independent experiments.

anti-MOG monoclonal antibody 8.18C-5. In mice that had received TCR<sup>1640</sup> serum, we noted a statistically significant increase in EAE severity similar to that of 8.18C-5 mAb (Fig. 8 A).

To examine the importance of B cells in the development of spontaneous EAE, we depleted B cells in TCR<sup>1640</sup> mice using a monoclonal mouse anti-mouse CD20 antibody.

TCR<sup>1640</sup> mice were treated with anti-CD20 or isotype control (mouse IgG2a) every 2 wk starting on day 3. This protocol removed the B cells from peripheral blood, as well as spleen and lymph nodes, but left significant numbers of B cells in the bone marrow (Fig. S5, A and B). B cell depletion went along with either complete or partial loss of anti-MOG IgG1

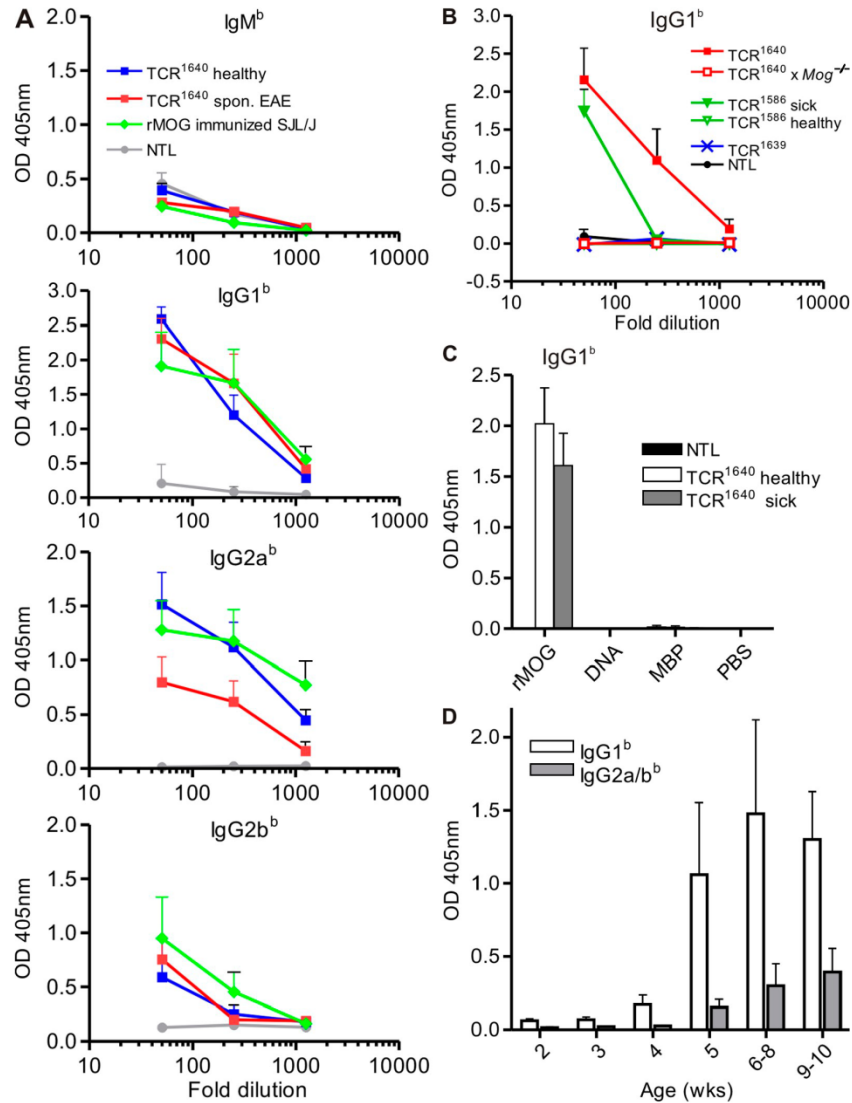


**Figure 6. MOG-specific antibodies in single TCR transgenic mice.** (A) Endogenous MOG binding antibodies of allotype *b* were measured by ELISA in sera of NTLs, healthy and sick TCR<sup>1640</sup>, and rMOG-immunized WT SJL/J ( $n = 6$  for each group). (B) Anti-MOG Igs of IgG1<sup>b</sup> isotype are formed in TCR<sup>1640</sup> and sick TCR<sup>1586</sup> but not in TCR<sup>1639</sup> or TCR<sup>1586</sup> mice. Control NTLs, as well as TCR<sup>1640</sup> mice deficient for MOG (*Mog*<sup>-/-</sup>), are devoid of MOG binding autoantibodies (each three to five mice per group). (C) Autoantibodies in sera from TCR<sup>1640</sup> mice are specific for MOG. Anti-MOG Ig antibodies, but not anti-MBP or anti-DNA-specific antibodies, were detected by ELISA in sera from TCR<sup>1640</sup> mice (1/50 diluted) using IgG1<sup>b</sup>-specific antibodies ( $n = 5$ ). (D) Appearance of anti-MOG IgG1<sup>b</sup> and IgG2a/b<sup>b</sup> in TCR<sup>1640</sup> mice by 5 wk of age. MOG binding antibodies were measured in 1/100 diluted sera from mice of different ages, each with three to five mice per group. Sera at the indicated dilutions were incubated with plates precoated with rMOG. Bound anti-MOG Ig was detected by allotype-specific antibodies as indicated. Mean absorbance at OD 405 nm is shown. Error bars indicate SEM. Data are representative of two independent experiments.



serum autoantibodies (Fig. S5 C). Within an observation period of up to 30 wk, only one out of nine anti-CD20-treated mice presented mild and transient EAE symptoms, whereas in mice receiving control antibody, spontaneous EAE was noted in >85% of the cases (Fig. 8 B and Table S3).

## DISCUSSION

The RR mouse, as described in this paper, is the first transgenic mouse model that recapitulates the major features of RR-MS, the most prevalent type of human inflammatory demyelination. The disease starts spontaneously and, in contrast to OSE mice described previously (2, 3), in most cases takes an RR course, with clinical signs differing between individual bouts. Importantly, development of spontaneous disease goes along with the expansion of myelin autoimmune B cells from the endogenous immune repertoire.

### Spontaneous RR-EAE

RR mice are transgenic SJL/J mice expressing at high frequency a TCR specific for MOG peptide 92–106 in the context of I-A<sup>b</sup>. RR mice differ substantially from previously created transgenic SJL/J mice expressing TCRs recognizing a dominant peptide of PLP (17). These animals, kept under specific pathogen-free conditions, developed spontaneous disease but, in contrast to RR mice, the disease was mostly progressive without remissions and subsequent relapses.

The course and clinical expression of autoimmune diseases are determined by diverse factors, both genetic and environmental. Indeed, SJL/J mice are predisposed to develop fluctuating disease. Depending on the protocol applied, active immunization against encephalitogenic proteins may trigger RR disease (18). Clearly, this response pattern is facilitated by distinct regulatory genes (19), which may also influence spontaneous EAE developing in RR mice. So far, our breeding results suggest that B10.S mice, which have a distinct genetic background but share the MHC and the TCR transgene with SJL/J RR mice, very rarely develop spontaneous EAE, and in the few cases observed, the disease took a chronic rather than RR course (unpublished data).

Most variants of induced EAE present a stereotypical clinical syndrome with motor deficiencies starting at tail and hind limbs and progressing cranially with ongoing disease. Histologically, this clinical picture is reflected by a caudocranial gradient of inflammatory lesions (20). In a few models, however, additional parts of the CNS are affected. For example, in C57BL/6 mice, MOG-induced EAE has a predilection to affect the optic nerve (2, 3), and cerebellar disease was noted in further antigen/mouse combinations (21, 22). Our RR mouse models are the first to show immune attacks against different CNS parts in subsequent inflammatory relapses. They thus provide a unique paradigm to study the mechanisms underlying the targeting of MS lesions within the CNS during ongoing disease.

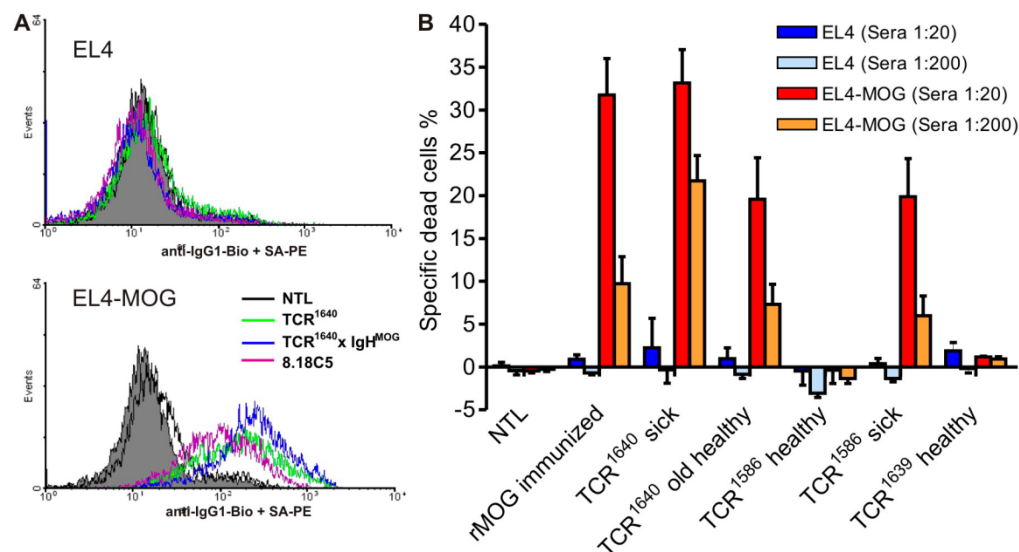


**Figure 7. MOG-specific autoantibodies bind MOG-expressing cells and activate complement.** (A) Binding of anti-MOG Ig from indicated mice to correctly conformed MOG on the cell surface of transduced EL4 cells (EL4-MOG) shown by flow cytometry. EL4 cells (top) and MOG-expressing EL4-MOG cells (bottom) were incubated with 1/200 diluted sera obtained from the indicated mice or 0.5  $\mu$ g/ml 8.18-C5 mAb. Bound antibodies were detected by FACS using biotinylated anti-IgG1-specific antibody (allotype unspecific) and streptavidin-PE (SA-PE). A representative plot of three independent experiments is shown. (B) Complement activating capability of MOG binding antibodies in sera from transgenic mice. EL4 and EL4-MOG cells were incubated with sera (1/20 and 1/200 diluted) obtained from the indicated mice, each with three to five per group. Complement activating capability was measured by cell lysis using propidium iodide (PI) staining after incubation of sera-bound EL4 cells with rabbit complement. Background values were subtracted, and shown are mean values with the SEM of one experiment representative of three similar experiments.

Several investigators reported that in RR-EAE actively induced by immunization with encephalitogenic peptides, relapses went along with the T cell reactivity against new epitopes (23), a phenomenon termed “determinant spreading” by Lehmann et al. (24). Recent work by McMahon et al. (25) suggests that in actively induced chronic EAE, initial bouts of CNS inflammation result in the induction of professional APCs within or near the affected CNS target tissue. By taking up myelin antigens and presenting crucial epitope components to newly arrived naive autoreactive T cells, the repertoire of target autoantigens spreads (25). It should, however, be mentioned that determinant spreading, i.e., recruitment of potentially encephalitogenic T cells specific for epitopes other

than MOG p92-106, has not been patent in spontaneous disease of our RR mice.

#### Expansion of MOG-specific B cells from endogenous repertoire

As described recently, in the C57BL/6 OSE model, MOG-reactive TCR transgenic T cells require the presence of MOG-specific B cells to kindle spontaneous EAE at high frequency. In this model, the MOG-specific B cells were transgenic with their germline IgJ region replaced by the rearranged H chain of a MOG-specific mAb (2, 3).

Based on these previous observations, we initially created double-transgenic mice by crossing our new MOG TCR

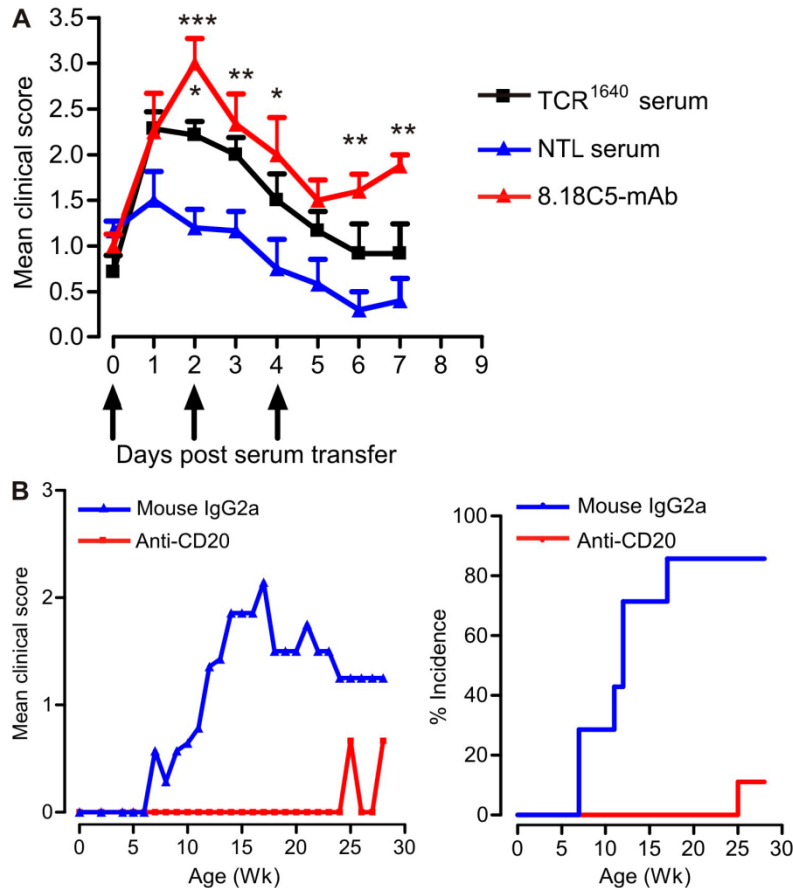


**Figure 8. B cells and anti-MOG antibodies are essential for spontaneous EAE.** (A) Spontaneously developed MOG-specific autoantibodies from TCR<sup>1640</sup> mice have pathogenic potential. EAE was induced in WT SJL/J mice by low-dose PLP 139–151 immunization. Serum from TCR<sup>1640</sup> mice, NTL mice, or 8.18c5 mAb were transferred after mice showed first clinical symptoms. Serum from TCR<sup>1640</sup> mice significantly increased disease severity in recipient mice compared with serum from NTL mice. Error bars indicate SEM. \*,  $P < 0.05$ ; \*\*,  $P < 0.01$ ; \*\*\*,  $P < 0.001$ . Data were pooled from two independent experiments, each six to seven per group. (B) B cell depletion protects TCR<sup>1640</sup> mice from spontaneous EAE. B cells were depleted from TCR<sup>1640</sup> mice by twice weekly injections of anti-CD20 antibodies from day 3 after birth, and control mice received mouse IgG2a antibodies. The development of spontaneous EAE was monitored regularly. Although 85% of isotype control antibody-treated mice developed spontaneous EAE, treatment with CD20 antibody protected TCR<sup>1640</sup> mice from disease development. Shown are the disease course (left) and the spontaneous EAE incidence (right) of TCR<sup>1640</sup> mice treated with these antibodies. Data were pooled from two independent experiments, each with six to seven per group.

transgenic SJL/J strain with MOG-specific B cell knock-in SJL/J mice. These mice presented with spontaneous RR-EAE at high frequency. Less expected spontaneous EAE was noted also in TCR single-transgenic SJL/J mice with a high proportion of MOG-reactive CD4 T cells but without transgenic B cells. It turned out that in these TCR single-transgenic mice, MOG-specific B cells were expanded from the endogenous B cell compartment. Substantial numbers of B cells were observed to invade the inflammatory lesions, and there were heavy local deposits of Ig along with some activated complement. Most importantly, TCR single transgenics produced high titers of anti-MOG autoantibodies of IgG1 and IgG2 isotypes, which bound to correctly conformed membrane bound autoantigen, destroyed MOG-expressing target cells, and, thus, have demyelinating potential (16).

MOG-reactive B cells are essential for the spontaneous development of RR-EAE. Depletion of B cells by treatment with anti-CD20 mAb profoundly suppressed RR-EAE when started at young age. Treatment of adult mice produced much more inconsistent results, a phenomenon which was recently noted in other investigations in actively induced EAE (26).

B cells contribute to immune and autoimmune responses by secreting humoral antibodies, by acting as APCs, and by releasing cytokines. RR mice, both single and double transgenic, produce MOG-specific autoantibodies that share their dominant isotype, IgG1, with the original demyelinating anti-MOG mAb 8.18-C5 and that, in vivo, aggravate EAE when transferred i.v. (27). Importantly, we found large Ig deposits in the demyelinating lesions of single- and double-transgenic RR mice. At least part of these antibodies may have been produced by local infiltrating B cells. In fact, B cells isolated from CNS infiltrates were found to secrete anti-MOG antibodies at high levels.

Beyond autoantibody secretion, MOG-specific B cells profoundly influence autoimmune responses by directly interacting with autoimmune T cells. In OSE mice, as well as in TCR<sup>1640</sup> × IgH<sup>MOG</sup> mice (unpublished data), MOG-specific B cells concentrate highly diluted MOG and present the antigen to MOG-reactive T cells. Hence, antigen-presenting B cells may contribute to the initiation and progression of spontaneous EAE. But, in addition, B cells may act into the opposite direction; they were shown to limit EAE by releasing IL-10 (28) and by influencing function of regulatory T cells (29).

The spontaneous recruitment and expansion of autoimmune B cells from the endogenous repertoire by organ-specific autoimmune T cells in the absence of exogenous autoantigen represents a mechanism of autoimmunity that has not yet been described. The MOG-specific B cell expansion process critically requires the presence of the endogenous target autoantigen, as *Mog*-deficient TCR transgenic SJL/J mice never produced anti-MOG autoantibodies, nor did they develop spontaneous RR-EAE.

The role of endogenous MOG is intriguing, considering that this target autoantigen is predominantly confined to the CNS tissues, which are largely inaccessible to circulating T and B cells. This hidden localization distinguishes the RR mouse paradigm from transgenic mice, where activation of

virus-specific B cell was noted in the presence of high numbers of virus-specific transgenic CD4<sup>+</sup> T cells and a viral pseudo-autoantigen expressed throughout the organism in cell types including DCs and macrophages (30).

Several mechanisms could be involved in MOG-specific B cell expansion. MOG-specific T cells could intrude into the naive CNS and create immunogenic conditions that allow the activation and expansion of naive B cells in the local milieu. This scenario has been forwarded recently as an explanation of epitope spreading in actively induced EAE (25). Alternatively, immunogenic MOG and/or myelin debris could be transported to local lymph nodes, either as cell-free material or by phagocytes, to be presented there to autoreactive B cells (31). Although MOG is predominantly expressed in the CNS, its messenger RNA was also found in some non-CNS organs, such as thymus, spleen, and liver (13, 32, 33), and low protein levels were found in the peripheral nervous system (34). Presentation of very low amounts of peripherally available MOG remains, at least in theory, an alternative mechanism of B cell expansion in RR mice.

Finally, animal models with spontaneously developing EAE show promise for the discovery of new drugs and the validation of existing medications. Thus, the opticospinal type of EAE described previously may represent essential features of human OSMS/Devic's disease (2), a disease variant which is rarely found in high prevalence populations. The spontaneous RR-EAE, with its conspicuous variation of neurological deficiencies, will provide a model for the most frequent type of MS, as it is seen typically in early phases of the disease.

## MATERIALS AND METHODS

**Mice.** SJL/J mice were purchased from Charles River Laboratories. *Mog* KO mice (13) were backcrossed into SJL/J for seven generations, crossed with TCR<sup>1640</sup> transgenic SJL/J mice, and then intercrossed to generate TCR<sup>1640</sup> transgenic *Mog* KO mice. All mouse strains were bred in the animal facilities of the Max Planck Institute of Neurobiology (Martinsried, Germany).

**Generation of TCR transgenic mice.** TCR donor clone (C3) was selected from a panel of MOG-specific T cell clones (series SL48) derived from a SJL/J mouse immunized with rMOG in CFA. The encephalitogenic clone C3 uses V $\alpha$ 8.3 along with V $\beta$ 4 and recognizes MOG<sub>92-106</sub> bound to I-A<sup>b</sup>. Total RNA of clone C3 was isolated by TRI reagent extraction (Sigma-Aldrich) and, after DNase I treatment, was converted into complementary DNA (cDNA) using hexanucleotide primers and Superscript II reverse transcription (Invitrogen). The rearranged cDNA of TCR- $\alpha$ 8.3 and TCR- $\beta$ 4 chains were amplified with the following primer pairs: TCR- $\alpha$ 8.3 sense with SalI restriction site, 5'-AGGTGTCGACCTTCCATGAACATGCGTCTGACACC-3'; TCR- $\alpha$  C terminus with BamHI restriction site, 5'-ATAGGATCCTCAACTGGACACAGCCCTCAGC-3'; TCR- $\beta$ 4 sense with SalI restriction site, 5'-AGGTGTCGACTGACACTGCTATGGGCTCCATTTTCTC-3'; and TCR- $\beta$  C2 terminus with BamHI restriction site, 5'-ATAGGATCCGGGTGAAGAACGGCTCAGGATGC-3' (all synthesized at Metabion). The rearranged TCR- $\alpha$ 8.3 and TCR- $\beta$ 4 chains from C3 cDNA were verified by sequencing. To eliminate a XhoI restriction site (CTC GAG) in TCR- $\beta$ 4 at aa 116, GAG was changed into GAA, both coding for glutamate, using a site-directed mutagenesis kit (Agilent Technologies) with the following primer pair: V $\beta$ 4 XhoI-Mut sense, 5'-CCAGACTGACTGTTCTCGAAGATCTGAGAAATGTG-3'; and V $\beta$ 4 XhoI-Mut, 5'-CACATTTCTCAGATCTCGAGAACAGTCAGCTGG-3'. The amino acid sequence of the CDR3 regions is as follows: T $\alpha$ 8.3, LYY

CALSGGNNAPR<sub>FG</sub> (V8.3J4); and TCR- $\beta$ 4, CASS QERT DSAE TLY (V4D1J2.3C2). The complete rearranged TCR chains were cloned into the pHSE3' vector (35), leading to expression under the control of the transgenic MHC class I H2-K<sup>b</sup> promoter. XhoI-linearized TCR-containing plasmids were coinjected into the pronuclei of fertilized FVB oocytes. Transgenic founders were identified by PCR using a specific primer for C3 V $\alpha$ -J $\alpha$  or V $\beta$ -J $\beta$  in combination with a pHSE3'-specific primer (TCR- $\alpha$  chain: mTCR-V $\alpha$ 8.3-CDR3 sense, 5'-CTCCATAAGAGCAGCAGCTCC-3', and hu  $\beta$ -globin antisense, 5'-CGTCTGTTTCCCATTCTAAACTGTACC-3'; TCR- $\beta$  chain: PH-2Kb sense, 5'-CTGGATATAAAGTCCACGCAGCC-3', and TCR-V $\beta$ 4-CDR3 antisense, 5'-CAATCTCTGCTTTTGATGGCTCAAAAC-3'). Transgenic mice were backcrossed for at least eight generations into the SJL/J background.

**EAE induction and scoring.** Mice were injected s.c. at the back with 200  $\mu$ l of recombinant MOG (200  $\mu$ g), which was emulsified in Freund's adjuvant and supplemented with 3 mg/ml *Mycobacterium tuberculosis* (strain H37Ra). 200 ng of pertussis toxin was injected i.p. on days 0 and 2 after immunization. Clinical scoring of classical paralytic EAE was performed as follows: score 0, healthy; 1, flaccid tail; 1.5, flaccid tail and impaired righting reflex; 2, impaired righting reflex and hind limb weakness; 2.5, one hind leg paralyzed; 3, both hind legs paralyzed with residual mobility in both legs; 3.5, both hind legs completely paralyzed; 4, both hind legs completely paralyzed and beginning front limb paralysis; and 5, moribund or death of the animal after preceding clinical disease. Ataxic scoring was as follows: score 0, healthy; 1, mouse partly tilted, feet fall into cage fence; 2, tilted and tumbles; 3, mouse heavily tilted and moves in circles; 4, inability to walk, is only rolling, and 5, moribund. All animal procedures used were in accordance with guidelines of the committee on animals of the Max Planck Institute of Neurobiology and with the license of the Regierung von Oberbayern (Munich, Germany).

**Antigens.** Recombinant histidine-tagged rat MOG protein (aa 1–125) was purified from bacterial inclusion bodies (36). MOG peptide 90–110 (SDEGGYTCFRRDHSYQEEAA), MOG 1–26 (GQFRVIGPGYPYRALVGDAAELPCRI), and MOG 92–106 (DEGGYTCFRRDHSYQ) were synthesized at the core facility of the Max Planck Institute of Biochemistry (Martinsried, Germany) or BioTrend (Köln, Germany). All antigens used in the study were of >95% purity, analyzed by silver staining of PAGE (proteins) or HPLC analysis (peptides).

**In vitro proliferation assay.** Proliferation assays were performed as previously described (2). Each sample was run in triplicates, the proliferative response of which is represented by the mean  $\pm$  SEM. All assays were replicated at least three times.

**ELISA.** Cytokine measurements and determination of serum titers of MOG-specific antibodies was performed as previously described (2). Antibodies were obtained from BD, except the anti-IL-17 which was obtained from R&D Systems. Each assay was repeated at least three times.

**Flow cytometric analysis.** Single cell suspensions were prepared from spleen, lymph node, thymus, or CNS tissue by mechanical disruption via forcing through 40- $\mu$ m cell strainers (BD). Erythrocytes of spleen cell suspensions were lysed by hypotonic treatment. CNS infiltrate cells were purified by Percoll gradient centrifugation. Cells were resuspended in Percoll (GE Healthcare) at a density of 1.035 g/ml and centrifuged over Percoll of a 1.08-g/ml density for 30 min at 20°C. The interphase was recovered and subjected to FACS analysis. For detection of cell surface markers by flow cytometric analysis, cells were stained in FACS medium (PBS containing 1% BSA and 0.1% NaN<sub>3</sub>) with different fluorochrome-labeled MAbs. For cytofluorometry, we used the FACSCalibur system with CellQuest software (BD), and for analysis we used WinMDI 2.9 software (Joe Trotter, The Scripps Institute, La Jolla, CA) was used. For intracellular cytokine staining, cells were first surface stained and then fixed and permeabilized in 4% PFA/0.1% saponin in Hepes-buffered HBSS, stained intracellularly, and washed. Before staining, cells were activated with 50 ng/ml PMA/500 ng/ml ionomycin in the presence of 5  $\mu$ g/ml brefeldin A for 4 h. The following

fluorochrome-labeled antibodies were purchased from BD or eBioscience: CD3 (145-2C11), CD4 (RM4-5), CD8 (53-6.7), V $\alpha$ 8.3 (B21.14), V $\beta$ 4 (KT4), CD11b (M1/70), CD45.1 (A20), CD19 (1D3), B220 (RA3-6B2), CD62L (MEL-14), CD25 (PC61), IFN- $\gamma$  (XMG1.2), IL-17 (TC11-18H10), and IgG1 (A85-1).

**Histological analysis.** Brain and spinal cord tissue from mice fixed by perfusion with 4% phosphate buffered paraformaldehyde were embedded in paraffin. Paraffin sections were stained with H&E, with Luxol fast blue for myelin, and by Bielschowsky silver impregnation for visualization of neurons and axons. Adjacent serial sections were stained by immunocytochemistry, using primary antibodies directed against CD3, B220, Mac-3, mouse Ig, and rat/mouse complement C9 neoantigen. Immunocytochemistry was performed with a biotin avidin technique.

**Quantitative real-time TaqMan PCR analysis.** Real time quantitative PCR analysis was performed as previously described (2). Quantification of the expression of mouse immune and housekeeping genes was performed by Taqman PCR using the following primer/probe combinations: GAPDH sense, 5'-TCACCACCATGGAGAAGGC-3'; GAPDH antisense, 5'-GCT-AAGCAGTTGGTGGTGCA-3'; GAPDH probe, 5'-ATGCCCCATG-TTTGTGATGGGTGT-3'; mIL-5 sense, 5'-CCGCTCACCGAGCTCT-GTT-3'; mIL-5 antisense, 5'-AGATTTCTCCAATGCATAGCTGG-3'; IL-5 probe, 5'-CAGGAAGCCTCATCGTCTCATTGCTTGT-3'; mIL-10 sense, 5'-CAGAGAAGCATGGCCAGAA-3'; mIL-10 antisense, 5'-TGCTCCACTGCCTTGCTCTT-3'; mIL-10 probe, 5'-TGAGGCGCT-GCATCGATTCTCC-3'; mIL-17 sense, 5'-AACTCCCTGGCG-CAAAAGT-3'; mIL-17 antisense, 5'-GGCACTGAGCTTCCCAGATC-3'; mIL-17 probe, 5'-CCACGTCACCCCTGGACTCTCCACC-3'; mCD4 sense, 5'-CGTTTCTCTCATCATCAATAAACTTA-3'; mCD4 antisense, 5'-GGTGGTACCCGGACTGAAG-3'; mCD4 probe, 5'-CACTTTG-AACACCCACAACCTCCACCTCCT-3'; TCR-V $\alpha$ 8.3 sense, 5'-CCAC-GCCACTCTCCATAAGAG-3'; TCR-V $\alpha$ 8.3 antisense, 5'-CAGTAG-TACAGCCAGAGTCTGACA-3'; TCR-V $\alpha$ 8.3 probe, 5'-CCTGAGC-GAAAATACAGCGTTT-3'; TCR-V $\beta$  sense, 5'-TAGTGCCTGGCC-ACATACTTC-3'; TCR-V $\beta$ 4 antisense, 5'-AGCAGCTCCTTCCATCT-GCAGAAGTCC-3'; TCR-V $\beta$ 4 probe, 5'-TGCCAGAGCCAAAGAACG-GACAGAT-3'; mFoxP3 sense, 5'-AGGAGAAGCTGGGAGCTATGC-3'; mFoxP3 antisense, 5'-TGGCTACGATGCAGCAAGAG-3'; mFoxP3 probe, 5'-AAGGCTCCATCTGTGGCCTCAATGGA-3'. IFN- $\gamma$ , TNF- $\alpha$ , IL-4, IL-13, and IP-10 Taqman probes were synthesized as described in Giulietti et al. (37).

**Cell surface serum binding and complement assay.** For EL4-MOG cells, the mouse *Mog* cDNA was cloned into the retroviral vector pLXSN (Clontech Laboratories, Inc.) and transformed into a GP+E-86 packaging cell line. Virus-containing supernatant was used to stably transduce the mouse EL4 lymphoma cell line. EL4 and MOG-transduced EL4 cells (EL4-MOG;  $2 \times 10^6$ /well) were incubated with sera at the indicated dilutions for 30–45 min at 4°C, washed intensively, and thereafter either stained with biotinylated anti-mouse IgG1 (BD) and streptavidin-PE diluted at 1/150 and PI at 1  $\mu$ g/ml or incubated with LOW-TOX-M rabbit complement (Cedarlane Laboratories) at a 1/10 dilution for 90 min at 37°C and thereafter analyzed for lysis by staining with PI. For analysis of binding only live (PI<sup>-</sup>) cells are gated for the histograms.

**Depletion of B cells.** For B cell depletion, 20  $\mu$ g of mouse anti-mouse CD20 (1B12; IgG2a; Biogen Idec) (38) or IgG2a control antibody (Sigma-Aldrich) was injected s.c. into 3-d-old TCR<sup>1640</sup> mice. 2 wk later, pups were injected with 80  $\mu$ g and, at 4 wk old, with 250  $\mu$ g of respective antibodies. Injections were repeated thereafter at 2-wk intervals with 250  $\mu$ g of respective antibodies.

**Serum transfer.** Sera were obtained through retroorbital bleeding from TCR<sup>1640</sup> or NTL. WT SJL/J mice were immunized with 100  $\mu$ g PLP139-151 in 5 mg/ml CFA. 200 ng of Pertussis toxin was injected on days 0 and 2. When mice showed clinical EAE signs (score  $\sim$ 1.0), they received i.p. injections of 250  $\mu$ l TCR<sup>1640</sup> serum or NTL serum or 8.18c5 mAb three times at 48-h intervals.

**Statistics.** Differential spontaneous EAE incidence of female to males was analyzed by logrank test (by an in-built survival curve analysis function from Prism 4 [Graph Pad Software, Inc.]), and the effect of serum transfer on EAE development was analyzed by two-way ANOVA. P-values < 0.05 were considered to be significant.

**Online supplemental material.** Fig. S1 shows the nature and encephalitogenicity of TCR donor clone C3. Fig. S2 shows the TCR expression in TCR<sup>1640</sup> transgenic mice splenocytes. Fig. S3 illustrates the spontaneous disease course of individual transgenic TCR<sup>1640</sup> animals. Fig. S4 shows the CNS messenger RNA expression analysis of spontaneous EAE- and MOG-immunized mice. Fig. S5 shows the efficiency of B cell depletion in TCR<sup>1640</sup> mice. Video S1 shows one diseased double-transgenic mouse in different EAE stages. Table S1 shows a summary of spontaneous EAE in TCR transgenic SJL/J mice. Table S2 shows a summary of histological analysis of representative individual mice with spontaneous EAE. Table S3 summarizes spontaneous EAE incidence and mortality in TCR<sup>1640</sup> mice treated with anti-CD20 and control isotype antibodies. Online supplemental material is available at <http://www.jem.org/cgi/content/full/jem.20090299/DC1>.

We are grateful to Irene Arnold-Ammer, Lydia Penner, Iris Jarsch, Michaela Krug, Marianne Leiszer, and Ulrike Kock for excellent technical support.

This project was supported by the Deutsche Forschungsgemeinschaft (SFB 571, Project B6) and the Max Planck society. S.H. Domingues is supported by a PhD fellowship (Portuguese FCT program SFRH/BD/15885/2005).

The authors have no conflicting financial interests.

Submitted: 6 February 2009

Accepted: 3 May 2009

## REFERENCES

- Krishnamoorthy, G., A. Holz, and H. Wekerle. 2007. Experimental models of spontaneous autoimmune disease in the central nervous system. *J. Mol. Med.* 85:1161–1173.
- Krishnamoorthy, G., H. Lassmann, H. Wekerle, and A. Holz. 2006. Spontaneous opticospinal encephalomyelitis in a double-transgenic mouse model of autoimmune T cell/B cell cooperation. *J. Clin. Invest.* 116:2385–2392.
- Bettelli, E., D. Baeten, A. Jäger, R.A. Sobel, and V.K. Kuchroo. 2006. Myelin oligodendrocyte glycoprotein-specific T and B cells cooperate to induce a Devic-like disease in mice. *J. Clin. Invest.* 116:2393–2402.
- Kira, J. 2003. Multiple sclerosis in the Japanese population. *Lancet Neurol.* 2:117–127.
- Compston, A. 2004. 'The marvellous harmony of the nervous parts': The origins of multiple sclerosis. *Clin. Med.* 4:346–354.
- Litzenburger, T., R. Fässler, J. Bauer, H. Lassmann, C. Lington, H. Wekerle, and A. Iglesias. 1998. B lymphocytes producing demyelinating autoantibodies: development and function in gene-targeted transgenic mice. *J. Exp. Med.* 188:169–180.
- Chen, Y., C.L. Langrish, B. McKenzie, B. Joyce-Shaikh, J.S. Stumhofer, T. McClanahan, W. Blumenschein, T. Churakova, J. Low, L. Presta, et al. 2006. Anti-IL-23 therapy inhibits multiple inflammatory pathways and ameliorates autoimmune encephalomyelitis. *J. Clin. Invest.* 116:1317–1326.
- Veldhoen, M., R.J. Hocking, R.A. Flavell, and B. Stockinger. 2006. Signals mediated by transforming growth factor- $\beta$  initiate autoimmune encephalomyelitis, but chronic inflammation is needed to sustain disease. *Nat. Immunol.* 7:1151–1156.
- Bettelli, E., Y. Carrier, W. Gao, T. Korn, T.B. Strom, M. Oukka, H.L. Weiner, and V.K. Kuchroo. 2006. Reciprocal developmental pathways for the generation of pathogenic effector TH17 and regulatory T cells. *Nature.* 441:235–238.
- Bailey, S.L., B. Schreiner, E.J. McMahon, and S.D. Miller. 2007. CNS myeloid DCs presenting endogenous myelin peptides 'preferentially' polarize CD4<sup>+</sup> TH-17 cells in relapsing EAE. *Nat. Immunol.* 8:172–180.
- Hori, S., T. Nomura, and S. Sakaguchi. 2003. Control of regulatory T cell development by the transcription factor *Foxp3*. *Science.* 299:1057–1061.
- Kishimoto, T., and T. Hirano. 1988. Molecular regulation of B lymphocyte response. *Annu. Rev. Immunol.* 6:485–512.
- Delarasse, C., P. Daubas, L.T. Mars, C. Vizler, T. Litzenburger, A. Iglesias, J. Bauer, B. Della Gaspera, A. Schubart, L. Decker, et al. 2003. Myelin/oligodendrocyte glycoprotein-deficient (MOG-deficient) mice reveal lack of immune tolerance to MOG in wild-type mice. *J. Clin. Invest.* 112:544–553.
- von Büdingen, H.C., S.L. Hauser, A. Fuhrmann, C.B. Nabavi, J.I. Lee, and C.P. Genain. 2002. Molecular characterization of antibody specificities against myelin/oligodendrocyte glycoprotein in autoimmune demyelination. *Proc. Natl. Acad. Sci. USA.* 99:8207–8212.
- Bourquin, C., A. Schubart, S. Tobollik, I. Mather, S. Ogg, R. Liblau, and C. Lington. 2003. Selective unresponsiveness to conformational B cell epitopes of the myelin oligodendrocyte glycoprotein in H-2<sup>b</sup> mice. *J. Immunol.* 171:455–461.
- Brehm, U., S.J. Piddlesden, M.V. Gardinier, and C. Lington. 1999. Epitope specificity of demyelinating monoclonal autoantibodies directed against the human myelin oligodendrocyte glycoprotein. *J. Neuroimmunol.* 97:9–15.
- Waldner, H., M.J. Whitters, R.A. Sobel, M. Collins, and V.K. Kuchroo. 2000. Fulminant spontaneous autoimmunity of the central nervous system in mice transgenic for the myelin proteolipid protein-specific T cell receptor. *Proc. Natl. Acad. Sci. USA.* 97:3412–3417.
- Moore, G.R., R.M. McCarron, D.E. McFarlin, and C.S. Raine. 1987. Chronic relapsing necrotizing encephalomyelitis produced by myelin basic protein. *Lab. Invest.* 57:157–167.
- Butterfield, R.J., E.P. Blankenhorn, R.J. Roper, J.F. Zachary, R.W. Doerge, J.D. Sudweeks, J. Rose, and C. Teuscher. 1999. Genetic analysis of disease subtypes and sexual dimorphisms in mouse experimental allergic encephalomyelitis (EAE): Relapsing/remitting and monophasic remitting/nonrelapsing EAE are immunogenetically distinct. *J. Immunol.* 162:3096–3102.
- Wekerle, H., and H. Lassmann. 2006. The immunology of inflammatory demyelinating disease. In *McAlpine's Multiple Sclerosis*. A. Compston, C. Confavreux, H. Lassmann, I. McDonald, D. Miller, J. Noseworthy, K. Smith, and H. Wekerle, editors. Churchill Livingstone, Oxford. 491–546.
- Abramson-Leeman, S., R. Bronson, Y. Luo, M. Berman, R. Leeman, J. Leeman, and M. Dorf. 2004. T-cell properties determine disease site, clinical presentation, and cellular pathology of experimental autoimmune encephalomyelitis. *Am. J. Pathol.* 165:1519–1533.
- Muller, D.M., M.P. Pender, and J.M. Greer. 2005. Blood-brain barrier disruption and lesion localization in experimental autoimmune encephalomyelitis with predominant cerebellar and brainstem involvement. *J. Neuroimmunol.* 160:162–169.
- McCarron, R.M., R.J. Fallis, and D.E. McFarlin. 1990. Alterations in T cell antigen specificity and class II restriction during the course of chronic relapsing experimental allergic encephalomyelitis. *J. Neuroimmunol.* 29:73–79.
- Lehmann, P.V., T. Forsthuber, A. Miller, and E.E. Sercarz. 1992. Spreading of T-cell autoimmunity to cryptic determinants of an autoantigen. *Nature.* 358:155–157.
- McMahon, E.J., S.L. Bailey, C.L. Vanderlugt-Castaneda, H. Waldner, and S.D. Miller. 2005. Epitope spreading initiates in the CNS in two mouse models of multiple sclerosis. *Nat. Med.* 11:335–339.
- Matsushita, T., K. Yanaba, J.-D. Bouaziz, M. Fujimoto, and T.F. Tedder. 2008. Regulatory B cells inhibit EAE initiation in mice while other B cells promote disease progression. *J. Clin. Invest.* 118:3420–3430.
- Gunn, C., A.J. Suckling, and C. Lington. 1989. Identification of a common idiotype of myelin oligodendrocyte glycoprotein-specific autoantibodies in chronic relapsing experimental allergic encephalomyelitis. *J. Neuroimmunol.* 23:101–108.
- Fillatreau, S., C.H. Sweeney, M.J. McGeachy, D. Gray, and S.M. Anderton. 2002. B cells regulate autoimmunity by provision of IL-10. *Nat. Immunol.* 3:944–950.
- Mann, M.K., K. Maresz, L.P. Shriver, Y.P. Tan, and B.N. Dittel. 2007. B cell regulation of CD4<sup>+</sup>CD25<sup>+</sup> T regulatory cells and IL-10 via B7 is essential for recovery from experimental autoimmune encephalomyelitis. *J. Immunol.* 178:3447–3456.

30. Guay, H.M., J. Larkin, C. Cozzo Picca, L. Panarey, and A.J. Caton. 2007. Spontaneous autoreactive memory B cell formation driven by a high frequency of autoreactive CD4<sup>+</sup> T cells. *J. Immunol.* 178:4793–4802.
31. De Vos, A.F., M. Van Meurs, H.P. Brok, L.A. Boven, R.Q. Hintzen, P. Van der Valk, R. Ravid, S. Rensing, L. Boon, B.A. 't Hart, and J.D. Laman. 2002. Transfer of central nervous system autoantigens and presentation in secondary lymphoid organs. *J. Immunol.* 169:5415–5423.
32. Derbinski, J., A. Schulte, B. Kyewski, and L. Klein. 2001. Promiscuous gene expression in medullary thymic epithelial cells mirrors the peripheral self. *Nat. Immunol.* 2:1032–1039.
33. Pagany, M., M. Jagodic, C. Bourquin, T. Olsson, and C. Linington. 2003. Genetic variation in myelin oligodendrocyte glycoprotein expression and susceptibility to experimental autoimmune encephalomyelitis. *J. Neuroimmunol.* 139:1–8.
34. Pagany, M., M. Jagodic, A. Schubart, D. Pham-Dinh, C. Bachelin, A.B. van Evercooren, F. Lachapelle, T. Olsson, and C. Linington. 2003. Myelin oligodendrocyte glycoprotein is expressed in the peripheral nervous system of rodents and primates. *Neurosci. Lett.* 350:165–168.
35. Pircher, H., T.W. Mak, R. Lang, W. Ballhausen, E. Rüedi, H. Hengartner, R.M. Zinkernagel, and K. Bürki. 1989. T cell tolerance to Mls<sup>+</sup> encoded antigens in T cell receptor V $\beta$ 8.1 chain transgenic mice. *EMBO J.* 8:719–727.
36. Adelman, M., J. Wood, I. Benzel, P. Fiori, H. Lassmann, J.-M. Mathieu, M.V. Gardinier, K. Dornmair, and C. Linington. 1995. The N-terminal domain of the myelin oligodendrocyte glycoprotein (MOG) induces acute demyelinating experimental autoimmune encephalomyelitis in the Lewis rat. *J. Neuroimmunol.* 63:17–27.
37. Giulietti, A., L. Overbergh, D. Valckx, B. Decallonee, R. Bouillon, and C. Mathieu. 2001. An overview of real-time quantitative PCR: Applications to quantify cytokine gene expression. *Methods.* 25:386–401.
38. Hamel, K., P. Doodes, Y.X. Cao, Y.M. Wang, J. Martinson, R. Dunn, M.R. Kehry, B. Farkas, and A. Finnegan. 2008. Suppression of proteoglycan-induced arthritis by anti-CD20 B cell depletion therapy is mediated by reduction in autoantibodies and CD4<sup>+</sup> T cell reactivity. *J. Immunol.* 180:4994–5003.

# **Publication 3**

## ARTICLES

nature  
medicine

## Myelin-specific T cells also recognize neuronal autoantigen in a transgenic mouse model of multiple sclerosis

Gurumoorthy Krishnamoorthy<sup>1</sup>, Amit Saxena<sup>2</sup>, Lennart T Mars<sup>2</sup>, Helena S Domingues<sup>1,3</sup>, Reinhard Mentele<sup>4,5</sup>, Avraham Ben-Nun<sup>6</sup>, Hans Lassmann<sup>7</sup>, Klaus Dornmair<sup>1,4,9</sup>, Florian C Kurschus<sup>1,8,9</sup>, Roland S Liblau<sup>2,9</sup> & Hartmut Wekerle<sup>1</sup>

We describe here the paradoxical development of spontaneous experimental autoimmune encephalomyelitis (EAE) in transgenic mice expressing a myelin oligodendrocyte glycoprotein (MOG)-specific T cell antigen receptor (TCR) in the absence of MOG. We report that in *Mog*-deficient mice (*Mog*<sup>-/-</sup>), the autoimmune response by transgenic T cells is redirected to a neuronal cytoskeletal self antigen, neurofilament-M (NF-M). Although components of radically different protein classes, the cross-reacting major histocompatibility complex I-A<sup>b</sup>-restricted epitope sequences of MOG<sub>35-55</sub> and NF-M<sub>18-30</sub> share essential TCR contact positions. This pattern of cross-reaction is not specific to the transgenic TCR but is also commonly seen in MOG<sub>35-55</sub>-I-A<sup>b</sup>-reactive T cells. We propose that in the C57BL/6 mouse, MOG and NF-M response components add up to overcome the general resistance of this strain to experimental induction of autoimmunity. Similar cumulative responses against more than one autoantigen may have a role in spontaneously developing human autoimmune diseases.

Organ-specific autoimmune disease is a key group of inflammatory disorders that includes rheumatoid arthritis, type 1 diabetes mellitus, thyroiditis and multiple sclerosis. The prevailing thinking is that the pathogenic changes are typically initiated and driven by T cells, which express receptors for autoantigens restricted to, or enriched within, the particular target tissues.

Unfortunately, it has been impossible so far to identify, with certainty, which autoantigens are the targets in individual humans. One reason for this limitation is the complexity of the human autoimmune response. Indeed, there is evidence that in one person more than one self antigen may be the target of the autoimmune attack and that, in addition, the profile of target autoantigens may fluctuate over time<sup>1</sup>. Furthermore, the peripheral immune repertoire of healthy humans contains a large number of T cells specific for many, if not all, autoantigens potentially related to autoimmune diseases<sup>2</sup>. There is no practical assay to distinguish T cells with high pathogenic potential from nonpathogenic counterparts and, moreover, to identify in humans the T cells participating in the pathogenesis from those that are uninvolved.

We report here a new mechanism of autoimmunity, ‘cumulative autoimmunity’, that may provide a solution to this dilemma. Cumulative autoimmunity designates an autoimmune response that

targets more than one particular cognate autoantigenic target at the same time, and the accumulation of these responses results in a tissue attack of enhanced vigor.

We observed a cumulative autoimmune response in transgenic mice with a TCR selected for reactivity to MOG peptide<sub>35-55</sub>, who develop spontaneous EAE in the presence of MOG and, unexpectedly, also in its absence. We found that in *Mog*-deficient mice, the transgenic T cells recognize a peptide fragment of the medium-sized neurofilament NF-M.

## RESULTS

## Spontaneous EAE in the absence of MOG

In an experiment designed to detail the role of the autoantigen in spontaneous autoimmunity, we bred transgenes encoding the MOG-specific TCR 2D2 (ref. 3) and immunoglobulin heavy chain specific for MOG (IgH<sup>MOG</sup>) (ref. 4) either separately or together into *Mog*<sup>-/-</sup> mice<sup>5</sup> (Fig. 1). To our surprise, spontaneous EAE developed in *Mog*-deficient 2D2 transgenic mice (2D2 × *Mog*<sup>-/-</sup>) with incidence and kinetics indistinguishable from those of wild-type (WT) counterparts. Between 15% and 20% of 2D2 × *Mog*<sup>-/-</sup> mice developed spontaneous EAE (Fig. 1a and Supplementary Table 1 online). *Mog*<sup>-/-</sup> mice and the *Mog*-deficient IgH<sup>MOG</sup> mice (IgH<sup>MOG</sup> × *Mog*<sup>-/-</sup>), whose B cells, but not T cells, are specific for MOG, remained healthy (Fig. 1a

<sup>1</sup>Department of Neuroimmunology, Max Planck Institute of Neurobiology, Martinsried, Germany. <sup>2</sup>Institut National de la Santé et de la Recherche Médicale, Unité 563, Université Toulouse III, Paul-Sabatier, Toulouse, France. <sup>3</sup>PhD Program in Experimental Biology and Biomedicine, Center for Neuroscience and Cell Biology, University of Coimbra, Coimbra, Portugal. <sup>4</sup>Institute of Clinical Neuroimmunology, University Hospital Grosshadern, Ludwig-Maximilians University, Munich, Germany.

<sup>5</sup>Department for Protein Analytics, Max Planck Institute of Biochemistry, Martinsried, Germany. <sup>6</sup>Department of Immunology, The Weizmann Institute of Science, Rehovot, Israel. <sup>7</sup>Center for Brain Research, Medical University of Vienna, Vienna, Austria. <sup>8</sup>Present address: I. Medizinische Klinik und Poliklinik, Johannes Gutenberg Universität, Mainz, Germany. <sup>9</sup>These authors contributed equally to this work. Correspondence should be addressed to H.W. (hwekerle@neuro.mpg.de).

Received 10 June 2008; accepted 29 April 2009; published online 31 May 2009; doi:10.1038/nm.1975



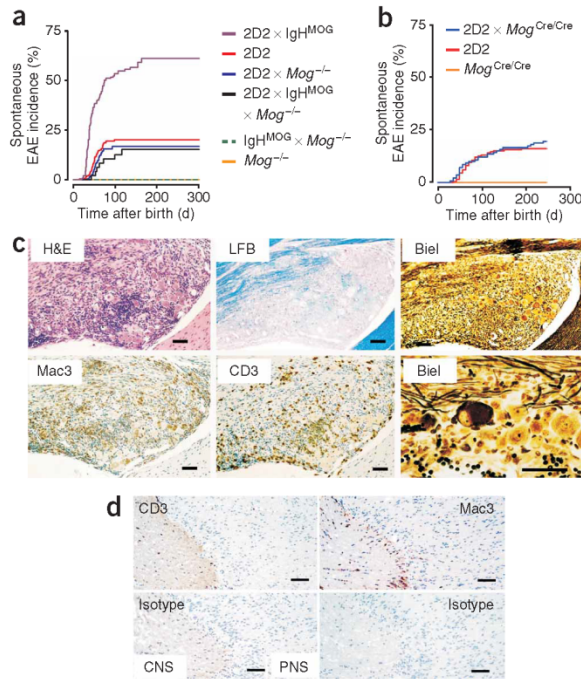


**Figure 1** Paradoxical development of spontaneous EAE in MOG-specific 2D2 TCR-transgenic mice in two different *Mog*-deficient strains. **(a)** Spontaneous incidence of EAE-like disease observed in transgenic mice carrying MOG-specific TCR (2D2), B cell receptor (IgH<sup>MOG</sup>) or both, on *Mog*-sufficient and *Mog*-deficient C57BL/6 backgrounds. Shown is the survival curve analysis of the mice that were observed for a minimum of 7 weeks after birth. 2D2,  $n = 440$ ; 2D2  $\times$  *Mog*<sup>-/-</sup>,  $n = 218$ ; 2D2  $\times$  IgH<sup>MOG</sup>,  $n = 258$ ; 2D2  $\times$  IgH<sup>MOG</sup>  $\times$  *Mog*<sup>-/-</sup>,  $n = 48$ ; IgH<sup>MOG</sup>  $\times$  *Mog*<sup>-/-</sup>,  $n = 63$ ; *Mog*<sup>-/-</sup>,  $n = 279$ . **(b)** Incidence of spontaneous EAE in MOG-specific 2D2-transgenic mice on a *Mog*-deficient background (different than in **a**). 2D2,  $n = 199$ ; 2D2  $\times$  *Mog*<sup>Cre/Cre</sup>,  $n = 140$ ; *Mog*<sup>Cre/Cre</sup>,  $n = 23$ . **(c)** Nervous system pathology of 2D2-transgenic mice with spontaneous EAE. Infiltration, demyelination and axonal damage in trigeminal ganglia were revealed by H&E, luxol fast blue (LFB) and Bielschowsky silver impregnation (Biel), respectively. The infiltrates are composed of macrophages (Mac3) as well as CD3<sup>+</sup> T cells. Scale bars, 100  $\mu$ m. **(d)** Nervous system pathology of C57BL/6 mice immunized with MOG<sub>35-55</sub>. The acute EAE lesions of CNS and PNS parts of the trigeminal nerve and ganglion were visualized by staining for macrophages (Mac3) and CD3<sup>+</sup> T cells. The bottom images show the respective isotype control antibody staining. Scale bars, 100  $\mu$ m.

**Fig. 1** online). To further exclude faulty MOG expression, we bred 2D2 TCR-transgenic mice with another line of *Mog*-knockout mice in which the 5' end of MOG exon 2 encoding the immunodominant MOG<sub>35-55</sub> epitope was deleted and replaced by the *Cre* recombinase gene (*Mog*<sup>Cre/Cre</sup>)<sup>8</sup> (**Supplementary Fig. 2** online). 2D2-transgenic mice crossed onto the *Mog*<sup>Cre/Cre</sup> background also developed spontaneous EAE at the same rate as 2D2-transgenic mice (**Fig. 1b**).

Spontaneous EAE in 2D2  $\times$  *Mog*<sup>-/-</sup> mice could also have been caused by T cells recruited from the endogenous repertoire or by T cells with dual TCR expression—expressing both 2D2 and endogenous receptor chains. Indeed, whereas in 2D2-transgenic mice most CD4<sup>+</sup> T cells use the transgenic TCR, there is also a considerable population with endogenous receptors (data not shown). In the absence of MOG, alternative TCRs might be stimulated to mount an attack against an alternative CNS target autoantigen. However, FACS analysis of 2D2 and 2D2  $\times$  *Mog*<sup>-/-</sup> thymus and spleen did not reveal any considerable differences in cell number or in activation markers such as CD25, CD44 and CD62 ligand (**Supplementary Fig. 3** online) or MOG-specific forkhead box P3-positive T regulatory cells (**Supplementary Fig. 4** online). In addition, the CNS infiltrates were predominantly composed of transgenic T cells with only a minor population of endogenous T cells (**Supplementary Fig. 5** online). Furthermore, we noted spontaneous EAE in two out of six triple-transgenic *Rag2*-deficient 2D2  $\times$  *Mog*<sup>-/-</sup> mice (2D2  $\times$  *Mog*<sup>-/-</sup>  $\times$  *Rag2*<sup>-/-</sup>), whose T cells express exclusively the transgenic TCR, indicating that transgenic T cells, not endogenous T cells, are the principal agents in the observed EAE.

Finally, the transgenic TCR might recognize an endogenous cross-reactive epitope. We tested some of the known encephalitogenic proteins and peptides such as myelin basic protein (MBP), S-100 calcium-binding protein, beta chain (S100 $\beta$ ) and proteolipid protein (PLP) amino acids 139–151, but none of them activated the 2D2-expressing T cells (**Fig. 2a**). Then we compared crude myelin preparations from *Mog*<sup>+/+</sup> and *Mog*<sup>-/-</sup> CNS isolated by classical protocols<sup>9,10</sup>. Both preparations activated MOG-specific 2D2-expressing cells to a comparable degree when presented by syngeneic bone marrow-derived dendritic cells (BMDCs) (**Fig. 2a**) but did not stimulate ovalbumin-specific OT-II TCR transgenic T cells, which we used as negative controls. Furthermore, myelin-induced proliferation of 2D2-transgenic T cells was blocked by antibodies to CD4 and major histocompatibility complex (MHC) class II but not by antibody to CD1d or control rat antibodies (**Fig. 2b**).

and **Supplementary Table 1**). Fifty percent of double-transgenic 2D2  $\times$  IgH<sup>MOG</sup> mice (also known as OSE/Devic mice<sup>6</sup>) spontaneously develop opticospinal myelitis<sup>3,6</sup>, but, in a limited cohort of MOG-deficient 2D2  $\times$  IgH<sup>MOG</sup> mice, fewer than 15% of the mice developed spontaneous EAE, a proportion similar to the one seen with *Mog*-deficient 2D2 mice but substantially lower than that in 2D2  $\times$  IgH<sup>MOG</sup> *Mog*-sufficient counterparts (**Fig. 1a** and **Supplementary Table 1**).

Clinically, spontaneous EAE was indistinguishable between *Mog*-sufficient and *Mog*-deficient transgenic mice. In all groups, disease started between 7 and 10 weeks of age, with classical paralytic EAE signs and, in a minority of cases, with a spastic component (**Supplementary Table 1** and **Supplementary Movies 1–6** online).

The lesions in *Mog*-sufficient and *Mog*-deficient groups were indistinguishable (data not shown), and they were restricted to the optic nerve and spinal cord<sup>6,7</sup>. In addition, we have now observed inflammatory infiltrates in the trigeminal ganglia, spinal ganglia, spinal roots and peripheral nerves, despite the absence of MOG within these tissues (**Fig. 1c** and **Supplementary Table 2** online). However, in mice immunized with MOG<sub>35-55</sub>, the acute EAE lesions were present only in the central nervous system (CNS) and not in the peripheral nervous system (PNS; **Fig. 1d**).

#### 2D2-transgenic T cells recognize a non-MOG CNS autoantigen

EAE in the *Mog*<sup>-/-</sup> mice might be explained by the incomplete deletion of *Mog*. The *Mog* knockout strain initially used in this study was created by the insertion of a cassette containing the LacZ and neomycin resistance genes behind the *Mog* promoter, leaving the MOG coding sequence intact<sup>5</sup>, which could leave some aberrant MOG expression in 2D2  $\times$  *Mog*<sup>-/-</sup> mice. However, in line with the original description of the *Mog*<sup>-/-</sup> mice<sup>5</sup>, western blot analyses with monoclonal as well as polyclonal antibodies did not detect any residual MOG protein expression in *Mog*<sup>-/-</sup> mice (**Supplementary**

## ARTICLES

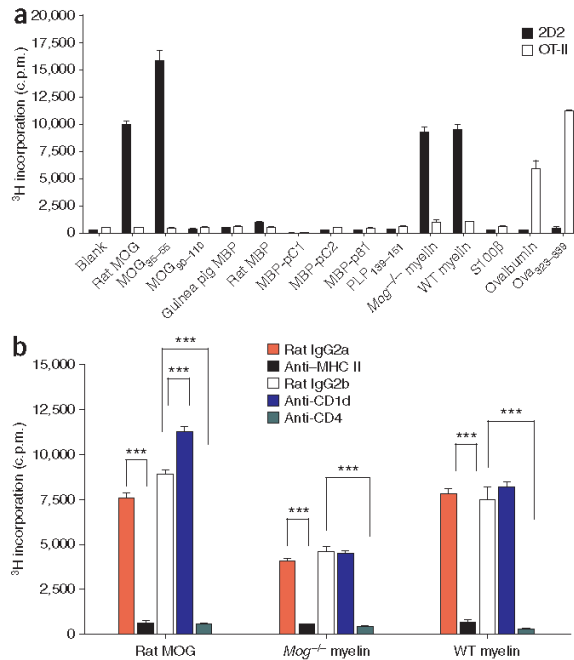


**Figure 2** MOG-specific T cells respond to myelin from *Mog*<sup>-/-</sup> mice.

(a) Proliferation, as measured by <sup>3</sup>H-thymidine incorporation assay, of spleen cells from 2D2-transgenic or control OT-II mice ( $2 \times 10^5$  cells per well) together with BMDCs ( $5 \times 10^4$  cells per well) cultured with the indicated proteins, peptides ( $20 \mu\text{g ml}^{-1}$ ) or myelin preparations ( $1 \mu\text{l}$  per well) from *Mog*<sup>-/-</sup> and WT mice. pC1, rat MBP<sub>68-84</sub>; pC2, guinea pig MBP<sub>45-67</sub>; p81, guinea pig MBP<sub>69-83</sub>. (b) Proliferation, as measured by <sup>3</sup>H-thymidine incorporation assay, of 2D2-transgenic spleen cells together with BMDCs incubated with rat MOG ( $20 \mu\text{g ml}^{-1}$ ) or myelin suspension ( $1 \mu\text{l}$  per well) preparations from *Mog*<sup>-/-</sup> and WT mice. The antibodies to MHC II (Anti-MHC II), CD1d (Anti-CD1d) or CD4 (Anti-CD4) or control rat IgG2a and rat IgG2b antibodies were added at  $10 \mu\text{g ml}^{-1}$ . Proliferation of T cells from a and b was measured by labeling with <sup>3</sup>H-thymidine during the last 16 h of a 72-h assay. Shown is the mean  $\pm$  s.e.m. of triplicate measurements. Statistical significance was analyzed by analysis of variance.  $***P < 0.001$ .

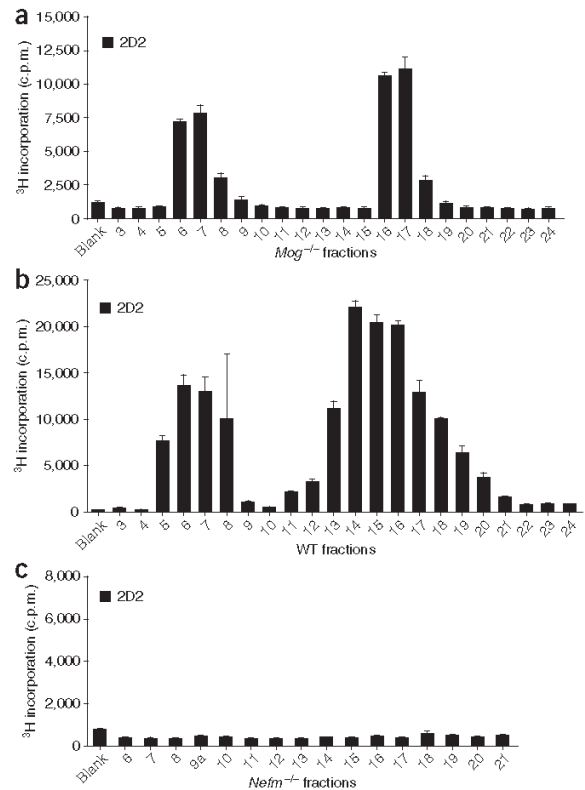
We tested the exclusive cross-reactivity of the NF-M with MOG-specific 2D2-transgenic T cells by an analysis of CNS proteins from NF-M-deficient (*Nefm*<sup>-/-</sup>) mice. None of the ion-exchange chromatography fractions from *Nefm*<sup>-/-</sup> mice activated 2D2-transgenic T cells (Fig. 3c and Supplementary Fig. 7c). In addition, we also found that the crude myelin preparations from both *Mog*<sup>-/-</sup> and WT mice that contained abundant amounts of NF-M (Supplementary Fig. 8a online), and not those from the *Mog*<sup>-/-</sup>  $\times$  *Nefm*<sup>-/-</sup> mice, activated 2D2-transgenic T cells (Fig. 2a and Supplementary Fig. 9 online). Full-length MOG, which is highly hydrophobic owing to its three membrane-spanning helices, was found mainly in the urea-insoluble fraction (data not shown). We detected only trace amounts of MOG in the urea-soluble extract but not in any of the 2D2-transgenic T cell-activating fractions from *Mog*-sufficient mice (Supplementary

### NF-M peptide cross-reacts with MOG-specific T cells

We systematically fractionated CNS tissue from *Mog*<sup>-/-</sup> mice (Fig. 3). We employed a purification regime composed of homogenization, lipid extraction and purification of the urea-dissolved proteins by ion-exchange and gel chromatography (Supplementary Fig. 6 online). Among the chromatography fractions presented to 2D2-expressing T cells by syngeneic antigen-presenting cells (BMDCs), we eluted several antigenic fractions from the anion-exchange column (Fig. 3a). Fractionation of *Mog*-sufficient CNS tissue led to a similar profile (Fig. 3b). Parallel fractionation of extracts from WT and *Mog*<sup>-/-</sup> CNS with the cation exchange column yielded similar results (Supplementary Fig. 7a,b online).

Gel filtration chromatography of both pooled positive fractions (fractions 16 and 17) from the anion exchange column resulted in one fraction (fraction 9) that was recognized by 2D2-expressing T cells (Fig. 4a). SDS-PAGE analysis revealed two prominent bands with molecular masses of approximately 68 kDa and 150 kDa (Fig. 4b). We excised both bands from the gel, in-gel digested them with trypsin and subjected them to matrix-assisted laser desorption/ionization-time-of-flight mass spectrometry. We identified the 68-kDa protein as the light chain of mouse neurofilament (NF-L) and the 150-kDa protein as NF-M.

**Figure 3** Fractionation of CNS proteins from *Mog*<sup>-/-</sup>, WT and *Nefm*<sup>-/-</sup> mice. (a–c) Proliferation, as measured by <sup>3</sup>H-thymidine incorporation assay, of 2D2 spleen cells in response to anion exchange column fractions of CNS tissue extracts from *Mog*<sup>-/-</sup> (a), WT C57BL/6 (b) and *Nefm*<sup>-/-</sup> (c) mice. <sup>3</sup>H-thymidine incorporation was measured during the last 16 h of the 72-h assay. Shown is the mean  $\pm$  s.e.m. of triplicate measurements. Shown is a representative of two individual protein purifications (with different pools of *Mog*<sup>-/-</sup> mice, WT mice or *Nefm*<sup>-/-</sup> mice) and stimulation experiments. The narrow elution profile of the *Mog*<sup>-/-</sup> CNS extract is due to the use of Mono Q column material instead of Source Q material, which was used for WT and *Nefm*<sup>-/-</sup> experiments.



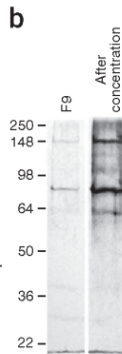
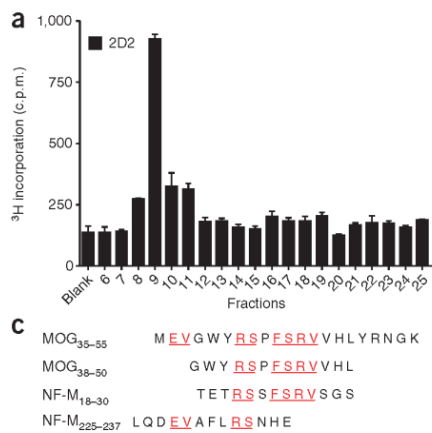


**Figure 4** Identification of a protein that cross-reacts with MOG-specific 2D2-transgenic T cells. **(a)** Proliferation, as measured by  $^3\text{H}$ -thymidine incorporation assay, of 2D2 spleen cells in response to the T cell-activating fractions (fractions 16 and 17 from **Fig. 3a**) from *Mog*<sup>-/-</sup> mice. The fractions were pooled and further separated by gel filtration chromatography. Proliferation was measured during the last 16 h of the 72-h assay. Shown is the mean  $\pm$  s.e.m. of triplicate measurements. **(b)** Silver staining of a 2D2 T cell-activating fraction from *Mog*<sup>-/-</sup> mice. T cell-activating fraction (fraction 9) from several similar gel filtrations were pooled and concentrated by re-chromatography with a Mono Q column. These fractions were resolved on a 10% Tris-glycine gel and stained by silver staining. F9, gel filtration fraction before concentration. **(c)** Amino acid alignment of the immunodominant epitopes of MOG and NF-M. MOG<sub>35-55</sub> and the minimal epitope MOG<sub>38-50</sub> were aligned with NF-M. Shown in red and underlined is the amino acid identity of MOG and NF-M peptides.

**Fig. 8b**). Hence, MOG is lost quantitatively during lipid extraction and urea solubilization, and these data exclude the presence of additional cross-reactive antigens, at least in the urea-soluble fraction we examined.

An *in silico* search identified a seven-amino acid peptide of NF-M nearly identical to the core region of the antigenic peptide MOG<sub>38-50</sub> (**Fig. 4c**), which spans from Tyr40 to Val47 and contains the amino acids Arg41, Phe44, Arg46 and Val47, which are known to be the crucial contact amino acids for the 2D2 TCR and other MOG-specific T cell lines<sup>11,12</sup>. These amino acids are completely preserved at identical positions in NF-M<sub>18-30</sub>; that is, positions Arg21, Phe24, Arg26 and Val27. Another candidate peptide, NF-M<sub>225-237</sub>, also showed some homology to MOG but lacked the essential residues of the core region (**Fig. 4c**).

2D2 T cells responded vigorously to the synthetic peptide NF-M<sub>18-30</sub> but not to NF-M<sub>225-237</sub> (**Fig. 5a**). In addition, NF-M<sub>18-30</sub> induced strong proliferation of 2D2  $\times$  *Rag2*<sup>-/-</sup> transgenic T cells, indicating that the cross-reactivity is intrinsic to the transgenic 2D2 TCR (**Fig. 5b**). This cross-reactivity is not limited to the synthetic MOG and NF-M peptides. 2D2 T cells also recognized the naturally processed recombinant MOG and NF-M proteins produced in *E. coli* (**Fig. 5a,b**). Notably, NF-M and MOG peptides mixed in a 1:1 ratio induced proliferation and cytokine secretion of 2D2-expressing T cells isolated either from the spleen or from the CNS of mice with spontaneous EAE without any signs of tolerance or anergy (**Fig. 5a** and **Supplementary Fig. 10** online).

2D2-transgenic T cell responses to MOG and NF-M peptides were similar but not identical. In dose-dependent proliferation tests, NF-M<sub>18-30</sub> peptide was superior to MOG<sub>35-55</sub> and MOG<sub>38-50</sub> peptides in inducing proliferation (**Fig. 5a,b**). We confirmed

this finding in cytokine assays, in which NF-M stimulated larger interferon- $\gamma$  (IFN- $\gamma$ ), interleukin-17 (IL-17), IL-2 and IL-10 releases than did MOG (**Fig. 5c**).

To clarify whether the cross-reactivity of 2D2-expressing T cells with NF-M reflects a 'private' clonotypic response (a response by a single T-cell clone) or represents a more general cross-reactivity between MOG<sub>35-55</sub>- and NF-M-specific T cells, we isolated fresh MOG<sub>35-55</sub>-specific T cells from C57BL/6 mice, expanded them and tested them for reactivity with NF-M. Indeed, a polyclonal MOG<sub>35-55</sub>-specific

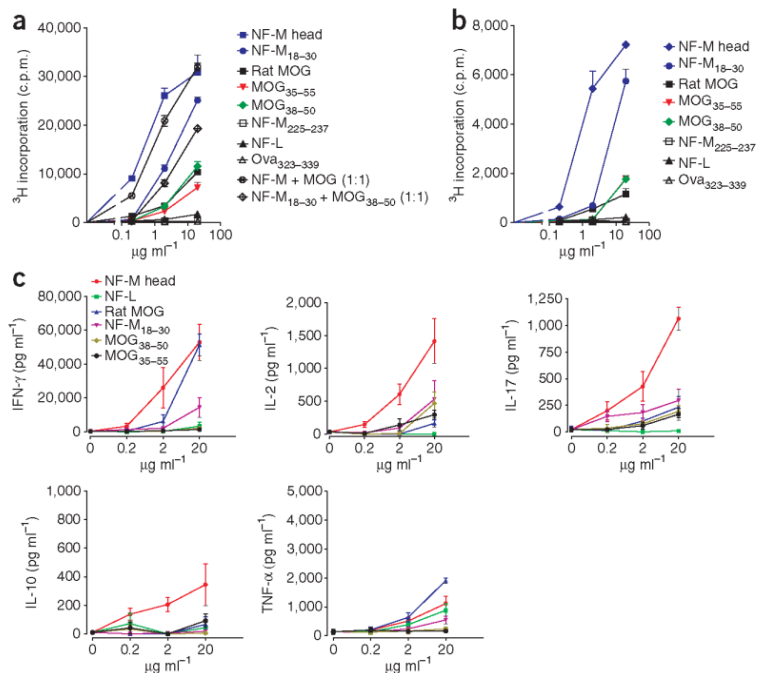


**Figure 5** NF-M reacts specifically with 2D2-transgenic T cells. **(a)** Proliferation, as measured by  $^3\text{H}$ -thymidine incorporation assay, of 2D2 splenocytes cultured with increasing concentrations of the indicated proteins, peptides or mixtures. Shown is a representative of more than three individual experiments consisting of more than six mice. **(b)** Proliferation, as measured by  $^3\text{H}$ -thymidine incorporation assay, of splenocytes from 2D2  $\times$  *Rag2*<sup>-/-</sup> mice cultured with the indicated proteins and peptides. Means  $\pm$  s.e.m. of triplicate measurements are shown. **(c)** Quantification of cytokines released by MOG-specific 2D2-transgenic T cells in response to cross-reactive NF-M peptide and protein. 2D2 splenocytes were cultured for 3 d with the indicated peptides and proteins in a dose-dependent fashion. The concentrations of the cytokines secreted by the T cells were measured in the supernatants in a sandwich ELISA composed of specific antibody pairs. The data were combined from three independent experiments. Each data point represents two to seven mice per group. Means  $\pm$  s.e.m. are shown.

## ARTICLES

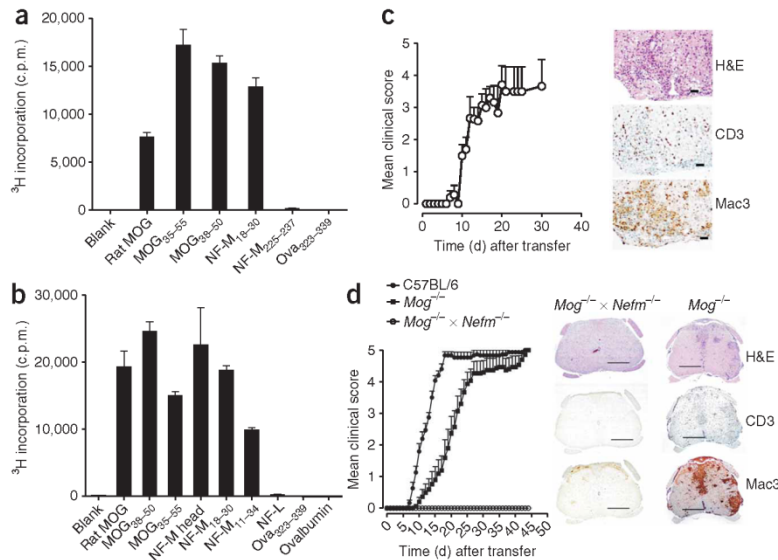


**Figure 6** *In vitro* and *in vivo* cross-reactivity between NF-M- and MOG-specific T cells. **(a,b)** Proliferation, as measured by  $^3\text{H}$ -thymidine incorporation assay, of MOG- and NF-M-specific T cell lines. A MOG<sub>35-55</sub>-specific T cell line **(a)** and NF-M-specific T cell line **(b)** generated from WT mice primed with its respective antigen were tested with the indicated protein and peptides ( $20 \mu\text{g ml}^{-1}$ ). The proliferation was measured during last 16 h of the 72-h assay. Shown is the mean  $\pm$  s.e.m. of triplicate measurements. **(c)** Clinical course of EAE induced by the NF-M-specific T-cell line. Naive WT C57BL/6 mice were lightly irradiated (400 rad) and injected intravenously with  $12 \times 10^6$  ( $n = 3$  mice) or  $6 \times 10^6$  ( $n = 7$  mice) activated T cells specific for NF-M<sub>15-35</sub> peptide. The T-cell line was derived from NF-M<sub>15-35</sub>-immunized WT C57BL/6 mice. Shown is the mean clinical score of mice from three experiments. Histopathology analysis of spinal cords (right) shows typical EAE pathology, with inflammatory infiltrates comprised of polymorphonuclear cells, T cells and macrophages or activated microglia. Scale bars, 100  $\mu\text{m}$ . **(d)** EAE induced by 2D2 T cells in WT C57BL/6 and *Mog*<sup>-/-</sup> but not in *Mog*<sup>-/-</sup>  $\times$  *Nefm*<sup>-/-</sup> double-knockout mice. We transferred  $15 \times 10^6$  2D2 *Rag2*<sup>-/-</sup> T helper type 1 cells into lightly irradiated (300 rad) syngenic WT ( $n = 15$ ), *Mog*<sup>-/-</sup> ( $n = 15$ ) and *Mog*<sup>-/-</sup>  $\times$  *Nefm*<sup>-/-</sup> double-knockout ( $n = 9$ ) C57BL/6 mice. Left, EAE clinical score of mice from three (WT, *Mog*<sup>-/-</sup>) or two (*Mog*<sup>-/-</sup>  $\times$  *Nefm*<sup>-/-</sup>) independent experiments. EAE frequency is significantly lower in double-knockout recipients as compared to either of the two other groups ( $X^2$ ;  $P < 1 \times 10^{-6}$ ). Kinetics of EAE differs significantly (Log-rank test;  $P < 10^{-4}$ ) between WT and *Mog*<sup>-/-</sup> mice. Data represent mean  $\pm$  s.e.m. Right, representative images comprising inflammatory infiltrates in the spinal cord of *Mog*<sup>-/-</sup> and *Mog*<sup>-/-</sup>  $\times$  *Nefm*<sup>-/-</sup> mice revealed by H&E, CD3 and Mac3 staining. Scale bars, 1 mm.

T cell line, which used  $V_{\alpha}$  and  $V_{\beta}$  regions distinct from the 2D2 TCR (Supplementary Fig. 11a online), readily responded to NF-M<sub>18-30</sub> but not to NF-M<sub>225-237</sub> or ovalbumin (Ova) amino acids 323–339 (Fig. 6a). Conversely, T cell lines from NF-M-immunized mice, also with  $V_{\alpha}$  and  $V_{\beta}$  gene segments different from those in the 2D2 TCR (Supplementary Fig. 11b), cross-reacted with MOG protein and peptides (Fig. 6b).

#### *In vivo* recognition of NF-M by MOG-specific T cells

To determine whether 2D2-transgenic T cells find their alternative target (that is, NF-M) *in vivo* during EAE, we transferred MOG peptide-activated, 2D2-transgenic CD4<sup>+</sup> T cells to *Rag2*<sup>-/-</sup> or *Rag2*<sup>-/-</sup>  $\times$  *Mog*<sup>-/-</sup> mice. Whereas both recipient groups developed EAE, in *Mog*-deficient *Rag2*<sup>-/-</sup> mice the disease was delayed (Supplementary Fig. 12 online).

We next examined whether NF-M-activated 2D2-T cells can also induce EAE. NF-M-activated 2D2-expressing T cells triggered EAE in WT hosts, which by incidence and kinetics was comparable to EAE caused by MOG-activated 2D2-expressing T cells (Supplementary

Fig. 13a,b online). To assess the impact of soluble MOG peptide tolerization, we transferred *in vitro* MOG peptide-activated 2D2-transgenic T cells into irradiated WT or *Mog*<sup>-/-</sup> mice and injected Ova<sub>323-339</sub> or MOG<sub>35-55</sub> peptides intravenously. We observed that treatment with MOG peptide delayed the onset of EAE in WT C57BL/6 recipients and, more notably, also in *Mog*<sup>-/-</sup> mice (Supplementary Fig. 13a). Similarly, MOG peptide tolerization lowered the encephalitogenic activity of 2D2-expressing T cells activated *in vitro* with NF-M peptide (Supplementary Fig. 13b).

Furthermore, we tested the encephalitogenic potential of ‘genuine’ NF-M-specific T cell lines, that is, CD4<sup>+</sup> T cells isolated from NF-M-primed C57BL/6 mice and propagated by serial NF-M-specific activation. T cells from an NF-M-specific line transferred to C57BL/6 mice induced severe EAE (Fig. 6c). The pathology in these mice was closely similar to that seen after transfer of 2D2-expressing cells in MOG-deficient mice. Lesions were most pronounced in the spinal cord and featured inflammation by T cells and macrophages (Fig. 6c), confluent demyelination and severe axonal loss (data not shown). We transferred NF-M peptide-activated transgenic T cells derived from 2D2  $\times$  *Rag2*<sup>-/-</sup> mice into both *Mog*<sup>-/-</sup> and WT mice. These monoclonal 2D2  $\times$  *Rag2*<sup>-/-</sup> T cells induced EAE in *Mog*<sup>-/-</sup> mice, albeit with a delayed onset as compared to WT recipients, confirming the autonomous capability of 2D2-expressing T cells to recognize the alternative target, NF-M (Fig. 6d).

The lesions developing in *Mog*<sup>-/-</sup> recipient mice injected with 2D2  $\times$  *Rag2*<sup>-/-</sup> T cells were severe, with large infiltrates in the spinal cord and cerebellum (Fig. 6d) and, remarkably, also in the trigeminal ganglia and in peripheral nerves (data now shown). These findings are reminiscent of the pathology seen in the spontaneous EAE of 2D2  $\times$  *Mog*<sup>-/-</sup> mice.

To confirm that the 2D2-transgenic T cell-mediated lesions in the *Mog*<sup>-/-</sup> recipient mice are due to *in vivo* recognition of NF-M, we transferred activated 2D2  $\times$  *Rag2*<sup>-/-</sup> T cells into *Mog*<sup>-/-</sup>  $\times$  *Nefm*<sup>-/-</sup> double-knockout mice. None of the double-knockout mice showed any clinical signs of EAE, and there were no lesions in the CNS (Fig. 6d).

#### DISCUSSION

C57BL/6 mice are resistant to the induction of most T cell-mediated organ-specific autoimmune diseases. In these mice, immunization with classical autoantigens elicits vigorous T cell responses but commonly fails to produce a clinical autoimmune disease. In contrast, immunization with MOG<sub>35-55</sub> peptide reliably induces clinical EAE, thus overcoming resistance of C57BL/6 mice<sup>13</sup>. Our observations may provide an unexpected clue explaining the unusual autoimmune potential of MOG<sub>35-55</sub>. We show that CD4<sup>+</sup> T cells selected from C57BL/6 mice for reactivity to MOG<sub>35-55</sub> also respond to an epitope

of the medium-sized neurofilament, NF-M. We propose that the combined response to the two target structures may overcome the innate resistance of C57BL/6 mice to autoimmune diseases.

It has previously been reported that the 2D2-transgenic C57BL/6 mice that harbor large populations of MOG-specific CD4<sup>+</sup> T cells tend to spontaneously develop optic neuritis and EAE<sup>3</sup>. This trend is markedly increased in the presence of MOG-specific transgenic B lymphocytes<sup>6,7</sup>. Paradoxically, however, as reported here, 2D2 mice develop spontaneous EAE also in the absence of MOG, the primary encephalitogenic target.

This was discovered in mice with disrupted exon 1 of the *Mog* gene<sup>5</sup>, and it was confirmed in another cohort of *Mog*-deficient 2D2-transgenic mice, whose *Mog* gene was deleted by an independent knock-in strategy<sup>8</sup>, excluding residual, atypical MOG material in these knockout animals as a possible encephalitogenic target.

We fractionated CNS tissue from *Mog*-knockout mice and found material that was presented to and recognized by 2D2-transgenic T cells. We identified the autoantigenic component, by classical biochemical methods and subsequent mass spectrometry, as NF-M. The salient target epitope of NF-M was finally determined by an *in silico* search for sequences related to the MOG<sub>35-55</sub> motif recognized by the 2D2 clone<sup>11</sup>. Given the marked degeneracy of peptide recognition by T cells<sup>14</sup>, cross-reaction of NF-M by 2D2 at the peptide level may not be very unexpected. However, less trivially, we confirmed NF-M as the stimulatory autoantigen at the protein level using both CNS white matter protein extracts and recombinant proteins.

Neurofilaments, including NF-M, are produced by neurons and also by some glial cells<sup>15</sup>. They were characterized recently as autoantigens in actively induced EAE and as possible targets in multiple sclerosis, too. Immunization of Biozzi ABH (antibody high, AB/H, ABH) mice with the light form of neurofilament, NF-L, causes EAE in a moderate proportion of treated animals<sup>16</sup>. Also, autoantibodies to NF-M have been detected in the cerebrospinal fluid of some individuals with multiple sclerosis<sup>17</sup>.

The CD4<sup>+</sup> T cell repertoire of 2D2-transgenic mice is dominated by the transgenic, MOG-reactive TCR but is by no means monoclonal. The NF-M-specific response could have been effected either by T cells from the residual endogenous repertoire or by T cells that escaped allelic exclusion and use endogenous TCR chains along with the transgenic one. We ruled out both possibilities, as 2D2-expressing T cells from *Rag2*-knockout mice showed a similar heteroclitic (stronger) cross-recognition of NF-M *in vitro* and *in vivo*, indistinguishable from their *Rag2*-sufficient counterparts. Furthermore, we observed spontaneous EAE in 2D2 × *Rag2*<sup>-/-</sup> × *Mog*<sup>-/-</sup> mice, suggesting the autonomous role of transgenic T cells in the cross-recognition.

EAE was readily mediated by T cell lines selected for reactivity to either MOG (2D2) or NF-M and by 2D2-expressing T cells activated by NF-M. In contrast, we were unable to induce disease by immunization with NF-M using protocols that allow active disease induction by MOG<sub>35-55</sub> (data not shown). This discrepancy between active and passive EAE induction is, however, not exceptional. It has been previously described for other models, including EAE induced in Lewis rats by glial fibrillary acidic protein<sup>18</sup> and S100-β<sup>19</sup> and MBP-induced EAE in BALB/c mice<sup>20</sup>.

Autoimmune cross-reactivity between MOG and NF-M has been discovered and analyzed in one clonal model, 2D2-transgenic T cells, but has been confirmed in other I-Ab-restricted MOG- and NF-M-specific CD4<sup>+</sup> T cells. MOG- or NF-M-primed polyclonal T cell populations isolated from WT C57BL/6 mice show extensive cross-reactivity between NF-M and MOG proteins and their salient epitopes, respectively. Of note, these populations rarely use V<sub>α3.2</sub> and

V<sub>β11</sub>, the variable chains used by the 2D2 clone, indicating that MOG and NF-M cross-reactivity is not limited to the 2D2 TCR.

Our *in vitro* results formally establish the cross-reactivity of 2D2 and other MOG<sub>35-55</sub> peptide-specific T cells with NF-M, but do these T cells respond to NF-M *in vivo*, and might there be additional cross-recognized autoantigens? *In vivo* NF-M-specific responses are suggested by several lines of evidence. We found lesions in trigeminal and spinal ganglia, tissues which even in WT mice are devoid of MOG autoantigen but contain NF-M. Furthermore, 2D2 × *Rag2*<sup>-/-</sup> T cells transferred into *Mog*<sup>-/-</sup> × *Nefm*<sup>-/-</sup> double-knockout recipients failed to develop EAE. This latter observation, together with the loss of autoantigen potential of myelin from double-knockout white matter, also rules out unknown autoantigens acting in addition to MOG and NF-M.

How would cross-reactive T cells respond to the simultaneous presence of both MOG and NF-M? Would the response components add up or would there be tolerization? Several observations suggest that MOG<sub>35-55</sub>-specific T cells respond both to the MOG epitopes as well as to the cross-reactive NF-M epitopes at the same time. *In vitro*, T cells isolated from CNS and spleen respond to both antigens in an additive fashion. *In vivo*, transfer of activated 2D2-expressing T cells caused substantially earlier appearance of EAE in *Mog*-sufficient mice compared to *Mog*<sup>-/-</sup> mice. Also, the clinical picture of *Mog*-sufficient and *Mog*-deficient 2D2-transgenic mice is very similar. However, a selective anti-MOG response component seems to prevail in transgenic mice with transgenic TCRs plus B cell receptors. In the presence of MOG, in T-B double-transgenic mice the incidence of spontaneous EAE rises to rates of 50% and more. In the absence of MOG, these double-transgenic mice develop EAE at proportions similar to their single-TCR transgenic counterparts. The MOG-dependent elevation of spontaneous EAE frequency, noted in double-transgenic 2D2 × IgH<sup>MOG</sup> mice<sup>5</sup>, is not seen in the absence of MOG.

To our knowledge, this is the first description of immunological self-mimicry, that is, the response of one T cell population to two independent target autoantigens in the same tissue, MOG and NF-M. Is such a response an exception to the norm or is it common? As mentioned, the MOG and NF-M response does not seem to be unique to the MOG-reactive 2D2 clone studied here but is also noted in polydonal MOG- and NF-M-reactive T cell populations from C57BL/6 mice. Furthermore, another case of self mimicry, though between structures from different tissues was reported by another group, who described in the Dark Agouti (DA) rat cross-reaction between MOG-specific T cells and an epitope of the milk protein butyrophilin<sup>21</sup>.

The dual response of T cells against two target autoantigens expressed within the same target tissue could have major implications for organ-specific autoimmune disease. It could have an additive role in determinant spreading (development of an immune response distinct from the initial disease-causing epitope) in the course of an autoimmune response. Beyond this, we propose that in C57BL/6 mice autoimmune response components directed against MOG and NF-M may accumulate to overcome the general resistance of these mice to induction of EAE. T cells with similar cumulative double self-reactivity could act as dominant pathogens in human multiple sclerosis, and genetic factors favoring bireactive T cells would enhance susceptibility to the disease. This study should provide a way to identify such T cells in humans and appreciate their role in the pathogenesis of multiple sclerosis.

## METHODS

Methods and any associated references are available in the online version of the paper at <http://www.nature.com/naturemedicine/>.

Note: Supplementary information is available on the Nature Medicine website.

## ARTICLES

## ACKNOWLEDGMENTS

*Mog*<sup>Cre/Cre</sup>, *Nefm*<sup>-/-</sup>, 2D2 and *Mog*<sup>-/-</sup> mice were generously provided by A. Waisman (Johannes Gutenberg University of Mainz), J.-P. Julien (Laval University), V.K. Kuchroo (Harvard Medical School) and D. Pham-Dinh (INSERM UMR 546). We thank F. Lottspeich for granting us permission to use his mass spectrometer. We thank L. Penner and I. Arnold-Ammer for technical support. This project was supported by the Deutsche Forschungsgemeinschaft (Sonderforschungsbereiche (SFB) 571, Projects A1 and B6) and the Max Planck Society. H.S.D. is supported by a PhD fellowship (Portuguese Fundação para a Ciência ea Tecnologia (PCT) program SPRH/BD/15885/2005). Part of the study (conducted by H.W., R.L. and H.L.) was funded by the EU Project Neuropromise (PL 018637), and A.B.-N. was supported by the Israel Science Foundation and the National Multiple Sclerosis Society of New York (RG3195B8/2). A.B.-N. is an Alexander von Humboldt Prize Awardee.

## AUTHOR CONTRIBUTIONS

G.K. performed most of the experiments. G.K. and H.W. designed the study and wrote the manuscript with input from co-authors. A.S., L.T.M. and R.S.L. contributed EAE and T cell data. K.D. supervised protein purification and mass spectrometry and performed *in silico* searches. R.M. performed mass spectrometry. H.S.D. assisted in EAE experiments. A.B.-N. performed T cell line transfer EAE experiments. H.L. performed and interpreted histology. E.C.K. designed experiments and performed protein purification.

Published online at <http://www.nature.com/naturemedicine/>

Reprints and permissions information is available online at <http://npg.nature.com/reprintsandpermissions/>

- Goebels, N. *et al.* Repertoire dynamics of autoreactive T cells in multiple sclerosis patients and healthy subjects. Epitope spreading versus clonal persistence. *Brain* **123**, 508–518 (2000).
- Wekerle, H. Breaking ignorance: the case of the brain. in *Current Concepts in Autoimmunity and Chronic Inflammation* (eds. Radbruch, A. & Lipsky, P.E.) 25–50 (Springer, Berlin, 2006).
- Bettelli, E. *et al.* Myelin oligodendrocyte glycoprotein-specific T cell receptor transgenic mice develop spontaneous autoimmune optic neuritis. *J. Exp. Med.* **197**, 1073–1081 (2003).
- Litzenburger, T. *et al.* B lymphocytes producing demyelinating autoantibodies: development and function in gene-targeted transgenic mice. *J. Exp. Med.* **188**, 169–180 (1998).
- Delarasse, C. *et al.* Myelin/oligodendrocyte glycoprotein-deficient (MOG-deficient) mice reveal lack of immune tolerance to MOG in wild-type mice. *J. Clin. Invest.* **112**, 544–553 (2003).
- Krishnamoorthy, G., Lassmann, H., Wekerle, H. & Holz, A. Spontaneous opticospinal encephalomyelitis in a double-transgenic mouse model of autoimmune T cell/B cell cooperation. *J. Clin. Invest.* **116**, 2385–2392 (2006).
- Bettelli, E., Baeten, D., Jäger, A., Sobel, R.A. & Kuchroo, V.K. Myelin oligodendrocyte glycoprotein-specific T and B cells cooperate to induce a Devic-like disease in mice. *J. Clin. Invest.* **116**, 2393–2402 (2006).
- Hövelmeyer, N. *et al.* Apoptosis of oligodendrocytes via Fas and TNF-R1 is a key event in the induction of experimental autoimmune encephalomyelitis. *J. Immunol.* **175**, 5875–5884 (2005).
- Norton, W.T. & Poduslo, S.E. Myelination in rat brain changes in myelin composition during maturation. *J. Neurochem.* **21**, 759–773 (1973).
- Chantry, A., Gregson, N.A. & Glynn, P. A novel metalloproteinase associated with brain myelin membranes. Isolation and characterization. *J. Biol. Chem.* **264**, 21603–21607 (1989).
- Petersen, T.R. *et al.* Characterization of MHC- and TCR-binding residues of the myelin oligodendrocyte glycoprotein 38–51 peptide. *Eur. J. Immunol.* **34**, 165–173 (2004).
- Ben-Nun, A. *et al.* Anatomy of T cell autoimmunity to myelin oligodendrocyte glycoprotein (MOG): prime role of MOG44F in selection and control of MOG-reactive T cells in H-2<sup>d</sup> mice. *Eur. J. Immunol.* **36**, 478–493 (2006).
- Mendel, I., Kerlero de Rosbo, N. & Ben-Nun, A. A myelin oligodendrocyte glycoprotein peptide induces typical chronic experimental autoimmune encephalomyelitis in H-2<sup>b</sup> mice: fine specificity and T cell receptor V $\beta$  expression of encephalitogenic T cells. *Eur. J. Immunol.* **25**, 1951–1959 (1995).
- Wucherpfennig, K.W. & Strominger, J.L. Molecular mimicry in T cell-mediated autoimmunity: viral peptides activate human T cell clones specific for myelin basic protein. *Cell* **80**, 695–705 (1995).
- Kelly, B.M., Gillespie, C.S., Sherman, D.L. & Brophy, P.J. Schwann cells of the myelin-forming phenotype express neurofilament protein NF-M. *J. Cell Biol.* **118**, 397–410 (1992).
- Huizinga, R. *et al.* Immunization with neurofilament light protein induces spastic paresis and axonal degeneration in Biozzi ABH mice. *J. Neuropathol. Exp. Neurol.* **66**, 295–304 (2007).
- Bartos, A. *et al.* Elevated intrathecal antibodies against the medium neurofilament subunit in multiple sclerosis. *J. Neurol.* **254**, 20–25 (2007).
- Berger, T. *et al.* Experimental autoimmune encephalomyelitis: the antigen specificity of T-lymphocytes determines the topography of lesions in the central and peripheral nervous system. *Lab. Invest.* **76**, 355–364 (1997).
- Kojima, K. *et al.* Experimental autoimmune panencephalitis and uveoretinitis in the Lewis rat transferred by T lymphocytes specific for the S100 $\beta$  molecule, a calcium binding protein of astroglia. *J. Exp. Med.* **180**, 817–829 (1994).
- Abromson-Leaman, S. *et al.* T cell responses to myelin basic protein in experimental autoimmune encephalomyelitis-resistant BALB/c mice. *J. Neuroimmunol.* **45**, 89–101 (1993).
- Steffler, A. *et al.* Butyrophilin, a milk protein, modulates the encephalitogenic T cell response to myelin oligodendrocyte glycoprotein in experimental autoimmune encephalomyelitis. *J. Immunol.* **165**, 2859–2865 (2000).

## ONLINE METHODS

**Transgenic mice.** We bred MOG-specific TCR transgenic mice (2D2)<sup>3</sup> and B cell knock-in IgH<sup>MOG</sup> (also known as Th)<sup>4</sup> on a C57BL/6 background into *Mog*<sup>-/-</sup> mice<sup>5</sup> to obtain 2D2 × *Mog*<sup>-/-</sup> and IgH<sup>MOG</sup> × *Mog*<sup>-/-</sup> and 2D2 × IgH<sup>MOG</sup> × *Mog*<sup>-/-</sup> mice. We obtained WT C57BL/6 mice from the animal facility of the Max Planck Institute of Biochemistry. We bred *Rag2*<sup>-/-</sup> mice and OT-II mice (Jackson Laboratories) in the conventional animal facilities along with other transgenic mice. We bred a second *Mog*<sup>-/-</sup> strain (*Mog*<sup>Cre/Cre</sup>) harboring the insertion of the gene encoding Cre recombinase in the first exon of *Mog*<sup>8</sup> with the 2D2-transgenic mice in the specific pathogen-free animal facility of Institut Fédératif de Recherche (IFR30). We also maintained *Nefm*<sup>-/-</sup> mice<sup>22</sup> in the specific pathogen-free animal facility of IFR30.

We routinely monitored a cohort of transgenic mice of the above genotypes at least one or two times a week for clinical EAE signs. The EAE disease scores were according to the classic scale<sup>6</sup>. To determine other neurological abnormalities, we lifted the mice by their tail and allowed them to grab the grid of a cage by their front limbs (see **Supplementary Movies 1–6**). We noted the clasp and hyperextension of hind limbs within 10–30 s of holding them by the tail.

All animal procedures were in accordance with guidelines of the Committee on Animals of the Max Planck Institute of Neurobiology or the Midi-Pyrénées Ethic Committee on Animal Experimentation and with the license of the Regierung von Oberbayern (or from the French Ministry of Agriculture).

**Peptides and proteins.** Mouse MOG<sub>35–55</sub> (MEVGWYRSPFSRVVHLYRNGK), mouse MOG<sub>38–50</sub> (GWYRSPFSRVVHLYR), mouse NF-M<sub>18–30</sub> (TETRSSFSRVSGS), mouse PLP<sub>139–151</sub> (HSLGKWLGHDPDKF), Ova<sub>323–339</sub> (ISQAVHAAHAEINEAGR), mouse MOG<sub>90–110</sub> (SDEGGYTCFFRDHSYQEEAA), rat MBP pC1 (MBP<sub>68–89</sub>) (HYGSLPQKSPRSQDENPV), guinea pig MBP pC2 (MBP<sub>45–67</sub>) (GSDRAAP KRGSGKDSHHAARTT) or guinea pig MBP p81 (MBP<sub>69–83</sub>) (YGSLPQKSR SQDEN) were synthesized either by BioTrend or by the core facility of Max Planck Institute of Biochemistry. We obtained mouse NF-M<sub>225–237</sub> (LQDEVA FLRSNHE) from Metabion. We purified the peptides by HPLC to >95% purity and analyzed them by mass spectrometry.

We purified recombinant soluble rat MOG protein (MOG<sub>1–125</sub>)<sup>23</sup>, mouse full-length NF-L and mouse head domain fragment of NF-M (NF-M 'head'; NF-M<sub>1–102</sub>) (**Supplementary Methods** online) from bacterial inclusion bodies. We purchased S100β and ovalbumin from Sigma. We purified guinea pig MBP and rat MBP using standard protocols.

**Histology.** We perfused mice with 4% paraformaldehyde in PBS and stored them in the same fixative for 24 h. We stained adjacent serial sections of CNS and PNS with H&E, luxol fast blue or Bielschowsky silver impregnation. We also stained some sections with CD3-specific (Serotec) and Mac3-specific (BD Biosciences) antibodies. We stained adjacent sections with the respective isotype controls.

**Adoptive transfer EAE.** For 2D2 × *Rag2*<sup>-/-</sup> T cell transfer, we purified CD4<sup>+</sup> T cells from 2D2 × *Rag2*<sup>-/-</sup> mice and stimulated them *in vitro* with 20 μg ml<sup>-1</sup> of NF-M<sub>15–35</sub> peptide in the presence of 20 ng ml<sup>-1</sup> IL-12 and 1 ng ml<sup>-1</sup> IL-2

(both from R&D Systems) and irradiated syngeneic splenocytes. On day 6, we re-stimulated viable cells with splenocytes and 20 μg ml<sup>-1</sup> of NF-M<sub>15–35</sub> in the presence of 20 μg ml<sup>-1</sup> IL-12 and 1 μg ml<sup>-1</sup> IL-2. On day 9, we injected FicolI-purified T helper type 1 cells into lightly irradiated (300 rad) syngeneic recipients.

**Myelin purification.** We purified crude myelin from *Mog*<sup>-/-</sup>, WT C57BL/6 or *Mog*<sup>-/-</sup> × *Nefm*<sup>-/-</sup> CNS tissues according to previously published protocols<sup>9,10</sup>. Briefly, we pooled brain and spinal cord and homogenized it in 0.32 M sucrose in 10 mM Tris HCl, pH 7.4. Then we centrifuged at 15,000g and washed the pellet twice with 0.32 M sucrose solution. Finally, we suspended the pellet in 0.32 M sucrose and overlaid on to 0.85 M sucrose and centrifuged at 26,000g. We collected the myelin at the interface, washed it twice and suspended it in 1 ml of sterile PBS.

**Proliferation assay.** For the analysis of fractions from biochemical separations, we mixed spleen cells from 2D2 or OT-II mice (2 × 10<sup>5</sup> cells) with LPS-activated BMDCs from WT C57BL/6 mice (5 × 10<sup>4</sup> cells) together with 1 in 50-diluted fractions.

Unless otherwise mentioned, in all other T cell proliferation experiments, we cultured 2 × 10<sup>5</sup> spleen cells with 20 μg ml<sup>-1</sup> peptides and proteins. We performed all proliferation assays in triplicate. We measured the T cell proliferation by the incorporation of <sup>3</sup>H-labeled thymidine during the last 6 h of a 48-h culture or the last 16 h of a 72-h culture.

**Enzyme-linked immunosorbent assay.** We assayed cell culture supernatants with antibody pairs or kits for IFN-γ, IL-2 (both from BD Biosciences), TNF-α (Peprotech), IL-10 (R&D Systems) or IL-17 (eBioscience) according to the manufacturer's instructions.

**T cell lines.** We established antigen-specific T cell lines from C57BL/6 mice immunized with MOG<sub>35–55</sub>, NF-M<sub>15–35</sub> or NF-M 'head' in complete Freund's adjuvant supplemented with 5 mg ml<sup>-1</sup> *Mycobacterium tuberculosis* (strain H37Ra) using established protocols. We collected spleen and draining lymph nodes 10–12 d after immunization and stimulated them with respective antigen at 20 μg ml<sup>-1</sup>. We supplemented T cell cultures with recombinant mouse IL-2 (Peprotech) and supernatant from concanavalin A-stimulated mouse spleen cells on days 0, 3 and 5. We purified live T cells by Nycoprep gradient (Progen Biotechnik) and repeated stimulation every 7–10 d.

**Statistical analyses.** We analyzed spontaneous EAE incidence by Kaplan-Meier survival curve analysis, and we analyzed adoptive transfer EAE data and proliferation assays by analysis of variance. We used GraphPad Prism for all statistical analyses. We considered *P* values less than 0.05 to be significant.

22. Jacomy, H., Zhu, Q.Z., Couillard-Despres, S., Beaulieu, J.M. & Julien, J.P. Disruption of type IV intermediate filament network in mice lacking the neurofilament medium and heavy subunits. *J. Neurochem.* **73**, 972–984 (1999).

23. Amor, S. *et al.* Identification of epitopes of myelin oligodendrocyte glycoprotein for the induction of experimental allergic encephalomyelitis in SJL and Biozzi AB/H mice. *J. Immunol.* **153**, 4349–4356 (1994).

# Publication 4



# Commensal microbiota and myelin autoantigen cooperate to trigger autoimmune demyelination

Kerstin Berer<sup>1</sup>, Marsilius Mues<sup>1</sup>, Michail Koutouros<sup>1</sup>, Zakeya Al Rasbi<sup>1</sup>, Marina Boziki<sup>1</sup>, Caroline Johner<sup>2</sup>, Hartmut Wekerle<sup>1</sup> & Gurumoorthy Krishnamoorthy<sup>1</sup>

**Active multiple sclerosis lesions show inflammatory changes suggestive of a combined attack by autoreactive T and B lymphocytes against brain white matter<sup>1</sup>. These pathogenic immune cells derive from progenitors that are normal, innocuous components of the healthy immune repertoire but become autoaggressive upon pathological activation. The stimuli triggering this autoimmune conversion have been commonly attributed to environmental factors, in particular microbial infection<sup>2</sup>. However, using the relapsing–remitting mouse model of spontaneously developing experimental autoimmune encephalomyelitis<sup>3</sup>, here we show that the commensal gut flora—in the absence of pathogenic agents—is essential in triggering immune processes, leading to a relapsing–remitting autoimmune disease driven by myelin-specific CD4<sup>+</sup> T cells. We show further that recruitment and activation of autoantibody-producing B cells from the endogenous immune repertoire depends on availability of the target autoantigen, myelin oligodendrocyte glycoprotein (MOG), and commensal microbiota. Our observations identify a sequence of events triggering organ-specific autoimmune disease and these processes may offer novel therapeutic targets.**

The relapsing–remitting (RR) mouse model uses transgenic SJL/J mice expressing, in a large proportion of their CD4<sup>+</sup> T cells, a transgenic T-cell antigen receptor (TCR) recognizing MOG peptide 92–106 in the context of MHC class II, I-A<sup>b</sup>. These mice spontaneously develop experimental autoimmune encephalomyelitis (EAE) with successive disease bouts that often affect different central nervous system (CNS) tissues. The disease is initiated by the transgenic CD4<sup>+</sup> T cells, which first infiltrate the CNS, and by MOG-autoantibody-producing B cells recruited from the natural immune repertoire<sup>3</sup>.

Whereas in our facility close to 80% of RR mice developed spontaneous EAE within 3–8 months of age, the rate was variable in other institutions, with spontaneous EAE incidences ranging from 35–90% (unpublished data). This recalled previous investigations that also observed that the frequency of spontaneous EAE in myelin-specific TCR transgenic mice varied in different breeding centres<sup>4</sup>. Because our mice were reared under specific pathogen-free (SPF) conditions, we tested the possible contributions of the non-pathogenic commensal flora to the triggering of a spontaneous CNS-specific autoimmune disease.

We first compared the incidence of spontaneous EAE between RR mice housed under SPF and completely germ-free conditions. The differences were marked. Whereas, as reported before, most SPF-bred RR mice came down with EAE within 3–8 months<sup>3</sup>, germ-free RR mice remained fully protected throughout their life (Fig. 1a). As the commensal microbiota have a central function in driving the correct development of the immune system<sup>5</sup>, the absence of spontaneous EAE in germ-free RR mice may have reflected a general immune deficiency due to missing microbial stimuli. However, two observations argue against a profound and irreversible non-reactivity. First, RR mice, which had been germ free (and disease free) for 6–12 weeks, promptly developed EAE when re-colonized with conventional commensal microbiota (Fig. 1b). Mono-colonization with segmented filamentous

bacteria (SFB), which restored autoimmunity in another mouse model, was of low efficiency (unpublished data). This suggests that the immune system of germ-free mice had grown efficient enough to mount a full autoimmune attack within a relatively brief period of time. Second, the basic immune competence of germ-free animals was confirmed by active immunization of germ-free wild-type SJL/J mice with recombinant MOG (rMOG) in complete Freund's adjuvant (CFA). In accord with one previous report<sup>6</sup>, although not with another more recent one<sup>7</sup>, all immunized germ-free mice developed EAE like their SPF counterparts, although with some delay (Fig. 1c), and transfer of pre-activated T cells induced comparable EAE in both germ-free and SPF mice (Supplementary Table 1). Moreover, germ-free and SPF SJL/J mice immunized with rMOG produced comparable levels of anti-MOG antibodies in their serum (Fig. 1d).

Recent studies established that components of the commensal microbiota profoundly shape the gut-associated lymphatic tissue (GALT),

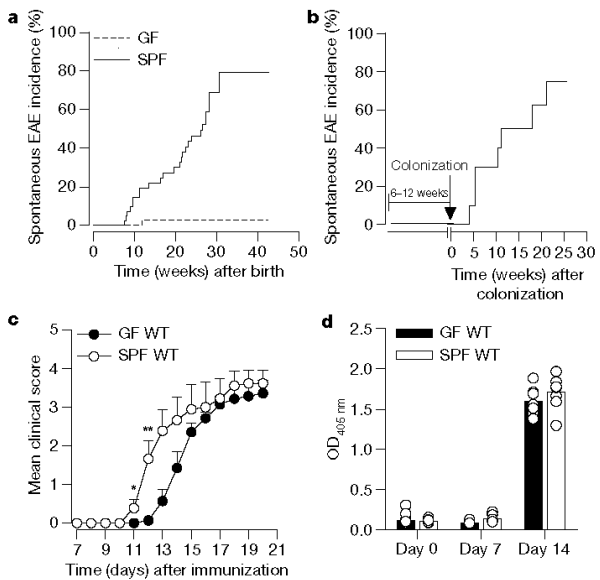


**Figure 1 | Commensal microbiota are required for the development of spontaneous EAE.** **a**, Incidence of spontaneous EAE in a cohort of RR mice housed in germ-free (GF;  $n = 35$ ) or SPF ( $n = 41$ ) conditions. **b**, Incidence of spontaneous EAE in germ-free RR mice ( $n = 10$ ) re-colonized with conventional flora from SPF mice. **c**, Delayed EAE onset in germ-free wild-type (GF WT) SJL/J mice immunized with rMOG/CFA. Mean EAE scores ( $\pm$  s.e.m.) of germ-free ( $n = 7$ ) and SPF ( $n = 8$ ) SJL/J mice are shown. \* $P < 0.05$ ; \*\* $P < 0.01$  (two-way ANOVA). **d**, Germ-free and SPF wild-type SJL/J mice produce similar levels of anti-MOG antibodies after immunization. Each circle represents an individual mouse and bars depict mean  $\pm$  s.e.m. Panels **c** and **d** represent two individual experiments.

<sup>1</sup>Department of Neuroimmunology, Max Planck Institute of Neurobiology, 82152 Martinsried, Germany. <sup>2</sup>Max Planck Institute of Immunobiology and Epigenetics, 79108 Freiburg, Germany.

some supporting differentiation of interleukin (IL)-17-producing  $T_H17$  cells<sup>8–10</sup> and others the generation of regulatory T lymphocytes ( $T_{reg}$ )<sup>11,12</sup>. We also found a marked deficit of  $T_H17$ -like cells in germ-free mice (Fig. 2a), which was most pronounced in T cells intimately connected to the intestinal wall, lamina propria T cells and in Peyer's patch but not in mesenteric lymph node populations. There were no notable changes in remote organs, such as spleen or pooled inguinal and axillary lymph nodes (Fig. 2a). Frequencies of IFN- $\gamma$ -, TNF- $\alpha$ - and IL-10-producing  $CD4^+$  T cells were comparable between germ-free and SPF RR mice (Fig. 2a and Supplementary Fig. 1). Apart from a minor increase in the frequency of  $CD4^+$  T cells in the spleen of germ-free RR mice and a reduction of the T cells expressing lower levels of T-cell receptor ( $TCR\alpha\beta^{low}$ ) (activated T cells) in the lamina propria (Supplementary Figs 2 and 3), the proportions of most lymphoid cell types examined, including Foxp3<sup>+</sup>  $T_{reg}$  cells, CD8<sup>+</sup> T cells, TCR $\gamma\delta^+$  cells, B cells, CD11b<sup>+</sup> macrophages, CD11c<sup>+</sup> dendritic cells, natural killer (NK) cells and Gr1<sup>+</sup> granulocytes were unchanged (Supplementary Fig. 2). Of note, although in the spleen the microbial colonization status did not affect cellular composition, it definitely impinged on cytokine production of splenic immune cells. As in MOG-immunized germ-free C57BL/6 mice<sup>7</sup>, germ-free RR mouse spleen cells released lower levels of IL-17 than their SPF counterparts upon MOG antigen or anti-CD3 monoclonal antibody stimulation, and in addition they showed reduced secretion of IFN- $\gamma$ . Re-colonization of germ-free mice not only restored T-cell cytokine production capacity but even led to overshooting reactions (Supplementary Fig. 4).

The commensal microbiota could act on MOG-specific T cells either via microbial structures mimicking MOG epitopes<sup>13</sup> or through innate immune signals creating a particular inflammatory milieu<sup>11,14</sup>. In an attempt to probe a potential MOG-specific mimicry response, we transferred carboxyfluorescein succinimidyl ester (CFSE)-labelled TCR transgenic or wild-type T cells into SPF wild-type mice and tested their proliferative responses in the gut. Proliferation rates of transgenic and polyspecific wild-type T cells in the GALT were equally high, whereas in the remote spleen of the same recipients the responses remained hardly detectable (Fig. 2b). Further, the microbial signals

seem to act persistently on local T cells. Transient depletion of gut flora by short-term antibiotic treatment significantly reduced the proliferation of T cells in the lamina propria, but not in spleen, pooled lymph nodes, mesenteric lymph nodes and Peyer's patches (Supplementary Fig. 5).

Activation of MOG-specific T cells in the GALT is necessary for the development of EAE in RR mice, but not sufficient. Full clinical EAE requires the participation of MOG-reactive B lymphocytes. We proposed that in RR mice, transgenic pathogenic T cells select the auto-immune B cells from the native B-cell repertoire and drive them to proliferate and release autoantibodies of IgG classes<sup>3</sup>. Indeed, we now found that germ-free RR mice, which, owing to missing microbial stimuli, lack activated autoimmune T cells, produced only low doses of anti-MOG autoantibodies. The autoantibody production was promptly increased in germ-free mice upon re-colonization (Fig. 3a). This response could involve antigenic mimicry at the B-cell level between MOG and epitopes on commensal microbes, reminiscent of Sydenham's chorea—the CNS manifestation of rheumatic fever—in which streptococcal antigens mimic neuronal B-cell epitopes<sup>15</sup>. However, this was not the case in spontaneous RR mouse EAE. We discovered that production of demyelinating autoantibodies critically depended on the expression of the target myelin autoantigen, MOG. RR mice deficient in MOG (RR  $\times$  MOG<sup>-/-</sup>), due to a transgenic mutation of the *Mog* gene<sup>16</sup>, failed to develop anti-MOG autoantibody titres despite their normal microbial status (Fig. 3a). Importantly, our data show that exogenous MOG injected into SPF RR  $\times$  MOG<sup>-/-</sup> mice via MOG in CFA readily induced anti-MOG antibodies (Supplementary Fig. 6).

Recruitment and activation of antigen-specific B cells involves signals by local helper T cells and surrounding stroma cells, which together drive the resting B cell into a germinal centre, where it undergoes proliferation, immunoglobulin class switching and somatic hypermutation<sup>17</sup>. Binding of the cognate antigen to the B-cell receptor has a central role in these processes. MOG-specific B cells could be recruited either in the CNS tissue via locally produced MOG material<sup>18</sup>, or in CNS draining peripheral lymph nodes (deep cervical lymph

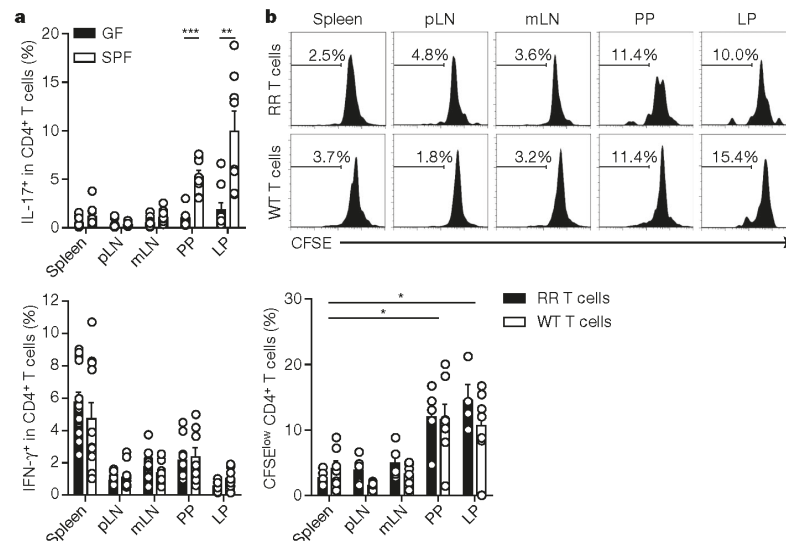


**Figure 2 | Effect of microbiota on T-cell activation and their cytokine profiles in the GALT.** **a**, Impaired  $T_H17$  differentiation in germ-free (GF) RR mice. Frequencies of IL-17- or IFN- $\gamma$ -producing T cells from the indicated organs of GF and SPF RR mice are shown. LP, lamina propria; mLN, mesenteric lymph nodes; pLN, pooled inguinal and axillary lymph nodes; PP, Peyer's patches.  $n = 8$ –13 mice per group. Data were pooled from four independent

experiments. \*\*\* $P = 0.0002$ ; \*\* $P = 0.0025$  (Mann–Whitney U test). **b**, Activation of T cells by commensal flora. Shown are the frequencies of CFSE<sup>low</sup>  $CD4^+$  T cells in the indicated organs of mice that received CFSE-labelled  $CD4^+$  T cells. Each circle represents an individual mouse and bars depict mean  $\pm$  s.e.m.  $n = 4$ –7 mice per group. Data represent two individual experiments. \* $P < 0.05$  (Mann–Whitney U test).

## RESEARCH LETTER

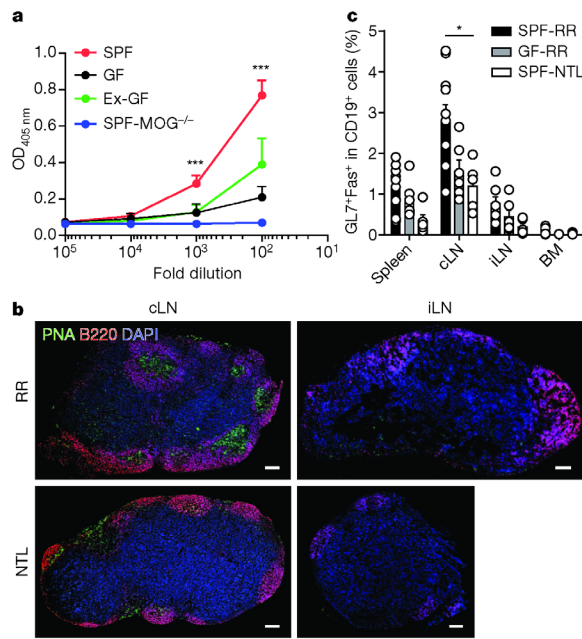


**Figure 3 | B-cell recruitment is impaired in germ-free RR mice.** **a**, Reduced production of MOG-specific IgG2a antibodies in sera of germ-free (GF) RR mice. SPF ( $n = 15$ ); germ-free ( $n = 24$ ); germ-free mice re-colonized with conventional commensal microbiota (Ex-GF;  $n = 7$ ); or SPF-MOG<sup>-/-</sup> ( $n = 13$ ) RR mice. Error bars indicate s.e.m. \*\*\* $P < 0.001$  (Kruskal–Wallis test). **b**, **c**, Spontaneously formed germinal centre B cells are enriched in the cervical lymph nodes (cLN) of RR mice. **b**, Immunofluorescence staining of cervical lymph nodes or inguinal lymph node (iLN) sections of RR and NTL mice. Peanut agglutinin (PNA) (green; germinal centre), B220 (red; B cells) and 4',6-diamidino-2-phenylindole (DAPI) (blue; cell nuclei). Representative data of 4–5 individual mice are shown. Scale bars, 100  $\mu\text{m}$ . **c**, Flow cytometric analysis of GL7<sup>+</sup> Fas<sup>+</sup> germinal centre B cells from spleen, cervical lymph nodes, inguinal lymph nodes and bone marrow (BM). Each circle represents an individual mouse and bars represent mean  $\pm$  s.e.m.  $n = 5–10$  per group. Data were pooled from three independent experiments. \* $P < 0.05$  (Mann–Whitney U test).

nodes) with MOG imported from the CNS via lymphatic vessels<sup>19</sup>. Our observations favour the latter alternative. Prior to the onset of clinical symptoms in SPF RR mice we found some scattered B cells in CNS infiltrates (Supplementary Fig. 7) but no follicle-like aggregates or follicular markers (data not shown). However, there were conspicuous changes in the cervical lymph nodes. Starting from the age of 3 weeks, cervical lymph nodes contained clearly delineated germinal centres (Fig. 3b). Furthermore, germinal centres and increased frequencies

of GL7<sup>+</sup> and Fas<sup>+</sup> germinal centre B cells were restricted to cervical lymph nodes of RR mice, but were significantly reduced in age-matched germ-free and non-transgenic littermates (NTL) (Fig. 3b, c).

Germinal centres are attractive milieus for B cells, provided they contain appropriate antigenic material and competent T-helper cells<sup>20</sup>. To investigate whether RR mouse cervical lymph nodes offer both prerequisites to MOG-reactive B cells, we transferred GFP-labelled, MOG-reactive B cells expressing the H chain of a MOG monoclonal antibody (IgH<sup>MOG</sup>)<sup>21</sup> into hosts with a distinct allotype and traced their homing behaviour (Fig. 4a). When examined 14 days after transfer, MOG-specific B cells were found densely packed within germinal centres of cervical lymph nodes (Fig. 4b). Further, donor IgH<sup>MOG</sup> B cells switched anti-MOG antibodies to IgG2a isotypes (Fig. 4c). However, GFP-labelled polyclonal wild-type B cells failed to accumulate in any of the lymph nodes of RR mice (Fig. 4b), and IgH<sup>MOG</sup> B cells neither homed to the cervical lymph nodes of wild-type or RR  $\times$  MOG<sup>-/-</sup> mice (Fig. 4b and Supplementary Fig. 8) nor produced class-switched anti-MOG antibodies (Fig. 4c and Supplementary Fig. 8c). Collectively, these data indicate an ongoing MOG-specific germinal centre reaction, which is critically dependent on the expression of MOG, in the cervical lymph nodes of RR mice.

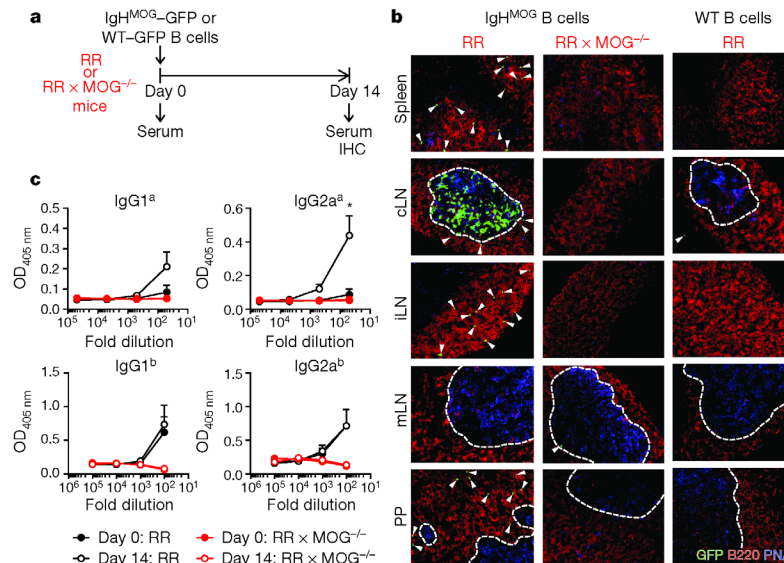


**Figure 4 | MOG-specific B cells home to the germinal centre of brain draining cervical lymph nodes.** **a**, Schematic representation of experimental set up. IHC, immunohistochemistry. **b**, MOG-specific B cells home to the germinal centre of brain draining cervical lymph nodes. PNA (blue; germinal centre) and B220 (red; B cells). Arrowheads indicate transferred GFP<sup>+</sup> B cells. Dotted lines define boundaries of germinal centre. Representative staining of

two independent experiments are shown.  $n = 4–5$  mice per group. Magnification:  $\times 20$ . **c**, Transgenic MOG-specific B cells spontaneously switch isotype in RR but not in RR  $\times$  MOG<sup>-/-</sup> mice. Titres of donor (a allotype) and recipient (b allotype) anti-MOG antibodies were measured. Error bars represent s.e.m.  $n = 4–5$  mice per group. Data were pooled from three independent experiments. \* $P < 0.05$  (Mann–Whitney U test).

This is the first report, to our knowledge, describing the sequential roles of the intact commensal gut flora and of myelin autoantigen in the initiation of a complex spontaneous demyelinating autoimmune disease. We propose a two-phase scenario that starts out in the GALT with expanding and activating CNS autoreactive T cells, which then recruit autoantibody-producing B cells. Together the autoimmune T and B cells trigger a demyelinating encephalomyelitis, which in the RR SJL/J mouse takes a relapsing–remitting course, very similar to early human multiple sclerosis.

Our findings are of direct relevance to multiple sclerosis, the pathogenesis of which is presently hotly debated. Some propose primary changes in the CNS target as the initiating process<sup>22</sup>, whereas others suggest that pathogenesis originates in the immune system<sup>23</sup>. Our present data support the latter concept. It is tempting to extend our finding of the gut origin of experimental CNS autoimmunity to human multiple sclerosis. There is now emerging evidence implicating gut microbiota in the starting phase of human autoimmune diseases. Besides inflammatory bowel diseases, in which bacteria may act on local tissue directly as well as indirectly<sup>24</sup>, inflammatory diseases with remote tissues affected seem to be modulated by the gut environment; for example, in rheumatoid arthritis<sup>25</sup> and type 1 diabetes mellitus<sup>26</sup>. In multiple sclerosis, evidence for commensal microbial contributions has remained less clear, so far. Dietary risk factors have been suggested to have a role<sup>27</sup>, and may contribute to a conspicuous increase of multiple sclerosis prevalence in Asian countries, like Japan, which has been ascribed to the spreading of a ‘westernized’ lifestyle<sup>28</sup>. It will be of interest now to search for the composition of intestinal microbiota associated with an increased susceptibility to multiple sclerosis, and this may provide a conceptual basis for exploring new, non-invasive treatment strategies.

## METHODS SUMMARY

**Mice.** Germ-free animals were re-derived from SJL/J anti-MOG TCR transgenic RR mice and kept germ free at the animal facility of the Max Planck Institute of Immunobiology and Epigenetics. Mice were re-colonized by housing in bedding material pre-conditioned by SPF mice.

**Cell purification, flow cytometry and adoptive transfers.** Single-cell suspensions were prepared from spleen, lymph nodes, Peyer’s patches and lamina propria by enzymatic digestion or mechanical disruption. Untouched T cells and B cells were purified using negative isolation kits (R&D Systems). Cells were stained with fluorochrome-labelled antibodies and acquired on FACSCalibur (BD Biosciences). Data were analysed using FlowJo (TreeStar) software. CFSE-labelled T cells or GFP<sup>+</sup> B cells were injected intravenously into SPF mice. CFSE<sup>low</sup> T cells were quantified by FACS 3 days after transfer. Localization of GFP<sup>+</sup> B cells was documented by immunofluorescence after 2 weeks.

**Immunofluorescence.** Sections of immune organs were stained with PNA (Vector Laboratories), anti-mouse B220 (BD Biosciences) and DAPI (Invitrogen). Images were obtained with a fluorescence microscope (Axiovert 200M; Carl Zeiss) and processed with MetaMorph 7.7 Software and Adobe Photoshop CSA.

**Full Methods** and any associated references are available in the online version of the paper at [www.nature.com/nature](http://www.nature.com/nature).

Received 16 June; accepted 12 September 2011.

Published online 26 October 2011.

1. Franciotta, D. *et al.* B cells and multiple sclerosis. *Lancet Neurol.* **79**, 852–858 (2008).
2. Ascherio, A. & Munger, K. L. Environmental risk factors for multiple sclerosis. Part I: the role of infection. *Ann. Neurol.* **61**, 288–299 (2007).
3. Pöhlinger, B. *et al.* Spontaneous relapsing–remitting EAE in the SJL/J mouse: MOG-reactive transgenic T cells recruit endogenous MOG-specific B cells. *J. Exp. Med.* **206**, 1303–1316 (2009).
4. Goverman, J. *et al.* Transgenic mice that express a myelin basic protein-specific T cell receptor develop spontaneous autoimmunity. *Cell* **72**, 551–560 (1993).
5. Hill, D. A. & Artis, D. Intestinal bacteria and the regulation of immune cell homeostasis. *Annu. Rev. Immunol.* **28**, 623–667 (2010).

6. Lampropoulou, V. *et al.* TLR-activated B cells suppress T cell-mediated autoimmunity. *J. Immunol.* **180**, 4763–4773 (2008).
7. Lee, Y. K., Menezes, J. S., Umesaki, Y. & Mazmanian, S. K. Proinflammatory T-cell responses to gut microbiota promote experimental autoimmune encephalomyelitis. *Proc. Natl Acad. Sci. USA* **108**, 4615–4622 (2011).
8. Ivanov, I. I. *et al.* Specific microbiota direct the differentiation of IL-17-producing T-helper cells in the mucosa of the small intestine. *Cell Host Microbe* **4**, 337–349 (2008).
9. Gaboriau-Routhiau, V. *et al.* The key role of segmented filamentous bacteria in the coordinated maturation of gut helper T cell responses. *Immunity* **31**, 677–689 (2009).
10. Ivanov, I. I. *et al.* Induction of intestinal Th17 cells by segmented filamentous bacteria. *Cell* **139**, 485–498 (2009).
11. Hall, J. A. *et al.* Commensal DNA limits regulatory T cell conversion and is a natural adjuvant of intestinal immune responses. *Immunity* **29**, 637–649 (2008).
12. Atarashi, K. *et al.* Induction of colonic regulatory T cells by indigenous *Clostridium* species. *Science* **331**, 337–341 (2011).
13. Ercolini, A. M. & Miller, S. D. Molecular mimics can induce novel self peptide-reactive CD4<sup>+</sup> T cell clonotypes in autoimmune disease. *J. Immunol.* **179**, 6604–6612 (2007).
14. Feng, T. *et al.* Microbiota in innate stimulation is a prerequisite for T cell spontaneous proliferation and induction of experimental colitis. *J. Exp. Med.* **207**, 1321–1332 (2010).
15. Kirvan, C. A., Cox, C. J., Swedo, S. E. & Cunningham, M. W. Tubulin is a neuronal target of autoantibodies in Sydenham’s chorea. *J. Immunol.* **178**, 7412–7421 (2007).
16. Delarasse, C. *et al.* Myelin/oligodendrocyte glycoprotein-deficient (MOG-deficient) mice reveal lack of immune tolerance to MOG in wild-type mice. *J. Clin. Invest.* **112**, 544–553 (2003).
17. Cyster, J. G. B cell follicles and antigen encounters of the third kind. *Nature Immunol.* **11**, 989–996 (2010).
18. McMahon, E. J. *et al.* Epitope spreading initiates in the CNS in two mouse models of multiple sclerosis. *Nature Med.* **11**, 335–339 (2005).
19. Cserr, H. F., Harling-Berg, C. J. & Knopf, P. M. Drainage of brain extracellular fluid into blood and deep cervical lymph and its immunological significance. *Brain Pathol.* **2**, 269–276 (1992).
20. Schwickert, T. A., Alabyev, B., Manser, T. & Nussenzweig, M. C. Germinal center reutilization by newly activated B cells. *J. Exp. Med.* **206**, 2907–2914 (2009).
21. Litzenburger, T. *et al.* B lymphocytes producing demyelinating autoantibodies: development and function in gene-targeted transgenic mice. *J. Exp. Med.* **188**, 169–180 (1998).
22. Barnett, M. H., Henderson, A. P. D. & Prineas, J. W. The macrophage in MS: just a scavenger after all? Pathology and pathogenesis of the acute MS lesion. *Ms* **12**, 121–132 (2006).
23. Hohlfeld, R. Multiple sclerosis: human model for EAE? *Eur. J. Immunol.* **39**, 2036–2039 (2009).
24. Kaser, A., Zeissig, S. & Blumberg, R. S. Inflammatory bowel disease. *Annu. Rev. Immunol.* **28**, 573–621 (2010).
25. Vaaheto, J. *et al.* Fecal microbiota in early rheumatoid arthritis. *J. Rheumatol.* **35**, 1500–1505 (2008).
26. Knip, M. *et al.* Dietary intervention in infancy and later signs of  $\beta$ -cell autoimmunity. *N. Engl. J. Med.* **363**, 1900–1908 (2010).
27. Lauer, K. Diet and multiple sclerosis. *Neurol. (Tokyo)* **49** (suppl. 2), S55–S61 (1997).
28. Kira, J. *et al.* Changes in the clinical phenotypes of multiple sclerosis during the past 50 years in Japan. *J. Neurol. Sci.* **166**, 53–57 (1999).

**Supplementary Information** is linked to the online version of the paper at [www.nature.com/nature](http://www.nature.com/nature).

**Acknowledgements** We thank I. Arnold-Ammer, N. Reißer and L. Penner for technical assistance and M. Pfunder, U. Stauffer, C. Hornung and N. Joswig for maintaining our germ-free colony and technical support. We are much obliged to R. Kemler for his support. This work was funded by SFB 571 (Project B6), the German Competence Network on Multiple Sclerosis (KKNMS), ARSEP (France), and by the Max Planck Society. K.B. is supported by a fellowship from ARSEP. Z.A.R. is supported by a PhD fellowship from the Emirates Foundation. M.B. receives a fellowship from the Hellenic Neurological Society.

**Author Contributions** K.B., H.W. and G.K. designed experiments and wrote the manuscript with input from co-authors. K.B. performed most of the experiments. M.M., M.K. and M.B. performed flow cytometry experiments or assisted in experiments. Z.A.R. performed flow cytometry and immunofluorescence staining for brain infiltrates. C.J. supervised the maintenance of germ-free mouse colony and colonization experiments.

**Author Information** Reprints and permissions information is available at [www.nature.com/reprints](http://www.nature.com/reprints). The authors declare no competing financial interests. Readers are welcome to comment on the online version of this article at [www.nature.com/nature](http://www.nature.com/nature). Correspondence and requests for materials should be addressed to H.W. ([hwekerle@neuro.mpg.de](mailto:hwekerle@neuro.mpg.de)) or G.K. ([guru@neuro.mpg.de](mailto:guru@neuro.mpg.de)).

## METHODS

**Mice and colonization.** Wild-type SJL/J, RR and RR  $\times$  MOG<sup>-/-</sup> SJL/J and IgH<sup>MOG</sup>  $\times$  actin-GFP and actin-GFP SJL/J mice were bred at the animal facility of the Max Planck Institute of Neurobiology. Germ-free RR mice were obtained by transferring embryos, isolated by sterile hysterectomy on embryonic day (E) 18.5, to sterile breeding conditions and by fostering on germ-free foster mothers. They were bred and maintained in positive-pressure plastic isolators and provided with  $\gamma$ -irradiated commercial rodent diet and autoclaved water at the animal facility of the Max Planck Institute of Immunobiology and Epigenetics. Fecal samples were routinely cultured in standard I-Bouillon and examined for contamination. In addition, mice from the colony were screened bi-annually according to FELASA health monitoring recommendations. For re-colonization experiments, germ-free mice were placed in cages with bedding material pre-conditioned by conventional (SPF) mice. All animal procedures were in accordance with the guidelines of the Committee on Animals of the Max Planck Institute of Neurobiology and with a license from the Regierung von Oberbayern.

**Active induction of EAE.** Mice were immunized subcutaneously with 200  $\mu$ g rMOG emulsified in Freund's adjuvant supplemented with 5 mg ml<sup>-1</sup> *Mycobacterium tuberculosis* (strain H37Ra; Difco). On days 0 and 2 after immunization, 200 ng of pertussis toxin (List Biological Laboratories) were injected intraperitoneally. Clinical scoring of EAE was done as published<sup>3</sup>.

**Antibiotic treatment.** For short-term antibiotic treatment, 8-week-old wild-type SJL/J mice were treated for 7 days with 1 g l<sup>-1</sup> of metronidazole (Sigma), 1 g l<sup>-1</sup> of neomycin (Sigma) and 0.5 g l<sup>-1</sup> of vancomycin (AppliChem) in their drinking water. **CFSE labelling and adoptive transfer.** Splenocytes from RR or wild-type mice were labelled at 37 °C for 10 min with 5  $\mu$ M CFSE (Invitrogen) in PBS containing 1% fetal bovine serum (FBS). Cells were washed twice in ice-cold PBS and subsequently CD4<sup>+</sup> T cells were isolated using a mouse CD4<sup>+</sup> T-cell isolation kit (R&D Systems). 5  $\times$  10<sup>6</sup> CFSE-labelled CD4<sup>+</sup> T cells were injected intravenously into wild-type SJL/J mice.

**B-cell isolation and adoptive transfer.** B cells were isolated from spleens using a mouse B-cell isolation kit (R&D Systems). B cells were enriched to >90% purity, as confirmed by flow cytometry. 10  $\times$  10<sup>6</sup> purified IgH<sup>MOG</sup>-GFP or wild-type-GFP B cells were intravenously injected into RR, wild-type or RR  $\times$  MOG<sup>-/-</sup> mice.

**Proliferation assay.** For the proliferation assay, 2  $\times$  10<sup>5</sup> splenocytes were cultured in the presence of various concentrations of rMOG or anti-CD3 antibody (BD Pharmingen), as indicated. Proliferative response was measured by the incorporation of [<sup>3</sup>H]-thymidine (1  $\mu$ Ci well<sup>-1</sup>) during the last 16 h of a 72 h culture period. Proliferation assays were performed in triplicates.

**Cell isolation and flow cytometry.** Single-cell suspensions were prepared from spleen, pooled peripheral lymph nodes (axillary plus inguinal), or individual lymph nodes (cervical and inguinal), mesenteric lymph nodes or Peyer's patches by mechanical disruption via forcing through 40- $\mu$ m cell strainers (BD Biosciences). For the isolation of lamina propria lymphocytes, small intestine was collected in ice-cold HBSS buffered with 15 mM HEPES. After careful removal

of Peyer's patches, fatty tissue and fecal contents, the intestine was opened longitudinally and cut into small pieces. The intestinal fragments were washed three times for 15 min with stirring (300 r.p.m.) in HBSS containing 5 mM EDTA, 15 mM HEPES and 10% FBS. Next, intestinal pieces were washed once for 5 min with stirring in RPMI containing 15 mM HEPES and 10% FBS, followed by an incubation step at 37 °C with stirring (500 r.p.m.) in RPMI with 15 mM HEPES, 10% FBS and 100 U ml<sup>-1</sup> Collagenase VII (Sigma). The digested tissue was washed once in RPMI with 15 mM HEPES and 10% FBS, before the lamina propria lymphocytes were subjected to FACS analysis. CNS infiltrating cells were purified by Percoll gradient centrifugation as described<sup>3</sup>. For detection of cell surface markers, cells were stained in FACS buffer (PBS containing 1% BSA and 0.1% Na<sub>2</sub>S<sub>2</sub>O<sub>8</sub>) with fluorochrome-labelled monoclonal antibodies: PerCP-conjugated anti-CD4 (RM4-5), PerCP-Cy5.5-conjugated anti-B220 (RA3-6B2), PE- and APC-conjugated anti-CD19 (1D3), APC-conjugated anti-CD8 $\alpha$  (53-6.7), PE-conjugated anti-TCR $\gamma\delta$  (eBioGL3), PE-conjugated anti-CD11b (M1/70), APC-conjugated anti-NKp46 (29A1.4), FITC-conjugated anti-CD11c (HL3), biotin-conjugated anti-Gr1 (RB6-8C5), FITC-conjugated anti-CD45.1 (A20), FITC-conjugated anti-V $\beta$ 4 (KT4), PE-conjugated anti-V $\alpha$ 8.3 (B21.14), FITC-conjugated anti-GL7, PE-conjugated anti-Fas (Jo2) and PE-conjugated streptavidin. For intracellular cytokine staining, cells were activated with 50 ng ml<sup>-1</sup> PMA (Sigma) and 500 ng ml<sup>-1</sup> ionomycin (Sigma) in the presence of 5  $\mu$ g ml<sup>-1</sup> brefeldin A (Sigma) for 4 h at 37 °C. After surface staining, cells were fixed and permeabilized in 4% paraformaldehyde/0.1% saponin in HEPES-buffered HBSS and stained intracellularly using the following antibodies: PE-conjugated anti-IL17 (TC11-18H10), APC-conjugated anti-IFN- $\gamma$  (XMG1.2), APC-conjugated anti-TNF- $\alpha$  (MP6-XT22), PE-conjugated anti-IL-10 (JES5-16E3) and APC-conjugated anti-FoxP3 (FJK-16 s). All antibodies were purchased from BD Pharmingen or eBioscience. Cells were acquired on a FACSCalibur (BD Biosciences) and analysis was performed using FlowJo (TreeStar) software.

**ELISA.** Serum titres of anti-MOG antibodies were quantified as previously described<sup>3</sup>. Cytokine levels in cell culture supernatants were determined with antibody pairs for IFN- $\gamma$  (BD Biosciences) or IL-17 (eBioscience).

**Immunofluorescence.** Organs were fixed in PBS with 4% paraformaldehyde and cryoprotected in PBS plus 30% sucrose before embedding in OCT medium (A. Hartenstein). Cryostat sections (10  $\mu$ m in thickness) of spleen, lymph nodes and brains were fixed in acetone. Sections were blocked with PBS and 5% BSA before being stained in a humidified chamber. The following antibodies were used for staining: biotin-conjugated anti-CD4 (BD Pharmingen), purified anti-B220 (BD Pharmingen), biotin-conjugated PNA (Vector Laboratories), Alexa Fluor 568-conjugated anti-rat IgG (Invitrogen), Alexa Fluor 488-conjugated Streptavidin (Invitrogen), APC-conjugated streptavidin (eBioscience) and DAPI (Invitrogen). Images were obtained with a fluorescence microscope (Axiovert 200M; Carl Zeiss) and processed with MetaMorph 7.7 Software and Adobe Photoshop CS4.

**Statistical analysis.** GraphPad Prism 5 (GraphPad Software) was used for all statistical analysis. *P* values <0.05 were considered to be significant.

## 7. Curriculum Vitae

### PERSONAL INFORMATION

Name: Gurumoorthy Krishnamoorthy  
 Position title: Project leader  
 Nationality: Indian  
 Date of birth: 05.06.1978  
 Office Address: Max-Lebsche-Platz 30, 81377 Munich, Germany  
 Tel: +49-89-44007 8385  
 Fax: +49-89-44007 8380  
 E-mail: guru@neuro.mpg.de

### EDUCATION

**2002 –2007** PhD student, Department of Neuroimmunology (Lab of Dr. Andreas Holz), Max Planck Institute of Neurobiology, Martinsried, Germany.

**2001 – 2002** Research fellow, Department of Biochemistry, Indian Institute of Science, Bangalore, India.

**1999 – 2000** M.S (Pharm.), National Institute of Pharmaceutical Education and Research (NIPER), Punjab, India.

**1995 –1999** B.Pharm, Adhiparasakthi College of Pharmacy, Tamilnadu Dr. M.G.R Medical University, Tamilnadu, India.

### CURRENT POSITION

**2008-present** Project leader, Department of Neuroimmunology (Director: Prof. Dr. Hartmut Wekerle), Max Planck Institute of Neurobiology, Martinsried, Germany.

### PREVIOUS POSITION

**2007 – 2008** Postdoctoral fellow, Department of Neuroimmunology (Lab. of Prof. Dr. Hartmut Wekerle), Max Planck Institute of Neurobiology, Martinsried, Germany.

### FELLOWSHIPS AND AWARDS

**2009** Junior Research Award of the German Multiple Sclerosis Society (Sobek Prize)

## 8. Acknowledgment

I would like to express my deep appreciation and gratitude to Prof. Dr. Hartmut Wekerle who has been a great mentor since my PhD thesis at his Department of Neuroimmunology at the Max Planck Institute of Neurobiology. My scientific career started and still continues in his department speaks volumes about how much I enjoyed working him over 12 years.

I also express my gratitude to Prof. Reinhard Hohlfeld, director of Institute of Clinical Neuroimmunology at the Ludwig-Maximilians University München who is my mentor for this habilitation work and a great motivator and supporter since my doctoral work.

I am also grateful to Dr. Andreas Holz who was my direct supervisor of my PhD work. His constructive comments, constant encouragement and discussions have sharpened my thinking about scientific problems.

I want to particularly thank my colleague Dr. Kerstin Berer for her companionship and all the help over the years. I want to thank all my present colleagues with a special mention to Birgit Kunkel and Clemens Goedel. I want to specially thank my former colleagues Bernadette Pöllinger, Sofia Domingues, Marsilius Mues, Michail Koutrolos, Irene Arnold-Ammer and Zakeya Al-Rasbi who were simply fantastic and I am very grateful to work with them.

I thank all my former and present colleagues of the department of Neuroimmunology at the Max Planck Institute of Neurobiology for their support and care. Especially, I thank Prof. Edgar Meinl, Dr. Naoto Kawakami and Dr. Klaus Dornmair for the collaboration and scientific discussion.

I want to thank my wife Jeeva and kids, Kavin & Yuvan for their efforts to cheer me up all the time. Most importantly, I want to thank my parents whose sacrifices brought me to this level.